Svoluji k zapůjčení své diplomové práce ke studijním účelům a prosím, aby byla vedena přesná evidence vypůjčovatelů. Převzaté údaje je vypůjčovatel povinen řádně ocitovat.

Charles University

Faculty of Science

Study programme: Biology

Branch of study: Microbiology

Bc. Klára Mikesková

The omega subunit of *Bacillus subtilis* RNA polymerase

Podjednotka omega RNA polymerázy z *Bacillus subtilis*

Diploma thesis

Supervisor: Doc.Mgr.Libor Krásný Ph.D.

Prague, 2022

Declaration:

I hereby declare that I have compiled this Thesis independently, using the listed literature and resources only. Content of the Thesis or any part of it has not been used to gain any other academic title.

Prohlášení:

Prohlašuji, že jsem závěrečnou práci zpracoval/a samostatně a že jsem uvedl/a všechny použité informační zdroje a literaturu. Tato práce ani její podstatná část nebyla předložena k získání jiného nebo stejného akademického titulu.

V Praze, 25.04.2022

Bc. Klára Mikesková

Abstract

Transcription is catalysed by the enzyme RNA polymerase (RNAP). RNAP contains a core made up of two α subunits, one of each β, β'and ω. These subunits are conserved in all bacteria. The ω subunit is a small subunit with a molecular weight of 7.6 kDa that binds β'. ω is important for the folding and integrity of RNAP and promoter selection. This was shown by experiments performed with Gram-negative bacteria but the knowledge about ω in Gram-positive bacteria is minimal. In my Diploma Thesis, I characterized ω from the model Gram-positive bacterium from the phylum Firmicutes, *Bacillus subtilis*. First, I prepared various expression strains for isolation of *Bacillus subtilis* ω. Then, I successfully isolated the ω subunit, which was the main initial aim of this Diploma Thesis. Subsequently, I tested the influence of the ω subunit on *in vitro* transcription by RNAP associated with the primary σ^A factor and alternative σ^F and σ^E factors that regulate sporulation in *Bacillus subtilis*. I also evaluated the effect of δ, a small RNAP subunit found in Firmicutes, both alone and in combination with ω. The experiments revealed that ω stimulated transcription both from vegetative promoters and sporulation-related promoters. Moreover, this stimulation was synergistically amplified by the δ subunit. This nicely correlated with a previous observation where *B. subtilis* strains lacking ω and δ displayed decreased sporulation efficiency. Overall, this Thesis has created the tools to study ω of *Bacillus subtilis*, performed an initial characterization of its effects on transcription, and paved the way to further exploration of its biological role.

Key words: ω subunit, δ subunit, RNA polymerase, transcription, sporulation, SigA, SigF, SigE

Abstrakt

Transkripce je zprostředkována enzymem RNA polymerázou (RNAP). RNAP obsahuje jádro tvořené dvěma podjednotkami α, a po jedné β, β' a ω. Tyto podjednotky jsou konzervované u všech bakterií. Podjednotka ω je malá podjednotka o velikosti 7,6 kDa, která se váže na podjednotku β'. Podjednotka ω je důležitá pro složení a integritu RNAP a výběr promotorů. Toto bylo ukázáno experimenty provedenými na Gram-negativních bakteriích, ale vědomosti o podjednotce ω u Gram-pozitivních bakterií jsou minimální. Ve své diplomové práci jsem charakterizovala ω z modelové Gram-pozitivní bakterie ze skupiny Firmicutes, *Bacillus subtilis*. Nejprve jsem připravila několik expresních kmenů pro izolaci podjednotky ω z *Bacillus subtilis*. Následně jsem úspěšně provedla její izolaci, což byl hlavní a původní cíl této Diplomové práce. Dále jsem testovala vliv podjednotky ω na transkripci *in vitro* pomocí asociace RNAP s primárním faktorem σ^A i s alternativními faktory σ^F a σ^E, které regulují sporulaci u *Bacillus subtilis*. Také jsem studovala vliv podjednotky δ, malé podjednotky RNAP nacházející se u skupiny Firmicutes, a to samostatně, i v kombinaci s podjednotkou ω. Mé výsledky odhalily, že podjednotka ω stimuluje transkripci z promotorů vegetativních i těch asociovaných se sporulací. Navíc, tato stimulace byla synergicky zesílena podjednotkou δ. Toto koreluje s předchozím pozorováním, ve kterém měly kmeny bez podjednotek ω a δ nižší účinnost sporulace. Shrnuto, v této práci jsem vytvořila nástroje k studiu podjednotky ω z *Bacillus subtilis*, provedla počáteční charakterizaci jejího vlivu na transkripci a naznačila cestu k dalšímu studiu její biologické role.

Klíčová slova: podjednotka ω, podjednotka δ, RNA polymeráza, transkripce, sporulace, SigA, SigF, SigE

Contents

Abbreviations

RNAP – RNA polymerase

Wt – Wild type

RP_C – Closed complex of RNAP with promoter

RP_I – Intermediate complex of RNAP with promoter

RP_O – Open complex of RNAP with promoter

SKF – Sporulation killing factor

SDP – Sporulation delaying protein

(p)ppGpp – Guanosin tetra(penta) phosphate

MBP-tag – Maltose binding protein tag

GST-tag – Gluthathion-S-transferase tag

His-tag – Hexahistidine tag

CTD – C-terminal domain

IPTG – Izopropyl–β–D–thiogalaktosid

iH_2O – Aqua pro injection

dH_2O – Distilled water

Falcone tube – Falcon® Conical Centrifuge Tube

MES – 2-(N-morpholino)ethanesulfonic acid

Tris Base – Tris(hydroxymethyl)aminomethane

ME – β-mercaptoethanol

SDS – Sodium dodecyl sulfate

1. Introduction

DNA is usually in the form of a double stranded helix, consisting of four types of nucleotides. These nucleotides are made up of sugar, base and phosphate moieties (Watson and Crick, 1953).

DNA is duplicated by the process of replication and serves as the template for transcription. Transcription is a process in which part of a DNA sequence is copied into an RNA sequence. Transcription is catalysed by the enzyme RNA polymerase (RNAP). RNA sequences that encode proteins are termed mRNAs. These mRNAs are then translated into amino acid sequences to form a protein.

The bacterial RNAP core consists of two α subunits (α_2), and one of each β, β', and ω subunits. These subunits, together with the σ subunit, which binds to the promoter region in DNA where transcription starts, form the holoenzyme. The holoenzyme can then initiate transcription. The α_2, β, β' subunits are essential in bacteria (Nudler, 2009). The ω subunit is an integral part of the holoenzyme. However, it is not essential and its absence can be substituted by the GroEL chaperone (Mukherjee et al., 1999). Furthermore, Gram-positive bacteria within the phylum Firmicutes, which includes the important model organism *Bacillus subtilis*, have additional nonessential subunits. These subunits are δ and ε (Weiss and Shaw, 2015).

Bacteria may have multiple different σ subunits (also known as sigma factors) that recognize specific promoters. There is usually one vegetative σ factor, which controls transcription in non-limiting conditions, particularly transcription of essential genes. It is called the housekeeping (also primary, vegetative) σ factor. The housekeeping σ factor in *B. subtilis* is σ^A, in *E. coli* it is σ^{70}. Under limiting and/or stress conditions, other σ factors become active and enable transcription of genes. An example of a process that is regulated by a cascade of various σ factors is sporulation in *B. subtilis* (Cook and Ussery, 2013; Haldenwang, 1995).

The result of sporulation is the resistant state of *B. subtilis*, the spore. Spores are formed when bacteria encounter unfavourable conditions such as: high temperatures, low concentrations of water, insufficient amounts of nutrients or UV light. Sporulation is regulated by σ^A, σ^H, σ^F, σ^E, σ^G, σ^K. It is a process that in defined steps turns a vegetative bacterial cell into an endospore that is highly resistant and can endure physical and chemical conditions that would be lethal for the vegetative cell., The spore can then germinate into a vegetative cell when the conditions in the environment improve (De Hoon et al., 2010).

Unpublished experiments from my lab had revealed that ω is important for sporulation in *Bacillus subtilis* (D. Kálalová). Hence, in this Thesis I focused on the process of transcription, the enzyme RNAP, and namely on the ω subunit of RNAP, using *Bacillus subtilis* as the model organism. The project started with cloning of the ω gene associated with sequences encoding various affinity tags. This was followed by optimisation of purification of the proteins. Subsequent *in vitro* experiments with a panel of vegetative and sporulation-specific promoters then showed a significant effect of ω on transcription and its synergistic effect together with δ. The Thesis thus helped define the role of ω during vegetative growth and sporulation, advancing our understanding of the transcription machinery in bacteria. Ultimately, this knowledge may aid future designs of antibacterial compounds targeting ω, hampering gene expression in pathogens such as *Bacillus anthracis* or *Staphylococcus aureus*.

2. Aims of the Thesis

The initial main aim of this Thesis was the isolation and purification of the ω subunit of *Bacillus subtilis* RNAP, as before this Thesis, the Krásný lab had struggled to obtain this protein for *in vitro* experiments in sufficient amounts and purity. Next, this protein was used to characterize its effect on transcription from selected promoters, both vegetative and sporulation-related.

The individual goals were to:

- prepare constructs with the ω subunit associated with various tags.
- test the overexpression of the ω subunit containing these tags.
- overexpress and purify the ω subunit containing selected tags.
- test the effect of the presence and absence of the ω subunit in *in vitro* transcription of selected promoters.

3. Literature Review

3.1 *Bacillus subtilis*

Bacillus subtilis is a Gram-positive rod-shaped bacterium that belongs to the phylum Firmicutes. It is non-pathogenic and an important model Gram-positive bacterium (Kovács, 2019). The complete genome of the *B. subtilis* strain 168 was sequenced already back in 1997 within a large collaborative project (Kunst et al., 1997), revealing a genome of 4,200 kbp. This sequence was then resequenced and cleared of errors yielding a total of approximately 4,500 kbp in 2009 (Barbe et al., 2009). This helped immensely to study this organism for which nowadays exist multiple genetic and molecular tools (van Tilburg et al., 2019).

B. *subtilis* is mainly a soil bacterium but it can be found also in water and the intestinal tract of various organisms. *B. subtilis* has multiple differentiation programs such as vegetative growth, competence (the ability to uptake exogenous DNA) sporulation, formation of biofilms or cannibalism (Arnaouteli et al., 2021; Chen et al., 2005; González-Pastor, 2011; Vlamakis et al., 2013). The process of sporulation is further described in detail in Chapter 3.5. It produces secondary metabolites, such as surfactin, which contributes to its motility. Motility can be facilitated in different ways, including movement of a single cell using peritrichous flagellum, by rafts of swarming cells or by sliding, which is enhanced, in addition to surfactin, also by hydrophobin (Kearns and Losick, 2003).

Furthermore, *B. subtilis* produces secondary metabolites that possess antibacterial and antifungal activity. These secondary metabolites are for example bacteriocins, AMP enzymes, polyketides and non-ribosomal proteins (NRPs). Bacteriocins are ribosomal peptides and are divided into three classes according to their biosynthetic pathways. AMP enzymes are lytic enzymes and enzymes for quorum quenching. Polyketides are synthesized from malonate and methyl malonate using a multifunctional polyketide synthase (e.g. macrolides and tetracyclines). NRPs are divided into thiotemplate NRPs (lipopeptides) and non-thiotemplate NRPs (Caulier et al., 2019). *B. subtilis* is also able to attach itself to plant roots or fungal hyphae (Benoit et al., 2015). Importantly, *B. subtilis* is used for industrial applications like production of hydrolytic enzymes, food fermentation and recently also used as a probiotic (Höfler et al., 2016; reviewed in Kovács, 2019; Marzorati et al., 2020).

3.1.1. Biofilm

The formation of biofilm occurs when microbial cells cluster together and form layers containing communities surrounded by polysaccharide/protein/DNA environment, so called extracellular matrix. Extracellular matrix is produced by the cells themselves and helps the cells adhere together in the biofilm and also has protective properties. During this process motile cells of *B. subtilis* transform into adherent (sessile) cells that form the biofilm. The extracellular matrix of *B. subtilis* is made up of proteins TasA, TapA and BslA (these are secreted proteins), eDNA (extracellular DNA), a mineral scaffold and EPS (extracellular polymeric substances). For more detail see the review by (Arnaouteli et al., 2021). According to Lopez *et al.*,2009 the subpopulation of cells, which produces the extracellular matrix is the same subpopulation of cells as the one that transforms into cannibalistic cells and these processes are triggered by surfactin (López et al., 2009).

3.1.2 Cannibalism

Cannibalism, as the name implies, is killing of sibling cells and then feeding on their lysed remnants. It is regulated through a phosphorelay system and two cannibalism toxins. The system is activated when the amount of nutrients is low and works as a last resort before the cell enters the process of sporulation to prolong the time before the cells commit to this process. The two toxins are: (i) the sporulation delaying protein (SDP) and (ii) the sporulation killing factor (SKF). The toxins are regulated by the master regulator Spo0A, which is active in sporulating cells and inactive in nonsporulating cells. For further review see (González-Pastor, 2011). The mechanism of regulation of cannibalism is depicted in Fig. 1.
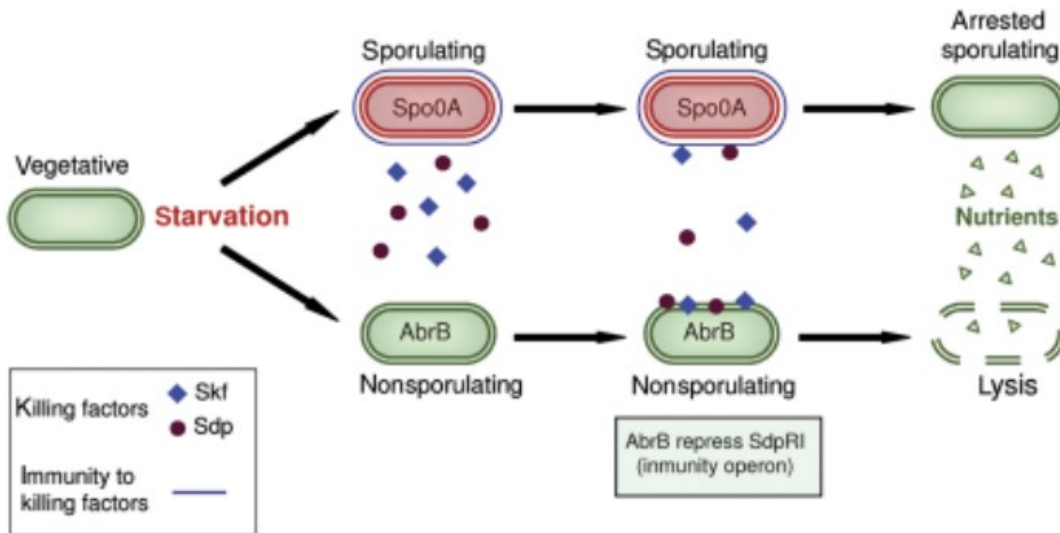
Figure 1. The mechanism of regulation of cannibalistic behaviour in *B. subtilis*. When the amount of nutrients are limited *B. subtilis* enters the process of sporulation. The master regulator (Spo0A) then becomes active only in part of the population. The population of cells in which Spo0A is activated produces toxins Skf and Sdp. The producing cells (with active Spo0A) are immune to these toxins. The cells with inactive Spo0A are sensitive to these toxins. This has two reasons. The first reason is that the ABC transporter and other genes for immunity (needed for the resistance to toxin SKF) are not transcribed. The other reason is that when Spo0A is inactive, AbrB can be expressed. AbrB then in turn can repress the transcription of the *sdpRI* operon. This operon gives the cells immunity to the SDP toxin. Thus, the non-sporulating cells are killed by the sporulating cells. The nutrients released in this way are then used by the sporulating cells that have not yet become irreversibly committed to sporulation. These cells then begin to grow again, and sporulation is arrested. Adapted from (González-Pastor, 2011)

3.2 RNA polymerase

RNAP is the enzyme (DNA-dependent RNA polymerase) that catalyses transcription. RNAP contains various subunits. The core bacterial subunits are α, α, β, β', and ω. These core subunits associate with a σ subunit that recognizes the specific promoter sequence. This RNAPσ complex is called the holoenzyme and is capable of initiating transcription. The bacterial core has a molecular weight of approximately 400 kDa (Browning and Busby, 2004; Helmann and DeHaseth, 1999; Nudler, 2009). The RNAP holoenzyme may exist in multiple forms according to the σ factor with which the core associates. The type of σ factor associated is dependent on the state of the bacteria (stress, exponential or stationary growth phase) (Gruber and Gross, 2003).

A dimer made of two α subunits provides a scaffold for β and β' subunits. The ω subunit helps the subunits β and β' with binding to this scaffold. It mainly interacts with the β' subunit. The structure of the holoenzyme resembles a crab claw. The subunits β and β' form the pincers (reviewed in Browning & Busby, 2004; Helmann & DeHaseth, 1999; L. Minakhin et al., 2001; Murakami et al., 2002). Some bacteria contain additional subunits, such as δ and ε that are

found in Gram-positive bacteria within the phylum *Firmicutes*. These subunits are nonessential (Weiss and Shaw, 2015).

RNAP has three major channels. Two of them (primary and secondary channels) are separated by the bridge helix. The bridge helix is found in the β' subunit of the RNAP and coordinates the movements of modules in RNAP. It is a metastable α-helix and spans the main channel of RNAP downstream of the active site (Hein and Landick, 2010). The cleft between the β and β' pincers is known as the main (primary) channel. Promoter DNA passes through this channel. The secondary channel, which is narrower is then supposed to serve as a means of transport for nucleoside 5'-triphosphates and therefore enables the access of these nucleosides to the active site (Landick, 2005). Multiple additional transcription factors, small proteins and small molecules enter and interact with the RNAP through the secondary channel as well as NTPs. These proteins and small molecules include for example DksA, Gre factors, HelD (p)ppGpp (nucleotides tetraphosphate and pentaphosphate) or TraR. This can have various effects on transcription (Paul et al., 2004a, 2004b; Perederina et al., 2004; Sutherland and Murakami, 2018). However, when DksA or TraR bind to the secondary channel of the RNAP they occupy it fully. This means there has to be an alternative route of entry for NTPs. According to Molodotsov *et al*., 2018 this alternative loading pathway is, in the open complex (RPo, a kinetic intermediate during transcription initiation where the transcription bubble is formed, see 3.3.1.), via the main channel of the RNAP. This is possible because in the RPo the main channel is occupied only by a DNA strand. On the other hand, the main channel of the elongation complex is occupied by the DNA/RNA hybrid. As the secondary channel is blocked by DksA or TraR the main channel is the only pathway of entry of NTPs during the initiation of transcription (Gopalkrishnan et al., 2017; Molodtsov et al., 2018).The third channel is then the RNA exit channel, which is formed by the flexible flap domain in RNAP's β subunit and a mobile clamp domain that includes several loops that cover RNAP's main channel and RNA exit channel (Toulokhonov and Landick, 2003). The RNA formed during transcription passes out of RNAP through this channel. Furthermore, when RNA hairpins form after the transcription of palindromic sequences it causes a change in conformation of the flap domain. This change is then the cause of transcription termination or pausing (Ray-Soni et al., 2016).

The σ subunit is responsible for the interaction of RNAP with promoter DNA. σ factors consist of several domains (from 1 to 4, each domain is then further subdivided). The σ region 4.2 (of the (C)-terminal domain) binds to the -35 element of the promoter. The σ region 2.3 - 2.4 then in turn binds to the -10 element of the promoter (for definition see the next chapter)

(Gruber and Gross, 2003; Minakhin et al., 2001; Murakami et al., 2002). The interaction between the promotor and σ^{70} RNAP during transcription initiation is shown in Fig 2.
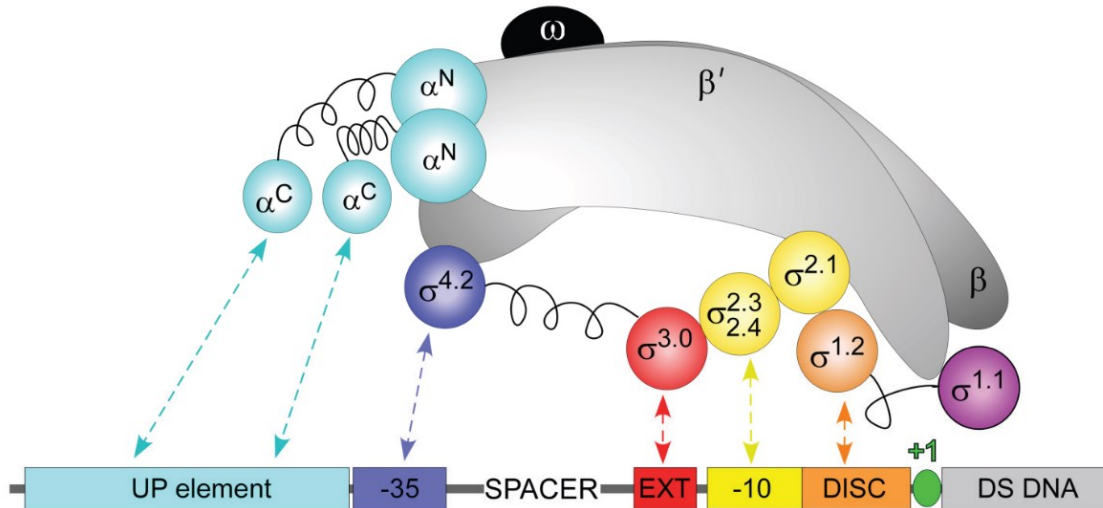
Figure 2. Interaction between the promoter regions and σ^{70} RNAP. Schematic demonstration of the interaction partners RNAP core and σ^{70} with the promoter. The two α subunits with the UP element in blue, σ 4.2 region with -35 element in purple, σ 2.3-2.4 region with -10 element in yellow, σ 1.2 with the discriminator in orange. The transcription start site is in green and the DNA downstream of the start site is in grey. The β and β' subunits are displayed in grey and the ω subunit in grey. CONS – the optimal consensus sequence. Adapted from (Ruff et al., 2015).

3.2.1 Promoter

The promoter contains specific DNA sequences. Two important hexameric DNA promoter elements are termed -10 (TATAAT) and -35 (TTGACA) (numbered relative to the transcription start site +1; sequences recognized by vegetative σ factors are shown). They interact with the σ factor of bacterial RNAP holoenzyme (Helmann and DeHaseth, 1999). The two hexamers are separated by the spacer region. The length of the spacer region affects the strength of the promoter. Typically, it is 17 bp long ±2 bp. The sequence and length of the region between -10 and +1 also affects promoter strength (Helmann, 1995; Lozinski et al., 1991).

Promoter activity is primarily determined by its affinity for RNAP and subsequently affected by kinetic parameters during transcription initiation and promoter escape. Furthermore, promoters are generally regulated by activators and repressors. Repressors are responsible for decreasing the promoter activity while activators increase the activity of the promoter. These regulators are proteins that bind to certain DNA sequences that are close to or overlap the binding site of RNAP. They can also bind to RNAP itself. Regulators that can bind to DNA

sequences can therefore only affect promoters which have transcription factor binding sites (Barne et al., 1997;reviewed in Browning & Busby, 2004).

Moreover, the activity of promoters can also be controlled by small molecules and proteins that bind to RNAP and affect the kinetics of transcription initiation. Examples are (p)ppGpp (nucleotides tetraphosphate and pentaphosphate), DksA or TraR (Molodtsov et al., 2018; Paul et al., 2005).

3.2.2 σ factors in *B. subtilis*

σ^A is the vegetative σ factor encoded by the *sigA* gene. It directs transcription from promoters for housekeeping genes. However, it was shown that it also plays a role in the expression of genes involved in the initiation of sporulation (Price and Doi, 1985). σ^A also plays a role in the transcription of some genes for the heat shock response (Chang et al., 1994).

σ^F is a σ factor associated with sporulation and post asymmetric cell division and can be found in the forespore. Before the asymmetric division, σ^F is sequestered as a complex with two molecules of the anti-sigma factor SpoIIAB. The release of the σ^F is induced when the anti-anti-sigma factor SpoIIAA binds to the complex (Campbell et al., 2002; Igoshin et al., 2006). The σ^F encoding gene is *sigF (spoIIAC)*. The most important function of σ^F is directing the transcription of the early stage forespore cell genes in sporulation. σ^F is the first activated regulator in the sporulation cascade that is compartment-specific and is responsible for transcription of approximately 50 genes (Steil et al., 2005).

σ^E, encoded by *sigE (spoIIG)*, is also a sporulation σ factor. After the asymmetric cell division, it is found in the mother cell. Specifically, it is responsible for transcription of early-stage mother cell genes. This σ factor is synthesized from its precursor protein pro-σ^E (LaBell et al., 1987). The synthesis of σ^E is controlled at two levels. The first level is transcription, when the promoter of the *spoIIG* operon becomes active only after sporulation begins. The second level is a posttranslational regulation, where the product of *spoIIG* (pro-σ^E) is an inactive precursor of σ^E. The processing of this precursor in the mother cell involves SpoIIGA (membrane aspartate protease) and SpoIIR (a signalling protein secreted in the forespore) that triggers the proteolytic cleavage (Karow et al., 1995; LaBell et al., 1987; Stragier et al., 1988). σ^E is responsible for directing the transcription of 262 genes. For further review see (Davis et al., 2017; Eichenberger et al., 2004; Haldenwang, 1995; De Hoon et al., 2010; Imamura et al., 2008). The activation of both σ^E and σ^F is dependent on the phosphorylation of Spo0A (Gholamhoseinian and Piggot, 1989; York et al., 1992).

3.2.3 δ subunit

The δ subunit is encoded by the *rpoE* gene in Gram-positive *Firmicutes*. It is a protein made up of 173 amino acids in *B. subtilis* and has a molecular mass of about 20.5 kDa. It is a highly acidic protein (pI is 3.6) (Lampe et al., 1988; Pero et al., 1975). The δ subunit co-purifies with the core of RNAP (Pero et al., 1975). According to the newest studies the δ subunit is considered as a component of the RNAP (De Jong et al., 2017; Pei et al., 2020) even though it was previously also suggested that it does not interact directly with the RNAP holoenzyme. It was proposed to bind upstream of the basal promotor, easing the recycling of the RNAP and transcription initiation (Prajapati et al., 2016).

The deletion of the δ subunit shows defects in altered cell morphology, lowered competitive fitness and sporulation. The effect of δ on sporulation is either direct or indirect and most probably at the level of transcription of some genes at stages II-III of sporulation as it was shown that inactivation of δ suppresses the sporulation defect of the inactive *pdhC* gene (E2 subunit of pyruvate dehydrogenase) (Gao et. al, 2004). Furthermore, δ has an effect on the regulation of RNAP through the concentration of initiating nucleotide triphosphates (iNTP) of sensitive promoters. These promoters form relatively unstable open complexes. This mechanism (regulation of RNAP through the concentration of the iNTP) is important for fast changes in gene expression as a response to environmental changes (Sojka et al., 2011).

Furthermore, according to De Jong *et al.*, 2017, the δ subunit interacts with the β' subunit of RNAP. There is a possibility that δ could possibly modulate promoter selectivity (De Jong et al., 2017). Furthermore, in synergy with the HelD protein, δ increases the recycling of RNAP. Both proteins are needed for *B. subtilis* to rapidly adapt to environmental changes (Rabatinová et al., 2013; Wiedermannová et al., 2014). HelD, which is found in Gram-positive bacteria is a putative nucleic acid-dependent NTPase, is related to UvrD and Rep helicases from *E. coli* (Kovaľ et al., 2019). The interaction of the δ subunit and HelD can be seen in Fig.3.

Moreover, it was shown by Kubáň *et al.*, 2019 that the δ subunit negatively affected transcription from promoters that form relatively unstable initiating complexes (P*ilv* and *rrnB* P1) (Krásny and Gourse, 2004; Krásný et al., 2008; Sojka et al., 2011; Whipple and Sonenshein, 1992) with RNAP (initiation of transcription described in 3.3.1) when the δ subunit contains a normal lysine tract (7 positively charged lysins KAKKKKAKK in the intrinsically disordered C-terminal domain of δ) and also when this lysine tract is mutated (lysin was replaced by glutamic acid) (Kubáň et al., 2019). This lysine tract enables the compact structure of the δ

subunit. The negatively charged segment that follows the lysine tract folds onto it. When this lysine tract is mutated the C-terminal domain remains in an extended form. Therefore, this extended form could have possibly interacted more strongly with the formation of the initiation complex and affected transcription more negatively when the tract was mutated.
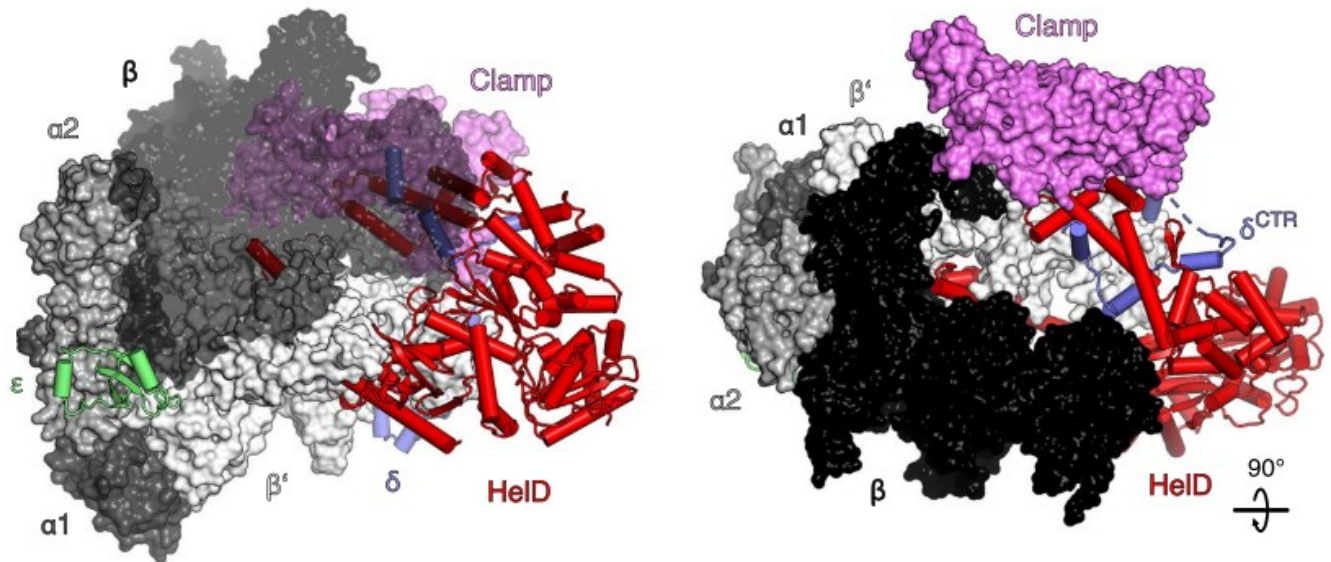
Figure 3. The structure of an RNAP-δ-HelD complex. In the structure on the left-hand side the surface of the β subunit is semi-transparent. The right-hand structure is rotated by 90° relative to the left-hand side structure. The colour coding is as follows α₁ is dark grey, α₂ is grey, β is black, β' is light grey, the β' clamp is violet, ε is lime green, δ is slate blue and HelD is red. Adapted from (Pei et al., 2020).

3.3 Bacterial transcription

Transcription in bacteria is catalysed by only one type of DNA-dependent RNA polymerase (RNAP)unlike Eukaryotes that have several types of this enzyme (Decker and Hinton, 2013). It is part of gene expression and is therefore part of the central dogma of molecular biology (Crick, 1970). The RNAP core is capable of catalysing the phosphodiester bond synthesis, however only the RNA polymerase holoenzyme including the σ factor is able to recognize a promoter and initiate transcription (Nudler, 2009). The structure of RNAP is described above in chapter 3.2. Transcription is divided into four parts: promoter recognition, initiation, elongation, and termination. These steps are shown in Fig. 4.
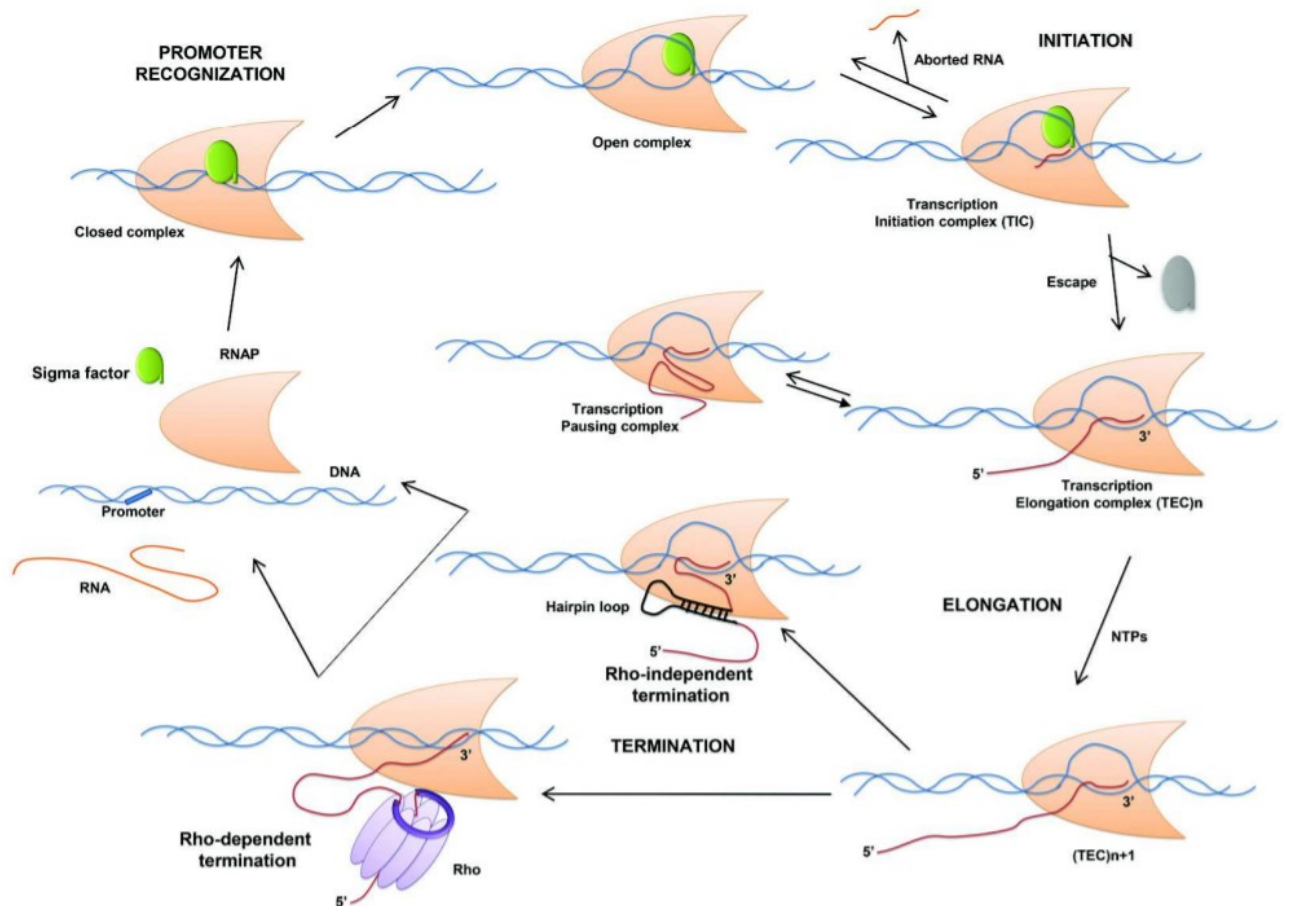
Figure 4. The transcription cycle in bacteria. This cycle consists of four stages: promoter recognition, initiation, elongation and termination. The bacterial holoenzyme consists of the core (α_2, β, β',ω) and the σ factor. The core selects a σ factor and becomes the RNAP-sigma factor holoenzyme. This holoenzyme can then recognize the promotor, which leads to the transition to the open complex (from the closed complex). The synthesis of RNA is initiated when the transcription initiation complex (TIC) forms. After the sigma factor is released, transcription elongation takes place when the transcription elongation complex forms (TEC). This leads to synthesis of RNA. During this process, the TEC may be stalled or become arrested, which depends on the DNA sequences. Transcription termination can then occur either by intrinsic (Rho-independent) termination or by extrinsic (Rho-dependent) termination. Intrinsic termination happens when a DNA sequence transcribes into an RNA forming hairpin loop. The Rho-dependent termination requires the homohexameric protein Rho that dislodges the elongation complex. Adapted from (Chhakchhuak et al., 2019).

3.3.1 Initiation

The bacterial RNAP holoenzyme recognizes the promoter DNA -10 and -35 elements (here I describe the situation for the main factor; for some alternative sigma factors, this numbering may differ (Chen and Helmann, 1995; Helmann, 1995). For transcription to initiate, a transient complex has to form and undergo multiple conformation changes. Supposedly, there is a mechanism common for all promoters. When the RNAP (R) binds the promoter (P), it forms three intermediate complexes: the closed (RP_C), intermediate (RP_I) and the open (RP_O) complex. In order for the conformation of these complexes to change from one to the other, the complex must undergo isomerizations. The machinery itself and its movements towards initiation are powered, not by the hydrolysis of ATP but by the free energy acquired from the

conformations of the earlier intermediates. When the complex is closed the two strands of DNA have not yet been separated, but when the RNAP isomerizes to the open complex the strands separate and the transcription bubble can then form. As transcription is initiated, short abortive products of RNA may be produced or the RNAP can slip. These two events can possibly have regulatory functions (Barne et al., 1997; reviewed in Helmann & DeHaseth, 1999).

3.3.2 Elongation

For elongation to take place, a mature elongation complex must form. It forms only once the σ factor is released from RNAP and RNAP is no longer in contact with the promoter. Once this occurs, RNAP uses the template strand to catalyse the addition of complementary nucleotides, using nucleotide triphosphates (NTPs) as substrates. At this point, a DNA-RNA hybrid forms as the complementary RNA is gradually synthesized. When the RNA is formed, it exits the RNAP through the RNA exit channel. Various factors exist, which influence transcription elongation. Among these factors belong for example GreA, GreB, NusG or Mfd. GreA plays a role in backtracking (by a few bp) of the transcription elongation complex, while GreB is supposed to be able to rescue arrested elongation complexes with more significant backtracking. These factors induce the hydrolytic activity of RNAP, causing the formation of new 3' ends in the active site of RNAP, allowing thus for resumption of transcription (Borukhov et al., 1993). Another factor important during elongation is NusG which is important for coupling of transcription and translation and binds to the lead ribosome (Valabhoju et al., 2016). Moreover, it also stimulates Rho dependent transcription termination. Mfd (Mutation frequency decline) is a transcription repair factor that recruits excision repair factors to stalled RNAPs. For further review see (Mustaev et al., 2017; Uptain et al., 1997).

3.3.3 Termination

In bacteria, transcription is usually terminated by two mechanisms: either by intrinsic (Rho-independent) termination or by extrinsic (Rho-dependent) termination. There are unique cases in which transcription may be terminated differently. This occurs when the RNAP becomes stalled or is inactive on the DNA. Termination of these stalled elongation complexes can then be mediated by proteins such as Mfd (a transcription-repair coupling factor)(Roberts, 2019; Roberts and Park, 2004), RNase J1(Šiková et al., 2020), or HelD(Pei et al., 2020).

Rho-dependent termination occurs with the assistance of the protein Rho. Protein Rho is an ATP-dependent RNA translocase. It is an homohexameric enzyme and releases RNA from the complex by changing the structure of the elongation complex itself(Mitra et al., 2017).

Intrinsic termination is based on the activity of the core RNAP and a DNA sequence, which encodes an RNA hairpin structure with a terminal segment rich in uridine. When the hairpin forms, it affects the conformation of RNAP. The RNA-DNA hybrid is then released. This is facilitated by the U-tract, which follows the hairpin. Finally, RNAP dissociates from the nucleic acid(Roberts, 2019).

In the case of the other factors, Mfd is an ATP-dependent translocase. This translocase binds both DNA and RNAP and by using the energy from ATP hydrolysis dissociates the stalled elongation complex (Roberts and Park, 2004; Smith et al., 2012).

RNase J1 is a 5' to 3' exonuclease. Besides its canonical function in RNA turnover, it also can dissociate stalled complexes of RNAP from DNA. RNase J1 recognizes free 5' ends of RNA protruding from stalled elongation complexes, degrades the RNA and, upon contact with RNAP, disassembles the stalled transcription complexes. This helps prevent collisions of transcription and replication, which could have dangerous consequences for the cell (Šiková et al., 2020; Svetlov and Nudler, 2020; Wiedermannová and Krásný, 2021).

Finally, HelD is an ATPase/GTPase that recognizes stalled RNAP. It binds to RNAP in a unique manner, protruding both into its primary and secondary channels, causing conformational changes resulting in release of nucleic acids. (Kouba et al., 2020; Pei et al., 2020). For further review of transcription termination see (Mitra et al., 2017; Roberts, 2019; Roberts and Park, 2004).

3.4 ω subunit of RNA polymerase

In the past, the ω subunit was not considered important because *in vivo* deletion of *rpoZ* (*yloH*) is tolerated in bacteria (Gentry et al., 1991). The redundancy of the ω subunit was also supported by the ability of *E. coli* RNAP to reconstitute only using purified α, β, β' subunits (Heil and Zillig, 1970). However, when the direct association of ω with the β' subunit of RNAP was found, it resulted in the validation of ω subunit as an integral part of the RNAP machinery *in vivo* (Dove and Hochschild, 1998). This idea of direct association was later also supported by the crystal structure of *Thermus aquaticus* RNAP (Zhang et al., 1999), and this stimulated further interest in this protein and its study.

The ω subunit is the smallest subunit of RNAP (7kDa-11.5kDa). The molecular weight of ω in *B. subtilis* is 7.62 kDa, its isoelectric point is 5.51 and the length of the protein is 67 amino acids (subtiwiki). The ω subunit gene in *B. subtilis* is organized in an operon with genes encoding an ATP-driven Ca^{2+} pump (*yloB*) (Raeymaekers et al., 2002), an endoribonuclease (*yloC*), a transcriptional regulator of extracellular matrix genes (*remA*) (Abecasis et al., 2013), guanylate kinase (*gmk*), or Coenzyme A biosynthesis protein (*yloI*) (Nicolas et al., 2012) and others. The exact order of the genes in the operon is *yloB-yloC-remA-gmk-yloH-yloI-priA-defA-fmt-yloM-yloN* and it is transcribed in 3 forms. Expression of this operon is σ^A-dependent. Also it belongs to the sigF regulon (Abecasis et al., 2013; Nicolas et al., 2012; Raeymaekers et al., 2002)

The ω subunit of eubacteria has three conserved α helices (α1, α2, α3). Helices α2 and α3 have five absolutely conserved amino acids (three aa in α2 and two aa in α3) (Kurkela et al., 2021). The structure of ω is shown in Fig. 5. Homologues of ω can be found in bacteria, archaea and eukaryotes. In bacteria, ω (RpoZ) is encoded by the *rpoZ* gene. In eukaryotes, ω has a structural and functional homologue termed RPB6. RPB6 is associated with RNAP I, II and III. In archaea, the ω homologue is known as RpoK (Minakhin et al., 2001). As described in detail below, it is generally a non-essential subunit in bacteria.
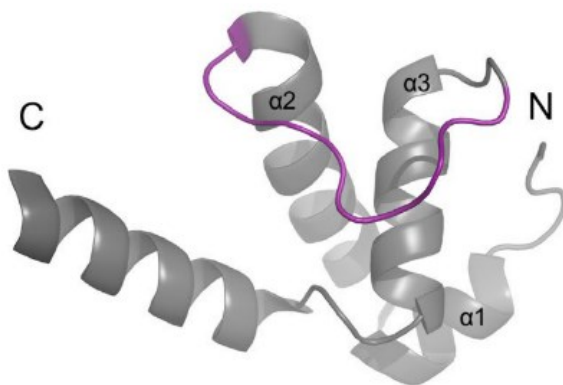
Figure 5. The structure of the ω subunit in *E. coli* with the variable loop connecting α helices α2 and α3 shown in purple. Adapted from (Kurkela et al., 2021).

For comparison of the structure of ω in different species, the structure of ω in *B. subtilis* is shown in Fig. 6. The ω subunit is also shown in complex with RNAP.
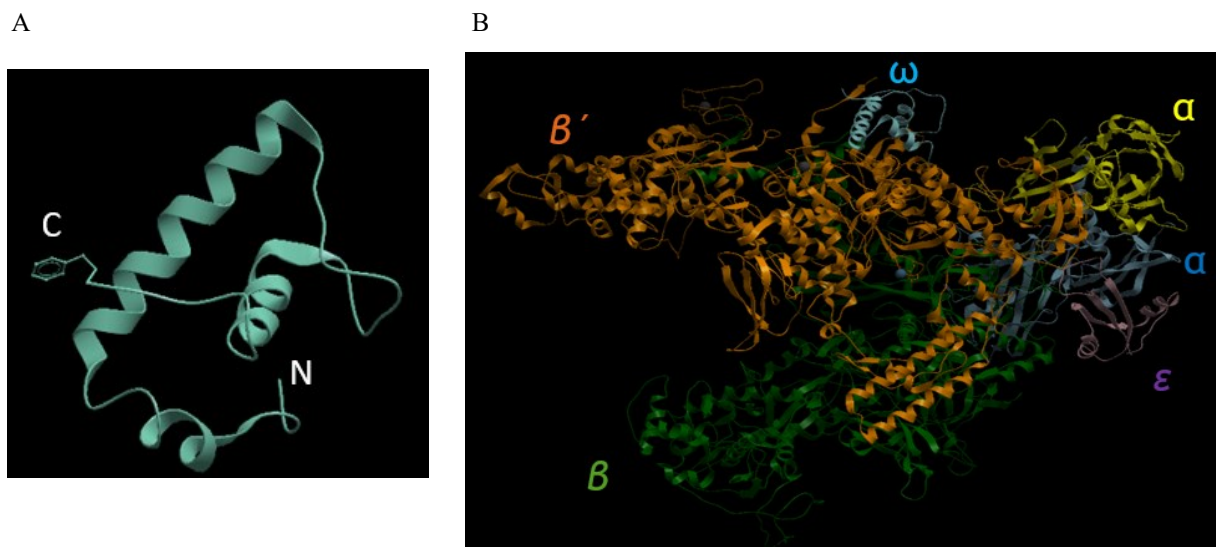
Figure 6. A: The structure of the ω subunit from *B. subtilis*. **B:** The structure of RNA polymerase of *B. subtilis* and ω subunit from *B. subtilis* Adapted and modified from (Newing et al., 2020). Individual subunits are labelled.

Expression and purification of the ω subunit in *E.coli* was first described by Gentry and Burgess, 1990 (Gentry and Burgess, 1990). This procedure was then improved, and the improved protocol was published by Vrentas *et al.*, 2010. This improvement resulted in a better yield from the soluble fraction (no need for denaturation and renaturation) and a more than 99% purity of the ω subunit from *E.coli* (Vrentas et al., 2010).

The ω subunit was studied also by mutagenesis. It was discovered that a point mutation, N60D (substitution of A to G in the codon), causes the inactivation of RNAP by changes in helicity of the ω subunit (Sarkar et al., 2013). Furthermore, Patel *et al.*, 2019, reported purification of the wt ω subunit and the ω subunit with a silent mutation (mutations that do not change amino acids but alter the respective codon). They found that when the RNAP was reconstituted with various silent mutations of ω, this structurally altered the ω subunit due to changes in the protein folding as it was being translated. This then inhibited transcription. The silent mutation in this case for alanine (A82) (codon change from GCC to GCT) (Patel et al., 2019). Purification of the *E. coli* ω subunit and the silent mutant are shown in Fig. 7. However, to my knowledge there are no studies reporting purification of the ω subunit from the Gram-positive *B. subtilis*.
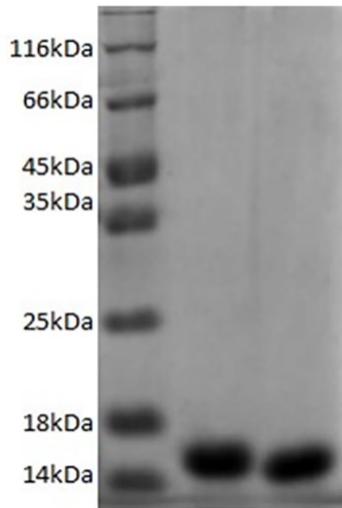
Figure 7. SDS-PAGE after purification of the proteins, wt ω and with the silent mutation ω_9 from *E. coli* (from left to right respectively). Adapted from (Patel et al., 2019)

3.4.1 ω and the stringent response

In *E. coli*, the *rpoZ* gene encoding the ω subunit is in the same operon as the *spoT* gene. The *spoT* gene encodes the pyrophosphatase enzyme, which is responsible for controlling the amounts of the signalling molecules ppGpp and pppGpp. These signalling molecules in turn regulate the stringent response, which is induced under stress conditions such as amino acid starvation (Gentry and Burgess, 1989). Multiple *in vitro* studies using the *E. coli* RNAP demonstrated that the (p)ppGpp molecule interacts with the core of the RNAP. Specifically, it binds at the interphase between the ω subunit and the β' subunit. (Mechold et al., 2013; Ross et al., 2013; Vrentas et al., 2005; Zuo et al., 2013).

Nevertheless, *E.coli* is able to induce the stringent response even without the *rpoZ* gene (Gentry et al., 1991). This is possible because a second binding site for (p)ppGpp molecule exists on RNAP. This second binding site enables the stringent response in the presence of DksA even when the ω subunit is absent (Vrentas et al., 2005). This binding site is situated at the rim of the secondary channel. It is more important for the stringent response than the first binding site and requires DksA for binding of (p)ppGpp (Ross et al., 2016). DksA/(p)ppGpp (DksA in complex with or without (p)ppGpp) influence the transcription initiation. DksA enhances the effect of (p)ppGpp and the effect is larger than the effect of either (p)ppGpp or DksA alone. For example, the decrease in transcription of rRNA genes or the increase in transcription of genes for amino acid biosynthesis and transcription from promoters recognized by the alternative σ^E is caused by the change in the conformation of RNAP and DksA once

(p)ppGpp binds to the RNAP-DksA complex (Gopalkrishnan et al., 2014, 2017; Molodtsov et al., 2018; Paul et al., 2004b, 2005; Perederina et al., 2004; Shin et al., 2021).

Deletion of the ω subunit does not affect the stringent response in Gram-positive *Staphylococcus aureus*. Also the majority of amino acids binding (p)ppGpp in RNAP of Gram-positive bacteria are not conserved and DksA is not present (Ross et al., 2013; Weiss et al., 2017; reviewed in Weiss & Shaw, 2015). In Gram-positive bacteria, the increase in the concentration of (p)ppGpp decreases the level of GTP in the cell by inhibiting guanylate kinase along with other GTP synthesising enzymes (Kriel et al., 2012; Liu et al., 2015). In *Bacillus subtilis*, the transcription activity from the rRNA promoters is regulated indirectly by (p)ppGpp, which affects the level of GTP. GTP is the initiating nucleotide of all rRNA promoters in *B. subtilis* and a major regulator of their activity (Krásny and Gourse, 2004; Natori et al., 2009).

A study by Hood *et al.*, 2016, revealed that the amount of (p)ppGpp can possibly regulate the growth rate in cyanobacterium *Synechococcus elongatus* (an obligatory autotroph). The elevated concentration of (p)ppGpp in the darkness halts growth (Hood et al., 2016). The change in gene expression such as the decrease in transcription of rRNA operons and the increase in transcription of genes for the biosynthesis of amino acids, that are typical of the stringent response, were found in the cyanobacterium S. 6803 (Huang et al., 2002). Furthermore, the cell differentiation in cyanobacteria, that are filamentous, is possibly also modulated by the signalling molecule (p)ppGpp (Zhang et al., 2013). This is due to the fact, that the homolog of RelA/SpoT in *Anabaena* sp. PCC7120 (a nitrogen fixing cyanobacterium) is crucial for the formation of heterocysts and the viability of cells in the absence of combined-nitrogen. In this case, ppGpp has a major role in rebalancing the activity of the metabolism in the cells. However, in these cases it is not clear whether there is a connection between the stringent response and the ω subunit. In cyanobacteria, the protein DksA is absent and GTP is the initiating nucleotide of rRNA operons. Moreover, these operons also have typical -10 and -35 elements (Koskinen et al., 2018). This is similar to the case of *B. subtilis* (Krásny and Gourse, 2004).

3.4.2 ω and stabilization of RNAP

One of the functions of the ω subunit is the stabilization of the RNAP structure and potentially helping with its assembly. In *E. coli*, experiments revealed that the assembly of RNAP starts with the formation of a homodimer containing two α subunits followed by the attachment of the β subunit and, then the β′ subunit joins the complex with the assistance of the ω subunit.

Also according to Ghosh *et al*., 2001 the ω subunit reduces aggregation of the β′ subunit and helps the assembly of RNAP *in vitro*, this suggests a chaperon-like function (Ghosh et al., 2001; Minakhin et al., 2001). However, this role of the ω subunit *in vivo* is challenged by well growing ω-less strains of *E. coli* (Gentry and Burgess, 1989), *Streptomyces kasugaensis* (Kojima et al., 2002)*, S. coelicolor* (Santos-Beneit et al., 2011) and *M. smegmatis*(Mathew et al., 2005). In *E. coli*, the absence of ω can be substituted by GroEL, a chaperone protein, substitutes the function of ω in protecting and recruiting β' during the assembly of RNAP in strains, which are omega deficient *in vitro* (Mukherjee et al., 1999).

To the contrary, deletion of ω in *S. aureus* caused structural changes in RNAP and this resulted in the increased misfolding and degradation of the β` subunit. It also caused changes in the abundance of δ and σ subunits (Weiss et al., 2017).

Furthermore, in *Mycobacterium tuberculosis* Mao *et al.*, 2018 showed that the assembly of the RNAP without the ω subunit was compromised *in vivo* as well as *in vitro* (Mao et al., 2018). The ω subunit is also required for reconstitution of RNAP of *Rhodobacter capsulatus in vitro* (Richard et al., 2003). The location of the β'CTD (C-terminal domain) and the ω loop (connects the α2 and α3 helices of ω) is close in *M. tuberculosis*, but not in *E. coli* and *T. thermofilus*. This closeness and interaction of the ω loop and the β' C-terminal domain in RNAP is essential for *M. tuberculosis*. This was shown by Mao *et al.*, 2018 through the deletion of the β' CTD region. This deletion caused a destabilization during the binding of ω to RNAP, as well as compromising the assembly of the core in *M. tuberculosis*. The alignments of sequences of the ω loop and β' CTD regions reveal that the crucial role of ω might be conserved only in mycobacteria, because these common specific sequences are not conserved and associated in other species for example in *E. coli* and *T. thermophilus*. The alignment of the ω loop sequences and the structural overlay can be seen in Fig. 8. This sheds light on why the ω subunit is so important in RNAP assembly in *M. tuberculosis* but not so much in other species. Furthermore, this is also nicely supported by the fact that the purified ω subunit from *E. coli* or *T. thermophilus* does not rescue the assembly of RNAP in *M. tuberculosis in vitro*. This indicates that the correct interactions between ω and β' are important to maintain the catalytic centre of RNAP active. To achieve this, the ω subunit has to be flexible enough. Also, the interactions between the ω subunit and β' subunit assist the formation and structural integrity of the functional RNAP. Nevertheless, as was stated above the importance of the ω subunit in the

structure of the RNAP varies between various bacterial species (Mao et al., 2018).
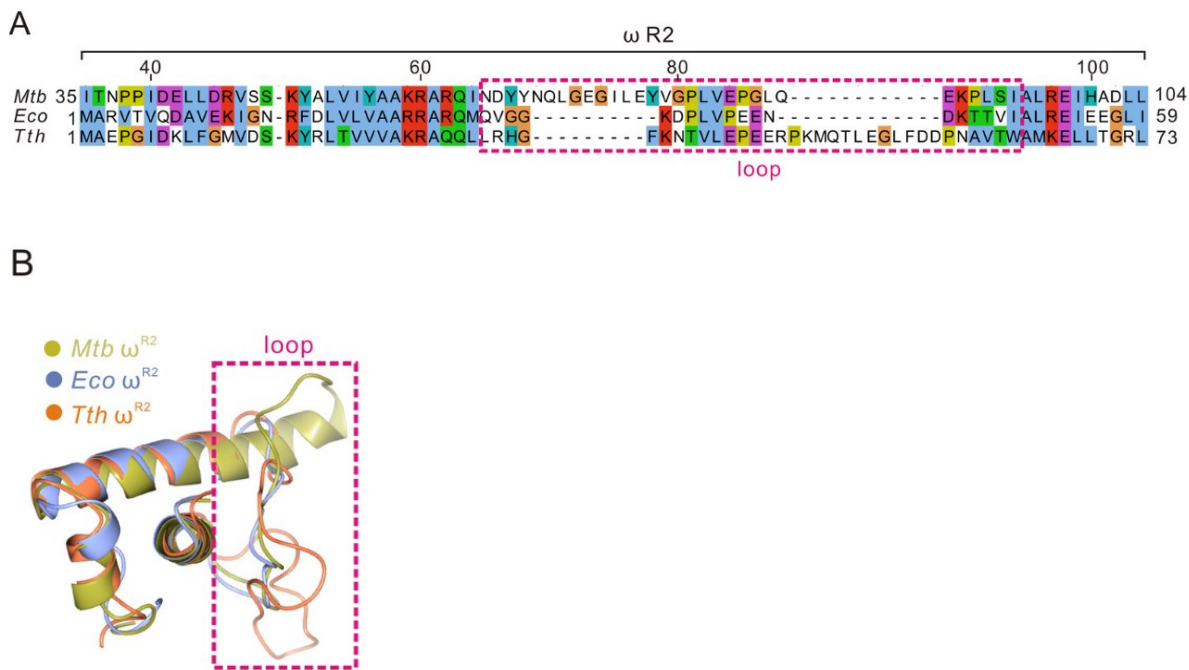
Figure 8. A: The alignment of sequences of the ω R2 regions from *M. tuberculosis*, *E. coli* and *T. thermophilus*. The ω loop is in the dashed red box. The numbering of the amino acids at the top is for *M. tuberculosis* ω. **B:** A structural overlay of the R2 regions of ω from *M. tuberculosis* (in yellow), *E. coli* (in blue) and *T. thermophilus* (in orange). Adapted from (Mao et al., 2018).

3.4.3 The effect of ω on the recruitment of σ factors and selection of promoters

In the past, in *E.coli* it was shown *in vitro* that ω-less RNAP has a lower affinity for DNA than wt RNAP (Mukherjee and Chatterji, 1999). It was also discovered that in an ω-less *E. coli* strain the formation of RNAP-σ^{38} holoenzyme increases, while the amount of RNAP-σ^{70} decreases (Geertz et al., 2011). The primary data and holoenzyme ratios are shown in Fig. 9. Corresponding with the decreased formation of the RNAP-σ^{70} holoenzyme, the *ΔrpoZ E. coli* has a slower growth rate in standard conditions. In the *ΔrpoZ* strain of *E. coli*, the preferred formation of the RNAP-σ^{38} holoenzyme induces upregulation of the σ^{38} regulon. The idea that the ω subunit influences selection of σ factors by the RNAP core is further supported by the fact that overexpression of σ^{70} significantly represses the *ΔrpoZ* phenotype (Geertz et al., 2011).

However, the slower growth rate may be possibly also caused by a polarity effect on the *spoT* gene that is in the same operon as *rpoZ* (Gentry and Burgess, 1989). Furthermore, *ΔrpoZ* knockout cells exhibit defects in biofilm formation in minimal medium, suggesting an effect on selection of σ factors (Bhardwaj et al., 2018).
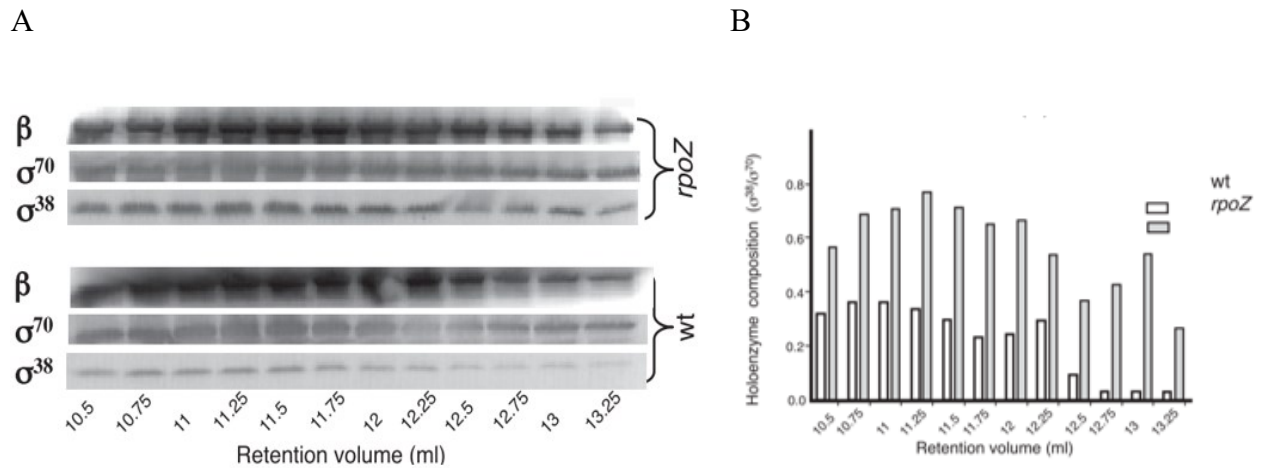
Figure 9. **A:** Fractionation of the wt and the $\Delta rpoZ$ mutant extracts from the whole cell (harvested at OD 1) by size exclusion chromatography. The fractions with the RNAP holoenzyme were subjected to Western blot analysis with antibodies against β, σ^{70} and σ^{38}.**B:** The quantification of the Western blot assays in part A into ratios of the σ^{38}/σ^{70} in the RNAP holoenzymes of wt and $rpoZ$ mutant cells. Adapted from (Geertz et al., 2011).

Various other experiments showed a similar occurrence in cyanobacterium S.6803 (*Synechosystis sp.* 6803) where the amount of the RNAP-σ^A holoenzyme decreased in the $\Delta rpoZ$ strain. This in turn decreased only a specific set of housekeeping genes, which included genes encoding carbon fixation and ATP synthase and carbon concentrating mechanisms (Rubisco, main carboxysome and bicarbonate transporter operons and all of the *ndh* operons). On the other hand, genes encoding proteins that were normally expressed, without any effect, were genes for RNAP, translation machinery, DNA replicating machinery and lastly for photosynthetic light reaction complexes. This is consistent with unchanged growth rate of the mutant strain compared to wt (Gunnelius et al., 2014a). Genes that were upregulated in the *rpoZ* knockout strain were genes with unknown function. Nevertheless, they also included various pilus genes and the heat shock gene *hspA* (Gunnelius et al., 2014b). The RNAP-σ^F holoenzyme transcribes the pilus-genes (Asayama and Imamura, 2008; Bhaya et al., 1999) and RNAP-σ^B holoenzyme transcribes the *hspA* gene (Tuominen et al., 2006). This suggests that, likewise as in *E. coli*, in the absence of the ω subunit the recruitment of alternative σ factors is favoured in comparison with the recruitment of the housekeeping σ^A factor. The data also indicate that the ω subunit has influence on promotor selection by RNAP-σ^A because there is a decrease in the expression of only specific housekeeping genes in the ω knockout strain (Gunnelius et al., 2014a). Interestingly, the promoter regions of the down-regulated genes in the ω knockout strain of *Synechocystis sp.* 6803 contained a typical -10 region, however a conserved -35 region was not detected (Gunnelius et al., 2014a).Some experiments also suggest that the ω subunit

plays a major role in adjusting the cyanobacteria to the amount of available inorganic carbon (Kurkela et al., 2017).

Similarly, as in the previous cases when the ω subunit was knocked out, the Gram-positive *S. aureus* also preferred the formation of a holoenzyme with the main alternative σ factor - RNAP-σ^B (Weiss et al., 2017). The knockout strain also showed multiple changes in the transcriptome. The expression of genes connected with the general stress response increased. However, the cells were able to grow well probably because of the simultaneous increase in expression of some genes of the transcription and translation machinery. This occurred supposedly to overcome the diminished function of RNAP (Weiss et al., 2017). This demonstrated that the relative reduction of RNAP holoenzymes with the vegetative σ factor in *ΔrpoZ* strains did not decrease transcription of all housekeeping genes. On the contrary, the ω knockout strains of *R. capsulatus* (Westbye et al., 2017), *S. coelicolor* (Santos-Beneit et al., 2011) and *M. smegmatis* (Mathew et al., 2006) grew slower than their wt strains even though the changes were not extreme. This could possibly mean that these strains might also recruit the vegetative σ factor with a decreased frequency. The ω subunit is needed for antibiotic production in *S. coelicolor* (Santos-Beneit et al., 2011) and *S. kasugaensis* (Kojima et al., 2002). Moreover, when the ω subunit is deleted the formation of aerial hyphae is defective in *S. kasugaensis* (Kojima et al., 2002) and *S. coelicolor* (Santos-Beneit et al., 2011). The *ΔrpoZ* strains of *S. aureus* (Weiss et al., 2017) and *M. smegmatis* (Mathew et al., 2006) showed defects in biofilm formation. The results from various experiments with different bacteria indicate that, when the ω subunit is deleted the preferred formation of the RNAP holoenzyme is with alternative σ factors rather than with the vegetative σ factor. In contradiction to this, the processes controlled by alternative σ factors in *ΔrpoZ* strains in general showed defects. These defects include biofilm formation, stress acclimation, antibiotic production and colony morphology. To resolve these contradictions will require further research.

Furthermore, Doherty *et al*., 2010 suggests that there could be two populations of RNAP in the cell, one population with ω and another without. This is an interesting possibility as wt RNAP and *ΔrpoZ* knockout RNAP manifest differences in the recruitment of σ factors and also in the recognition of promoters. However, in *E. coli*, this might not play a key role as most of the RNAPs seem to have the ω subunit. The comparison of quantified amounts of ω in *E. coli* and *B. subtilis* is shown in Fig. 10. This supports the hypothesis that in *B. subtilis*, GroEL, or other proteins might play a more significant role in maturation of RNAP than in *E. coli*. Furthermore, the recycling factor HelD was suggested to influence the amount of ω associated

with the RNAP. The RNAP$^{\Delta HelD}$ showed a loss of the ω subunit (Doherty et al., 2010; Pei et al., 2020; Wiedermannová et al., 2014).
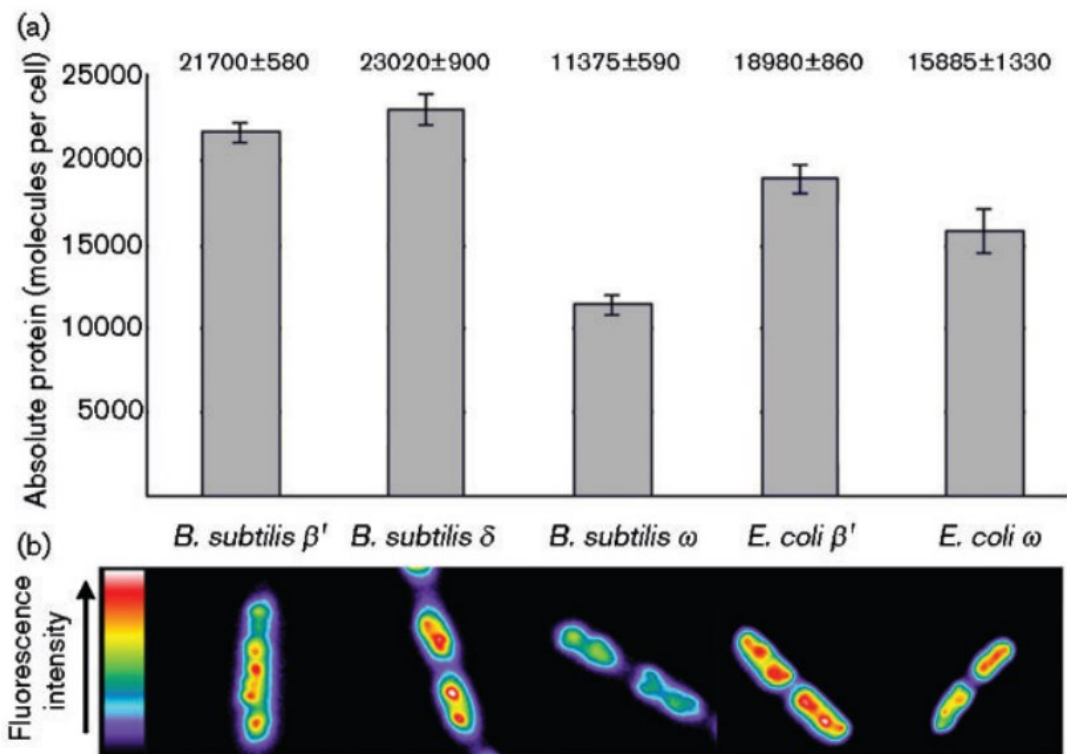
Figure 10. Quantification of subunits β' and ω in *E. coli* and of subunits β', ω and δ in *B. subtilis*. A: Displays absolute quantification of the proteins. **B**: Displays normalized representative micrographs. They are heat-ramped and show relative GFP intensity in the cells. Adapted from (Doherty et al., 2010).

Another important fact is that the normal flexible structure of the ω subunit is essential for the efficient recruitment of all the σ factors (Bhowmik et al., 2017). When the ω subunit in *E. coli* was mutated to be more rigid (dominantly α helical), it associated with RNAP too tightly and negatively affected the initiation of transcription. It decreased the binding affinity of the RNAP core to σ^{70}, σ^{32} and σ^{38} when compared with the binding affinity of the core with the wt unstructured ω subunit.

3.4.4 The ω subunit and DNA topology

As stated above, according to Geertz *et al.*, 2011, the knockout of the ω subunit changes the selection of the σ factor in *E. coli*. In their experiments, they showed that in the *ΔrpoZ* strains there was a noticeable decrease in the amount of the vegetative σ factor, σ^{70}. They also observed a slight increase in the amount of σ^{38}. However, along with the decrease of σ^{70} and increase of σ^{38} they noticed a change in the overall DNA topology *in vivo*. The *ΔrpoZ* strain had generally more relaxed DNA (less negative supercoiling) than the wt strain. In turn, the overproduction

of σ^{70} then increased the amount of negative supercoiling to levels similar to the wt strain. The primary data can be seen in Fig. 11 below. This supports the hypothesis that deletion of the ω subunit causes a global change in DNA topology through the selection of specific σ factors (Geertz et al., 2011).
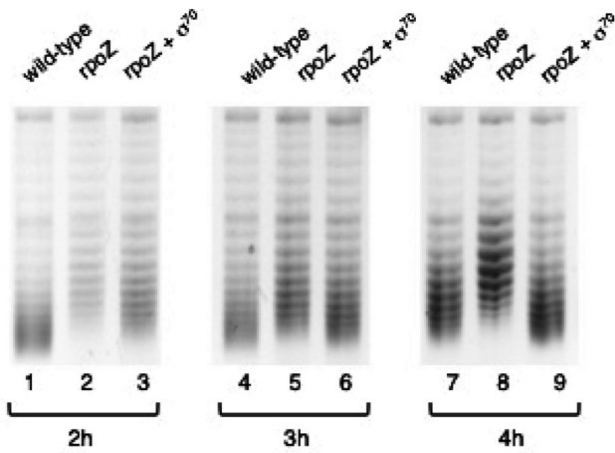
Figure 11. A high-resolution agarose gel electrophoresis of plasmids pACYC184. The plasmids were isolated from the exponential phase of growth from wt and *rpoZ* mutant cells. Samples with the overproduction and without it can also be seen. The tracks labelled as 2h, 3h and 4h correspond to hours from inoculation. 2h and 3h is the mid-log phase while 4h is the late-log phase. The more negative supercoiling the faster the migration on this gel. Adapted from (Geertz et al., 2011).

3.5 Sporulation

Here, I introduce the process of sporulation in more detail, focusing on the σ factors associated with this process as they are the subject of the experimental part of this Thesis. A scheme of sporulation is shown in Fig. 12.

Sporulation is typical for *B. subtilis*. It occurs when the cell is in unhospitable conditions (high temperatures, UV light, low humidity). Once sporulation reaches a specific point (formation of the asymmetric septum) it cannot be reversed, therefore it is a process of last resort and takes places only when all other options and resources are exhausted. This process forms an endospore. It is a very resilient form that can survive in this dormant state for an extremely long time without nutrients(Cano and Borucki, 1995). Endospore formation can also be found in other bacteria. Bacteria from classes Bacilli (aerobic) and Clostridia (anaerobic) are also capable of sporulation (e.g. *B. anthracis, Clostridium difficile*). Furthermore, the master regulator of sporulation, Spo0A, and the sporulation σ factors are according to Hoon *et al.*, 2010 conserved in all spore forming species. The key sporulation factors are σ^A, σ^H, σ^F, σ^E, σ^G,σ^K and along with the master regulator, the phosphorelay and other sporulation transcription

factors regulate sporulation. They help modulate and separate sporulation temporally and spatially(De Hoon et al., 2010; Losick and Stragier, 1992).

3.5.1 Regulation of sporulation

Regulation of sporulation begins with a group of histidine kinases (auto-phosphorylation) that sense environmental change, that then pass on a signal to the master response regulator of sporulation (Spo0A) using a phosphorelay. The phosphate group is consecutively transferred from the histidine kinases (HK). From HK to Spo0B and from there to Spo0F and finally to Spo0A. The phosphorylation of the master response regulator, Spo0A, then in turn activates sporulation (Burbulys et al., 1991).The result of this last phosphorylation is the altered transcription of over 500 genes (Molle et al., 2003). Before the division of the cell, the transcription of *spo0A* is increased by σ^H via a promotor specific for sporulation. Furthermore, phosphorylated Spo0A represses the transcription of AbrB (a repressor of σ^H) and in this way works as an indirect positive regulator of the gene encoding σ^H (*sigH*). The Spo0A-P regulon is made up off high and low threshold genes (Fujita et al., 2005).

Furthermore, σ^H also regulates transcription of the *spoIIAA-spoIIAB-sigF* operon. This operon encodes the anti-sigma factor SpoIIAB, the anti-anti-sigma factor SpoIIAA and finally σ^F, that is specific for the early forespore. σ^F is the first activated regulator that is compartment-specific. It regulates transcription of over 50 genes. *sigG* (σ^G) is one of the genes that is directed by σ^F as well as another gene RsfA(Steil et al., 2005; Wang et al., 2006). RsfA represses and activates various genes transcribed by σ^F. In this way RsfA forms coherent and incoherent feed-forward loops. These loops are common topological motifs in cells, where one gene is regulated by another gene. In turn these two genes together regulate a downstream gene(Alon, 2019; Kashtan et al., 2004). When RsfA works as an activator, it forms together with σ^F a coherent feed-forward loop. This results in delayed and prolonged kinetics of gene expression. On the contrary, when RsfA functions as a repressor, it forms together with σ^F an incoherent feed-forward loop. This then produces a brief pulse of gene expression. SpoVT is the last transcription factor specific for the forespore in the sporulation cascade and together with σ^G forms coherent and incoherent feed forward loops. σ^G is a late forespore specific σ factor. It directs around 100 genes (Steil et al., 2005; Wang et al., 2006).

In the case of the mother cell, the regulation of gene expression is similar. σ^E is responsible for transcription of genes that are specific to the early mother cell. The synthesis of σ^E is dependent on a promoter specific to σ^A. This promoter is upstream of the *spoIIGA-sigE*

operon and is activated by phosphorylated Spo0A. σ^E regulates transcription of various genes, including genes for transcription factors GerR and SpoIIID (Eichenberger et al., 2004; Steil et al., 2005). Both of these factors form feed-forward loops with σ^E. SpoIIID represses and activates some of the genes dependent on σ^E. On the other hand, GerR seems to play only the role of a repressor of genes dependent on σ^E, but is an activator of genes dependent on σ^K (Kuwana et al., 2005). The expression of *sigK* depends on the σ factor σ^E and SpoIIID (Kroos et al., 1989). The gene *sigK* encodes the final σ factor of sporulation σ^K. This factor directs around 150 genes (Eichenberger et al., 2004; Steil et al., 2005). These genes include the gene for GerE. GerE is the last transcription factor specific to the mother cell. Similarly, as SpoIIID, GerE can be a repressor or an activator of transcription depending on the situation and the promoter.
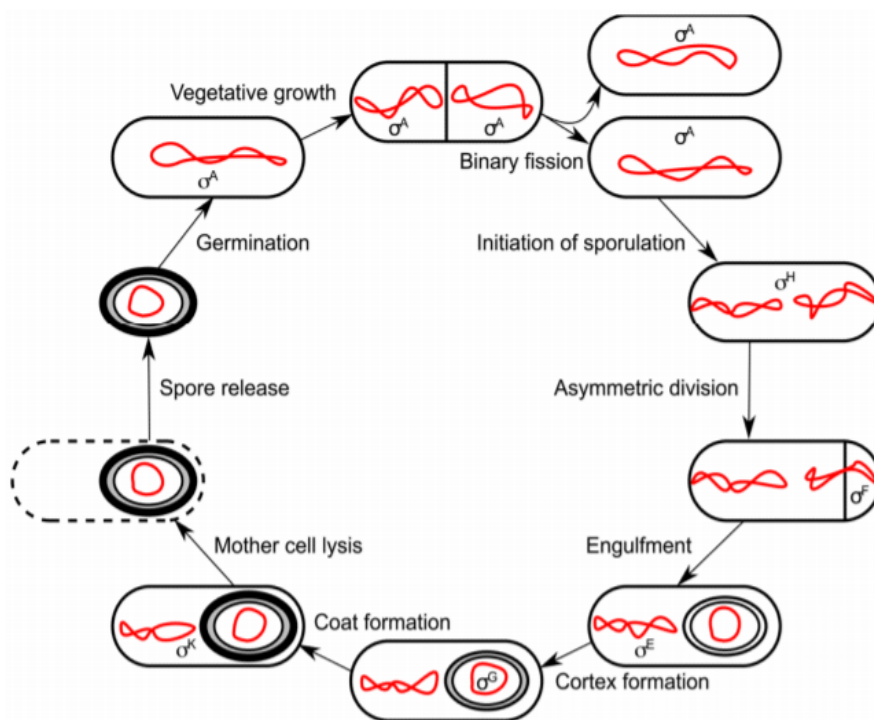
Figure 12. The life cycle and morphological stages of *B. subtilis*. The order and compartmentalisation of each of the σ factors involved in sporulation are displayed above. Throughout the phase of vegetative growth cells divide and form two identical daughter cells. The initiation of sporulation occurs when the cell starves. Inside the sporulating cell, prior to division, we can see that the chromosomes (in red) have their origin-proximal region oriented and anchored towards the cell poles. Next asymmetric division takes place during, which two membrane compartments (separated by a membrane) are formed: a large mother cell and a small forespore. After this division, the rest of the forespore chromosome is translocated into the forespore. When the forespore is engulfed by the mother cell, the forespore is released as a free protoplast inside the mother cell cytoplasm. We can find the cortex (modified peptidoglycan showed in grey) between the two membranes around the forespore. The coat (in black) is assembled around the surface of the forespore. It is a complex structure and consists of at least 70 different proteins. After the mother cells undergoes lysis, the mature spore can then be released. Cells of *B. subtilis* can stay in this dormant form for long periods of time, however spores can again germinate in reaction to various small molecules (sugars or fragments of peptidoglycan, single amino acids) and vegetative growth can restart. Adapted from (De Hoon et al., 2010).

3.5.2 Association of various sigma factors with RNAP during sporulation

It was shown in various publications that the vegetative σ factor (σ^A) has a strong affinity towards RNAP in *B. subtilis*. This was stated because σ^A was present during vegetative growth and in smaller amounts during sporulation. The sporulation σ factors seem to have a smaller affinity to RNAP. This is illustrated by a competition experiment of σ^A and σ^H shown in Fig. 13. (Fujita, 2000; Fujita and Sadaie, 1998a, 1998b; Ju et al., 1999).
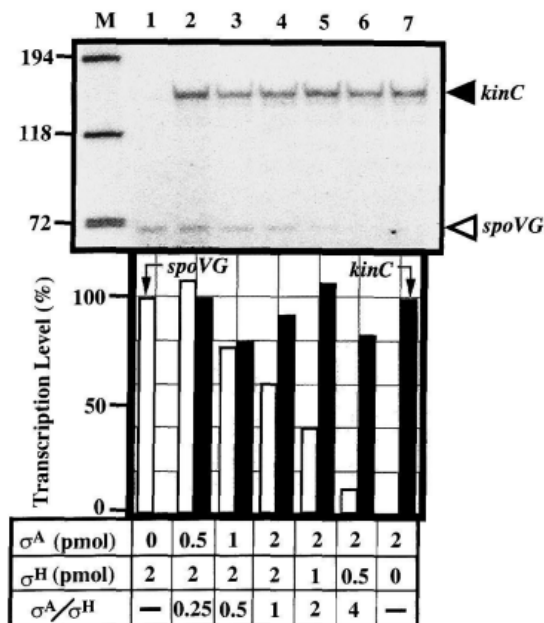
Figure 13. Competition in binding of σ^A and σ^H to the RNAP core. *In vitro* transcription (single round) was performed using a constant amount of the RNAP core and different amounts of each σ factor. The RNAP core (conc. 0.5 pmol) and the different amounts of σ factors (σ^A and σ^H) were mixed in transcription buffer. These mixtures were then incubated for 10 min at 0°C in order to from holoenzymes. Template mixture containing *kinC* (σ^{A}dependent promoter) and *spoVG* (σ^H dependent promoter) with template DNAs was added to the RNAP holoenzymes and incubated for 3 min at 37°C. A substrate mixture containing heparin was added and RNA synthesis took place for 5 min at 37°C. The synthesized RNA was analysed using gel electrophoresis. The band intensity was quantified using a BAS-2000 Bio-Imaging Analyzer and normalized to the maximum level. The intensity is expressed in arbitrary units. The lanes and corresponding concentrations of components are displayed in the table in the Figure. Lane M was used as a size marker and indicates the number of bases. Adapted from (Fujita and Sadaie, 1998a).

However, the association of σ factors with RNAP during sporulation and the mechanism behind the temporal association of these σ factors is still unclear. It has been suggested, that sporulation σ factors might be able to replace each other and, in this way, regulate the association of σ factors with RNAP temporally. According to Ju *et al*, 1999, the σ factors σ^E and σ^K replace σ^A and further σ^K consecutively is needed to replace σ^E (Ju et al., 1999). This theory is also partially supported by Lord *et al*., 1999, where they state that after asymmetric

septation the concentration of the RNAP core is lower than the concentration of σ factors (σ^A and σ^F) and hypothesises that the replacement of σ^A by σ^F might require an additional factor along with the concentration of the σ^E. This factor/event could be for example the activation of an anti-σ^A (Lord et al., 1999). Furthermore, Fujita *et al.*, 1998, also suggested that the replacement of σ^A by σ^H may also require an additional factor or a modification of RNAP core or σ factor (Fujita and Sadaie, 1998a). On the other hand, according to Fujita, 2000, the results suggest that the RNAP core is in excess and the successive σ factors do not have to compete for the RNAP core. Therefore, there is no need for the σ factors to replace σ factors that were present earlier (Fujita, 2000).

3.5.3 Effect of ω and δ on sporulation

A set of experiments done in the Krásný showed that both small subunits (δ and ω) of *B. subtilis* seem to affect sporulation. The deletion of δ had an effect on sporulation and when the ω subunit was also knocked-out, the effect on sporulation was even more significant. In the absence of both these subunits sporulation was practically inhibited (unpublished data, Kálalová). This is displayed in Fig. 14.
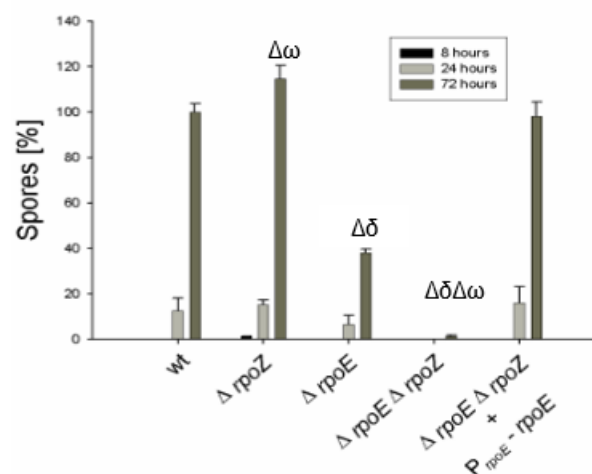
Figure 14. Effect of the deletion of ω and δ on sporulation. Wt- wt RNAP; *ΔrpoZ*-RNAP without the ω subunit; *ΔrpoE*-RNAP without the δ subunit; *ΔrpoEΔrpoZ*- double mutant RNAP without δ and ω; the last bar represents the results after complementation with the δ subunit. Adapted and modified from (unpublished data, Kálalová).

4. Materials and methods

4.1 Chemicals

The chemicals used in this Thesis are listed in Table 1.

Table 1 List of chemicals used in this Thesis.

Chemical	Manufacturer
^{32}P-UTP	M. G. P.
β-mercaptoethanol (ME)	Serva
Agarose for molecular biology	Amresco
Ammonium persulfate (APS)	Sigma
Ampicillin	Biotika
Amylose resin beads	NEB
Boric acid (H_3BO_3)	Penta
Bovine serum albumin (BSA)	Sigma
Bromphenol blue	Dr. G. Gruber & Co.
Calcium chloride ($CaCl_2$)	Lach-Ner
Chloramphenicol	Sigma
Chlorophorm	Penta
Coomassie Brilliant Blue G-250	Serva
Disodium phosphate (Na_2HPO_4)	Lach-Ner
Dithiotreitol (DTT)	Serva
Erythromycin	Serva
Ethanol 96%	Penta
Ethanol 70%	Penta
Ethylenediaminetetraacetic acid (EDTA)	Lachema
Factor Xa	NEB
Formamid	Penta
Gel Red	Biotium
Glycerol	Sigma
iH_2O (Aqua pro injection)	Braun
Imidazol	Sigma
Izopropyl–β–D–thiogalaktosid (IPTG)	Sigma
Kanamycin	Serva
Magnesium chloride ($MgCl_2$)	Penta
Magnesium sulphate ($MgSO_4$)	Lachema
Magnesium sulphate heptahydrate ($MgSO_4 \cdot 7H_2O$)	Penta
Monopotassium phosphate (KH_2PO_4)	Penta
Monosodium phosphate (NaH_2PO_4)	Lachema
NTP (ATP, GTP, CTP, UTP)	Roche
Ni-NTA agarose	Qiagen
NuPAGE^{TM} LDS Sample Buffer (4x)	Invitrogen
Phenol	AppliChem
Phosphate acid (H_3PO_4)	Penta

Phenylmethylsulfonyl fluoride (PMSF)	P - LAB
Polyacrylamide (PAA)	Serva
Potassium chloride (KCl)	Lachema
Shrimp Alkaline Phosphatase (SAP)	NEB
SimplyBlue^{TM} SafeStain	Invitrogen
Sodium acetate (NaCl)	Lach-Ner
Sodium hydroxide (NaOH)	Penta
Spectinomycin	Sigma
Tetrametyletylendiamin (TEMED)	Serva
Tris(hydroxymethyl)aminomethane (Tris-acetate)	Serva
Tris(hydroxymetyl)aminomethane hydrochloride (Tris-HCl)	Sigma
Tryptone	Oxoid
Xylene cyanol	Sigma-Aldrich
Yeast extract	Difco
dNTP (dATP, dCTP, dGTP. dTTP)	Roche

4.2 Enzymes

The enzymes used in this Thesis are listed in Table 2.

Table 2 List of enzymes used in this Thesis.

Enzymes	Manufacturer
Shrimp Alkaline Phosphatase (rSAP)	NEB
T4 DNA Ligase	NEB
Restriction endonuclease *EcoRI*	NEB
Restriction endonuclease *BamHI*	NEB
Restriction endonuclease *NdeI*	NEB
Expand High Fidelity PCR system	Roche

4.4 Media, buffers and solutions

- **10x NEB Buffer 3.1** for *EcoRI*, *BamHI, NdeI* (pH 7.9) NEB

Composition 1x:

- 100 mM NaCl
- 50 mM Tris-HCl
- 10 mM $MgCl_2$
- 100 µg/ml BSA

- **10x Expand High Fidelity PCR System Buffer** (pH 8.9) Roche
  - 500 mM Tris-HCl
  - 220 mM $(NH_4)_2SO_4$
  - 15 mM $MgCl_2$

- **10x DNA ligase Buffer** (pH 7.5) NEB

Composition 1x:
  - 50 mM Tris-HCl
  - 10 mM $MgCl_2$
  - 1 mM ATP
  - 10 mM DTT

- **4x SDS loading dye**

Composition 1x:
  - 125 mM Tris-HCl (pH 8)
  - 10 % glycerol
  - 0.1 % SDS
  - 0.05 % bromphenolblue
  - 2 % β-mercaptoethanol

- **10x rCutSmart™ buffer (for rSAP)** (pH 7.9) NEB

Composition 1x:

  - 50 mM Potassium Acetate
  - 20 mM Tris-Acetate
  - 10 mM Magnesium Acetate
  - 100 μl/ml Recombinant Albumin

- **20x NuPAGE MES SDS Running Buffer** (Invitrogen)

Composition 1x:

  - 50 mM MES
  - 50 mM Tris Base (pH 7.3)
  - 0.1 % SDS
  - 1mM EDTA

- **Dilution buffer (for dilution of proteins)**
  - 50 mM Tris-HCl (pH8)
  - 100 mM NaCl

- 50 % glycerol

- **50× TAE buffer**
  - 50 mM EDTA (pH 8)
  - 2 M Tris-acetate

- **10× TBE buffer**
  - 0.02 M EDTA (pH 8)
  - 0.9 M Tris-HCl (pH8)
  - 0.9 M H_3BO_3

- **LB medium** (pH 7), 1l
  - 10g Tryptone
  - 10g NaCl
  - 5g Yeast extract

- **Bradford reagent**, 1l
  - 50 ml 96% EtOH
  - 100 ml 85% H_3PO_4
  - 100 mg Coomassie Brilliant Blue G-250

- **10× PBS buffer**
  - 27 mM KCl
  - 1.37 mM NaCl
  - 100 mM Na_2HPO_4
  - 18 mM KH_2PO_4

- **Stop solution**
  - 0.05% bromphenol blue
  - 20 mM EDTA (pH 8)
  - 95% formamide
  - 0.05% xylene cyanol

- **2x P buffer**
  - 600 mM NaCl
  - 100 mM Na_2HPO_4
  - 10 % glycerol

- **Storage buffer for ω-His**
  - 50 mM, Tris HCl, pH 8
  - 300 mM NaCl
  - 50 % glycerol
  - 3 mM β-mercaptoethanol

- **Storage buffer**
  - 50 mM Tris-HCl, pH 8
  - 100 mM NaCl
  - 50 % glycerol
  - 3mM β-mercaptoethanol

- **MBP buffer**
  - 20 mM Tris-HCl, pH 8
  - 200 mM NaCl
  - 3 mM β-mercaptoethanol
  - 5 % glycerol

- **Filtered maltose**
  - 10 mM maltose

- **Factor Xa buffer**
  - 20 mM Tris-HCl, pH 8
  - 200 mM NaCl
  - 5 % glycerol
  - 2 mM $CaCl_2$
  - 3 mM β-mercaptoethanol

- **MBP storage buffer**
  - 50 mM Tris- HCl, pH 8
  - 200 mM NaCl
  - 50% glycerol
  - 3 mM β-mercaptoethanol

4.3 Markers

DNA markers:

- GeneRuler Low Range DNA Ladder (25-700 bp) (ThermoFisher Scientific)
- GeneRuler DNA Ladder Mix (100-10000 bp) (ThermoFisher Scientific)
- GeneRuler 1kb DNA Ladder (250-10000bp) (ThermoFisher Scientific)

Protein markers:

- Novex^{TM} Sharp Pre-stained Protein Standard (3.5-260 kDa) (Manufactured by Invitrogen)

4.5 Equipment

4.5.1 Power sources and electrophoresis

PowerPac 3000 Electrophoresis Power Supply (Manufactured by Bio Rad)

➢ Power source for various gel electrophoreses with maximum voltage of 300V.

ENDURO 300V Power Supplies (Manufactured by LABNET INC.)

➢ Power source for various gel electrophoreses with maximum voltage of 300V

Owl^{TM} EasyCast B1A Mini Gel Electrophoresis System (Manufactured by ThermoFisher Scientific)

➢ Horizontal agarose electrophoresis for analysing DNA fragments.

XCell SureLock^{TM} Mini-Cell Electrophoresis system (Manufactured by ThermoFisher scientific)

➢ Vertical electrophoresis for analysis of proteins using Novex SDS-PAGE minigels.

SC20-CDC unit for dual plate vertical electrophoresis (Manufactured by Sigma-Aldrich)

➢ Vertical electrophoresis used for the analysis of RNA fragments marked with ^{32}P radioactive isotope.

4.5.2 Equipment for work with radioactivity

BAS-MS2040 (Manufactured by FUJI)

➢ A cassette containing a phosphor screen for evaluation of radioactive phosphorus ^{32}P gels after *in vitro* transcription.

Amersham^{TM} Typhoon (Manufactured by GE Healthcare)

➢ A gel and blot imaging system used for imaging of radioactive ^{32}P polyacrylamide gel.

GD-4534 (Manufactured by Scie-Plas)

➢ Vacuum dryer used for drying polyacrylamide ^{32}P gels.

Mini 900EP15 Contamination and Radiation Monitor (Manufactured by ThermoFisher Scientific)

➢ A Geiger-Müller radiation counter with sensitivity 0.5 – 2000 cps (portable)

4.5.3 Shakers and thermostats

Mini rocker MR 1 (Manufactured by Biosan)

➢ A shaker with a rocking motion of 5 – 30 oscillations/minute staining of SDS-PAGE protein gels.

Multifunctional Shaker PSU 20 (Manufactured by Biosan)

➢ Adjustable shaker with options for reciprocal/orbital shaking or vibrations.
➢ Rotations 20-250 rpm.

Bio RS-24 Mini-Rotator (Manufactured by Biosan)

➢ Rotator with vertical rotation.

Horizontal shaker HS250 BS1 (Manufactured by IKA laboratortechnik)

➢ Horizontal shaker with adjustable length of incubation of cell cultures in Erlenmeyer flasks.

➢ Maximum 500 rpm.

Vortex Genie 2 (Manufactured by Scientific industries)

➢ Rotation range: 600 – 3200 rpm

➢ Two modes: continues or touch sensitive

Biological Thermostat BT120 (Manufactured by Lab System)

➢ Temperature range 5-75 °C

➢ Used for the incubation of Petri dishes.

Thermo Shaker Ts 100C (Manufactured by Biosan)

➢ Thermostat with a maximum capacity of 24 x 1.5 ml Eppendorf tubes that enables shaking of samples.

➢ Range of temperature: 24-100°C

➢ Rotations: 250-1400 rpm

Thermostat (Manufactured by Brouwer)

➢ Thermostat for incubation of cultures in Erlenmeyer flasks.

Block Heater SBH 130D (Manufactured by Stuart)

➢ For incubation of Eppendorf tubes.

➢ Temperatures: 24-130°C

➢ Maximum of 36 x 1.5 ml Eppendorf tubes

4.5.4 Centrifuges

Universal 320 R (Manufactured by Hettich)

➢ Centrifuge with cooling and exchangeable rotors.

➢ Rotor 1420-B, maximum speed 21 382xg, maximum of 24x 2 ml Eppendorf tubes.

➢ Rotor 1620-A, maximum speed 9 509xg, maximum of 6x 50 ml cuvettes.

Microfuge 20R (Manufactured by Beckman)

- ➢ Centrifuge with cooling
- ➢ Rotor FA241.5, maximum speed 20 627xg
- ➢ Maximum of 24x 1.5 ml Eppendorf tubes

Avanti J-26XPI (Manufactured by Beckman Coulter)

- ➢ Centrifuge with cooling and exchangeable rotors.
- ➢ Rotor JA-10: maximum speed 17 700xg, maximum of 6x 500ml cuvettes
- ➢ Rotor JA-25.50: maximum speed 45 000xg, maximum of 8x 50ml cuvettes

Allegra X-15R Centrifuge (Manufactured by Beckman)

- ➢ Centrifuge with cooling.
- ➢ Rotor head SX4750A.
- ➢ Maximum speed 5 250xg
- ➢ Maximum of 28x 50ml cuvettes /56x 15 ml cuvettes.

Mini-Centrifuge (Manufactured by Rotilabo)

- ➢ Maximum speed 2000g with a maximum of 6x 1.5 ml Eppendorf tubes.

4.5.5 Other equipment
ÄKTA pure 25L FPLC system

- ➢ For gel chromatography and ionex separation of proteins.

Qubit™ 4 fluorometer (Manufactured by Invitrogen)

- ➢ For measuring concentration of proteins, DNA and RNA.

UV-1601PC UV Visible (Manufactured by Shimadzu)

- ➢ Double beam spectrophotometer with UV and visible light.

KAR-230 (Manufactured by Kartell)

- ➢ A vacuum desiccator.

UVT-20M (Manufactured by Herolab)

➢ Transilluminator for UV irradiation of gels.

NanoDrop^{TM} Lite (Manufacutred by Thermo Scientific)

➢ A UV spectrophotometer for measuring concentrations of DNA, RNA and proteins.

UP200S (Manufactured by Hielsher)

➢ Sonicator with exchangeable probes.

EG 2200 (Manufactured by Kern)

➢ Analytic scales.
➢ Minimum weight 0.01 g and maximum weight 2200g.

ABJ 220-4NM (Manufactured by Kern)

➢ Analytical scales.
➢ Minimum weight 1mg and maximum weight 220 g.

pH/ION 510 (Manufactured by Oakton Instruments)

➢ pH meter.

T100^{TM} Thermal Cycler (Manufactured by BioRad)

➢ Cycler with two thermoblocks for PCR.

KNFLAB (Manufactured by Labport)

➢ Vacuum pump.

Slide A Lyzer Dialysis Cassette (Manufactured by ThermoFischer Scientific)

➢ Dialysis cassette for exchanging protein buffers.

4.6 Vectors

Plasmid pMal-c5x

The plasmid (5 677 bp) contains the maltose binding protein tag (MBP-tag) (42 kDa) and the Factor Xa cleavage site used in the overexpression of ω. It was acquired from NEB. The gene for the ω subunit was inserted between the cleavage sites *NdeI* and *EcoRI*. It also encodes the resistance for ampicillin and includes a T7 promoter and terminator. It was acquired from NEB. The map of the plasmid can be seen in Fig. 15.
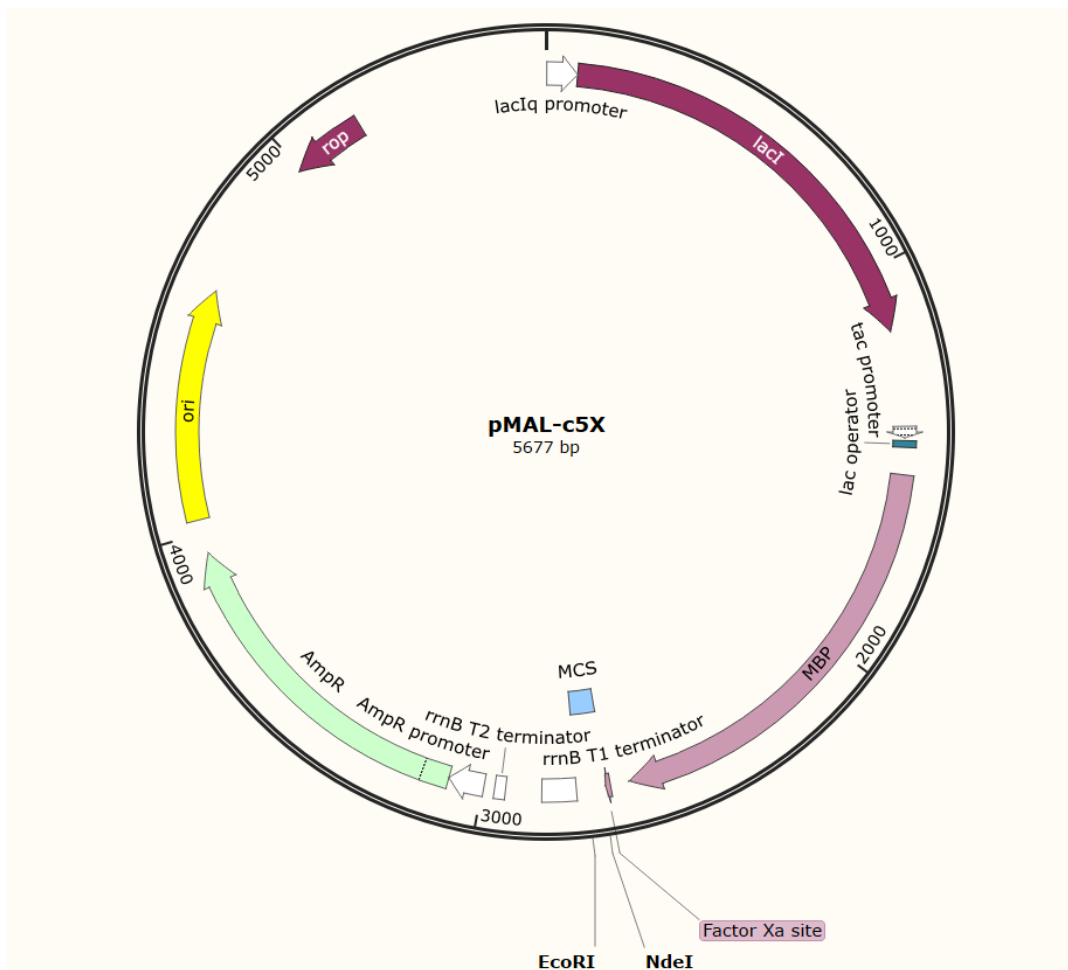
Figure 15. Plasmid map of pMAL-c5x. The map source was SnapGene: pMAL-c5X Sequence and Map (snapgene.com).

Plasmid pGEX-1

This plasmid (4 932 bp) contains the gluthathion-S-transferase tag (GST tag) (26 kDa) used in the overexpression of the ω subunit from *B. subtilis*. It was acquired from M. Fábry. The gene for the ω subunit was inserted between the *EcoRI* and *BamHI* cleavage sites using site-specific restriction endonucleases. Factor Xa cleavage site (found in the primer) was inserted along with the ω subunit. It also contains resistance for ampicillin and the LacI promoter for induction. The map of the plasmid is shown in Fig. 16.
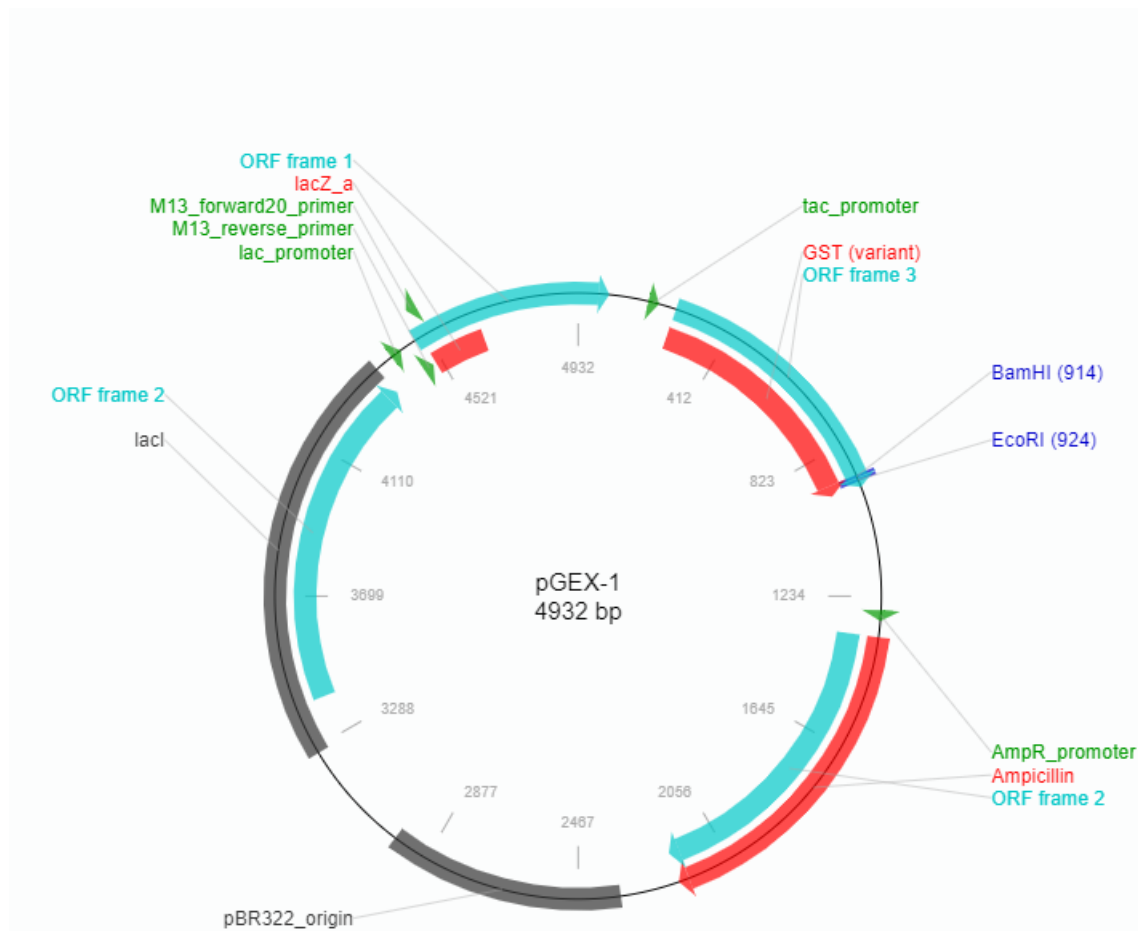
Figure 16. The map of plasmid pGEX-1. The map was acquired from Addgene: Vector Database - pGEX-1.

Plasmid pET-22b

Plasmid pET-22b (5 493 bp) contains a Hexahistidin tag (6xHis tag). The gene for ω subunit was inserted using cleavage sites *XhoI* and *NdeI*. The antibiotic resistance encoded is for ampicillin. The plasmid contains T7 promoter. The map of the plasmid is shown in Fig. 17.
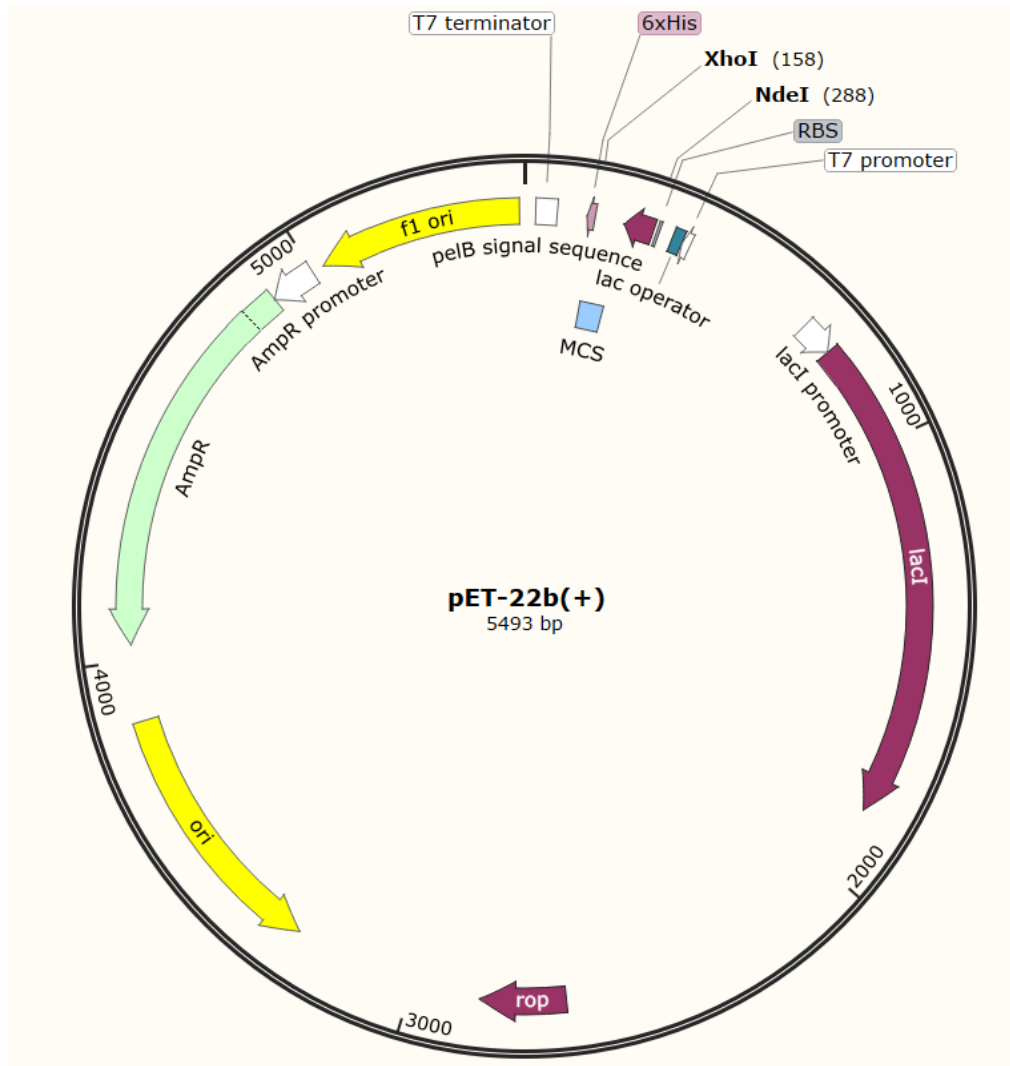
Figure 17. Map of plasmid pET-22b. Source SnapGene: pET-22b(+) Sequence and Map (snapgene.com).

Plasmid p770

This plasmid (5 080 bp) long and was acquired from the Richard Gourse lab (Ross et al., 1990). The promoters used in *in vitro* transcription were inserted between the restriction sites *EcoRI* and *HindIII* using restriction enzymes. The promoters are followed by a 150 bp transcript and a terminator. The plasmid contains the origin of replication, the β-lactamase gene that provides resistance to ampicillin and a terminator (intrinsic termination). The map of the plasmid and the sequence where the promoters were inserted is shown in Fig. 18.
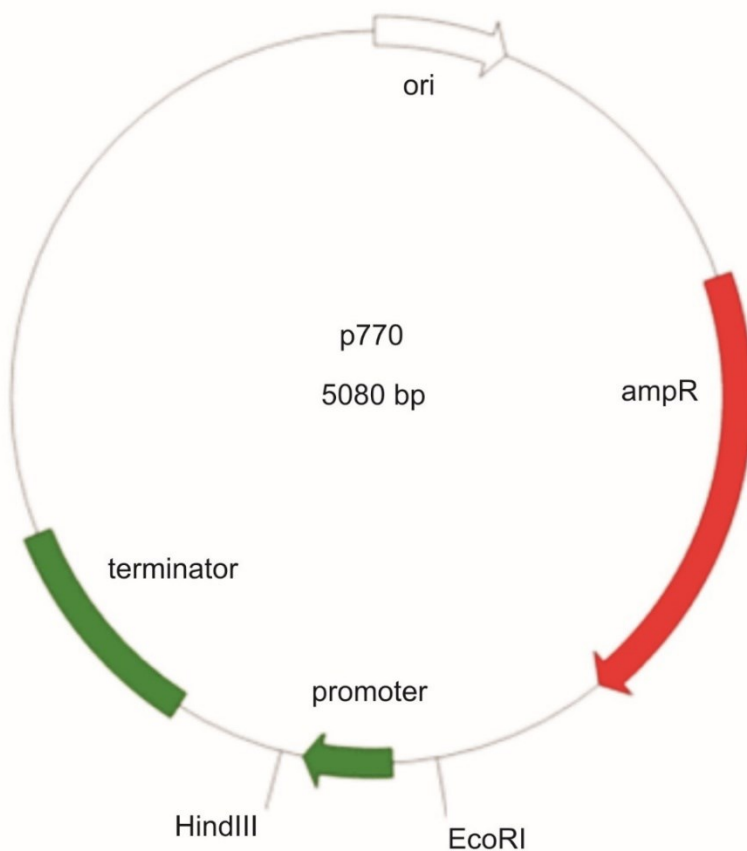
EcoRI   HindIII
GAATTCTCATGTTTGACAGCTTATCATCGGAGCTCTCGAGTCTAGAATCGATCCCGGG**AAGCTT**GG
GTCCCACCTGACCCCATGCCGAACTCAGAAGTGAAACGCCGTAGCGCCGATGGTAGTGTGGGGTCT
CCCCATGCGAGAGTAGGGAACTGCCAGGCATCAAATAAAACGAAAGGCTCAGTCGAAAGACTGGG
CCTTTCG**TTTT**
              Terminator

Figure 18. Map of plasmid p770. Map of the plasmid p770. The detailed sequence where insertion took place is shown below the map. The map was constructed in the program SnapGene Viewer available at https://www.snapgene.com/snapgene–viewer/.

4.7 Promoters

The promoters used in this Thesis were P*veg*, *rrnB* P1, P*spoIIQ*, P*katX* and P*yknT*. P*veg* and *rrnB* P1 are vegetative promoters of *B. subtilis*. The sequences of these promoters are shown in Table 3. P*veg* is a non-ribosomal promoter that is mainly vegetative but is expressed also during sporulation and is σ^A-dependent (Fukushima et al., 2003). The *rrnB* P1 promoter is a ribosomal promoter also σ^A-dependent and initiated by GTP (Krásný and Gourse, 2004; Natori et al., 2009). P*spoIIQ*, P*katX* and P*yknT* are sporulation-related promoters in *B. subtilis*.

P*spoIIQ* is σ^F-dependent, encodes the protein spoIIQ, that is responsible for the encasement of the forespore by the spore coat (McKenney and Eichenberger, 2012). P*katX* is σ^F-dependent and encodes a catalase. It is expressed at early stages of sporulation in the forespore (Wang et al., 2006). P*yknT* is σ^E-dependent, encodes a spore coat protein (cse15) and is expressed at early stages of sporulation in the mother cell (McKenney and Eichenberger, 2012; Steil et al., 2005).

Table 3 List of promoter sequences.

Promoter	Sequence	Source
P*veg*	-35　　　　　　　　　　　　　　　　-10　　　　+1 TAT**TTGACA**AAAAATGGGCTCGTGTTG**TACAAT**AAATGT**G**	(Helmann, 1995)
rrnB P1	-35　　　　　　　　　　　　　　　-10　　　　+1 CTA**TTGCAA**TAAATAAATACAGGTGT**TATATT**ATTAAAC**G**	(Helmann, 1995)
P*spoIIQ*	-35　　　　　　　　　-10　　+1 AGGTT**GTATAT**ATTTTCAGAAAAGTGTT**CAGAATG**TTGCT**G**AGGTGATGAAACAATGAGAGAGGAAG	(Amaya et al., 2001)
P*katX*	-35　　　　　　　　　　　　　　　-10　　　　+1 GC**TGTTTT**AAAATCTTTCCATTCAGGG**AATATTG**TTACC**G**TT	(Bagyan et al., 1998)
P*yknT*	CTCCCCCTGCCAGCAGTACGTTTACATGCTTCATATCATCTCACCTCTAGTTTCGTTAAAAGCATAGCAAAAGC 　　　　　　　　　　　　　　　　　　　　　　　　　-35　　　　　　　　-10 AAAGGCTCAACGCTACTGCTTGTCTGTTTATTAAAGAGGA**ATAGCT**GTTCAGTATTTG**CATATTGT**AGTGTTA +1 ACA**T**CATGAGGGA	(Henriques et al., 1997)

4.8 Bacterial strains

Table 4 List of strains used in this Thesis.

Number	Strain	Source
B. subtilis		
LK1477	MH5636 *rpoC*-His10, *rpoE*:KAN, *rpoZ*:SPC	Lab stock
LK1922	Wt BaSySBio, MLS	Lab stock
E.coli		
DH5α	supE44; ΔlacU169(Φ80 lacZΔM15); hsdR17; recA1; endA1; gyrA96; thi–1; rel–A1	Lab stock
DE3 (BL21)	F– ompT hsdS(rB– mB–) gal dcm λ(DE3)	Lab stock
RLG7023	DE3, pFL31/*Bsu_rpoE*	(De Saro et al., 1995)
LK1365	DE3, pET3/s*igA*	(Chang and Doi, 1990)
LK242	pGEX-1M	M. Fábry
LK700	pET22b/*rpoZ*	Lab stock
LK1177	p770/P*veg*(-38/+1)	(Krásný and Gourse, 2004)
LK1340	DH5α, pMAL-c5x	NEB
LK1425	DE3, pET22b/SigF	(Sudzinová et al., 2021)
LK1495	DH5α, p770/P*spoIIQ*(-251/+9)	(Sudzinová et al., 2021)
LK1496	DH5α, p770/P*katX*(-225/+15)	Lab stock
LK1522	DH5α, p770/P*rrnB* P1(-39/+10)	(Krásný and Gourse, 2004)
LK2580	DH5α, pET22b/*SigE*	(Sudzinová et al., 2021)
LK2593	DH5α, p770/P*yknT*(-150/+10)	Lab stock
LK2594	DH5α, p770/P*spoIIID*	(Sudzinová et al., 2021)
LK2685	DE3, pGEX-1/*rpoZ*	This work
LK2686	DE3, pGEX-1/*rpoZ*	This work
LK2687	DE3, pMAL-c5x/*rpoZ*	This work
LK2688	DH5α, pGEX-1/*rpoZ*	This work
LK2689	DH5α, pGEX-1/*rpoZ*	This work
LK2690	DH5α, pMAL-c5x/*rpoZ*	This work
LK3033	DE3, pMAL-c5x	This work

4.9 Primer

Table 5 List of primers used in this Thesis.

Oligonucleotide number	Use	Sequence
301	Reverse for sequencing pGEX-1	CTCCGGGAGCTGCATGTGTCAGAGG
1318	Forward for sequencing pMAL-c5x	GAAGCCCTGAAAGACGCGC
3398	Forward for PCR into pGEX-1	CGCGGATCCCATCGAAGGTCGTATGTTAGATCCGTCAATTG
3399	Reverse for PCR into pGEX-1 and pMAL-c5x	CGCGCGAATTCTGCTACTATTCGCGGTCTTCCTTTTC
3400	Forward for PCR into pMAL-c5x	CGCCATATGTTAGATCCGTCAATTG

4.10 Bacterial growth

E. coli and *B. subtilis* strains were cultivated in liquid LB medium in Falcon tubes (volume 2-10 ml) and in Erlenmeyer flasks at continuous shaking at 37 °C or at 16 °C (for induction of protein expression). The volume of the liquid culture filled a maximum of 1/3 of the flask. They were also cultivated on LB agar at 37 °C (LB medium with 1.5 % agar).

The overnight cultures were prepared by inoculation of liquid LB media containing specific antibiotic [*B. subtilis* - kanamycin (5 µg/ml), chloramphenicol (2.5 µg/ml) and spectinomycin (100 µg/ml); *E. coli* - ampicillin 100 µg/ml] from the glycerol stock and incubated overnight (16 h) at 37 °C with constant shaking.

4.10.1 *Bacillus subtilis* strain cultivation

The 1l/2l of LB media without antibiotics was inoculated from overnight culture to $OD_{600} = 0.03$ and incubated at 37 °C at constant shaking to $OD_{600} = 1$ [expression of mutant RNAP (LK1477) was not induced, His-tag was integrated into the genome].

4.10.2 *Escherichia coli* strain cultivation for overexpression of proteins

Overexpression of proteins was induced at room temperature (i) or at 16°C (ii).

(i) The 1l/2l/200 ml of LB media with suitable antibiotics was inoculated from overnight culture to OD_{600} = 0.03 and incubated at 37 °C at constant shaking to OD_{600} =0.5-0.6, then overexpression of protein was induced by addition of IPTG (final concentration 0.3 mM) and cultivation continued at room temperature (~24°C) for 3 hours.

(ii) For overexpression at 16°C, 50 ml of LB media with the given antibiotic was inoculated from overnight culture to OD_{600} = 0.03 and this culture was incubated at 37 °C at constant shaking. After 4-5 hours, a larger volume (1l/2l/200 ml) was inoculated from the 50ml culture to OD_{600} = 0.03. This culture was grown until OD_{600} = 0.5-0.6 at 37 °C at constant shaking and then transferred into 16 °C for 1.5 hours also at constant shaking to cool the culture. Then the expression of ω subunit was induced by the addition of IPTG (final concentration 0.05 or 0.005 mM) and cultivation continued overnight.

After cultivation, the OD_{600} was measured, and the bacterial cells were harvested by centrifugation at 6000xg. The pellets were washed with 10 ml 1xP buffer and transferred into Falcon Tubes. Cell suspensions were subsequently centrifuged at 6000xg for 10 minutes at 4°C. The supernatant was discarded, and the pellet was stored at -20 °C.

A 1 ml sample was taken before and after induction for analysis of overexpression. These samples were centrifuged at 13 000xg, at room temperature for 3 minutes. The supernatant was discarded, and the pellet was stored in -20 °C.

4.10.3 Measurement of optical density

The sample of the culture was diluted in ratio of 1:9 with distilled water (100 μl culture + 900 μl H_2O) and the OD was measured on the spectrophotometer UV – 1601PC at the wavelength 600 nm. To get optical density of the culture the measured optical density on the spectrophotometer was multiplied by 10.

4.10.4 Glycerol stock preparation

850 μl of liquid bacterial overnight culture in LB media was mixed with 150 μl of sterile glycerol and stored at – 80 °C, which enables storage of bacterial strains for years.

4.11 Work with plasmid DNA

4.11.1 Midiprep isolation of plasmids

The Wizard Plus Midipreps DNA purification System from Promega was used for the isolation of < 20kbp plasmids.

Cells were grown in 100 ml cultures in LB medium with specific antibiotics at 37 °C overnight (chapter 4.10). The next day, the cells were centrifuged at 4750xg, for 10 min, at 4°C. The supernatant was discarded, and the pellet was resuspended in 3 ml of Cell Resuspension Solution by mixing on a vortex. 3 ml of Cell Lysis solution was added, and the tube was gently inverted. After 2-5 minutes, Cell Neutralization Solution was added, and the tube was gently inverted. This mixture was centrifuged at 27 000xg for 10 min, 4°C. The supernatant was poured into a clean Falcon tube.

A Midicolumn was assembled and connected to a vacuum pump. Wizard Midiprep DNA Purification Resin was well resuspended, and 7.5 ml was added to the supernatant. The vacuum pump was turned on and the mixture of DNA and resin was poured to the Midicolumn. When the mixture passed through the column, 10 ml of Column Wash Solution was added 2 times. Once the solution passed through the Midicolumn the resin was dried by drawing the vacuum for a maximum of 30 additional seconds. The vacuum pump was removed and turned off. The reservoir with the resin was separated from the rest of the Midicolumn using a scalpel or scissors. The Midicolumn reservoir was placed into a 1.5 ml Eppendorf tube and centrifuged at 10 000xg for 2 minutes, at room temperature. The reservoir was then placed into a new Eppendorf tube and 300 μl of preheated iH$_2$O (70°C) was added. This was left to stand for 1 minute and then centrifuged at 10 000xg, 20s, at room temperature. The reservoir was discarded, and the tube was again centrifuged at 10 000xg, at room temperature for 5 minutes. The supernatant was transferred into a new Eppendorf tube.

4.11.2 Phenol-chloroform extraction

To remove any RNAses in the sample for use in *in vitro* transcription phenol-chloroform extraction was performed:

200 μl of iH$_2$O was added to the supernatant (to final volume 500 μl). Next 500 μl of phenol was added and DNA was extracted by rotating on a rotator for 5 min. The mixture was centrifuged at 10 000xg, 5 min, room temperature. The upper phase (aqueous phase) was

transferred to a new Eppendorf tube and 250 µl of phenol and 250 µl chloroform were added. The extraction of DNA and centrifugation was repeated. The upper phase was again transferred to a clean Eppendorf tube. 500 µl of chloroform was added. The mixture was again rotated (DNA was extracted) and centrifuged. The water phase was again transferred into a new Eppendorf tube and the volume of the water phase was measured.

4.11.3 DNA Precipitation

0.1 volumes of 3M CH_3COONa and 2.2 volumes of cooled 96% ethanol were added. This mixture was mixed by inverting the tube and incubated for 10 min at -80°C. The solution was centrifuged at 12 000xg for 20 min at 4 °C. The supernatant was discarded and 50 µl of cooled 70% ethanol was added. The pellet with ethanol was gently vortexed and again centrifuged at 12 000xg, 20 min, 4 °C. The supernatant was discarded. Pellet was dried in a desiccator for 10-15 minutes. The DNA was dissolved in 30 µl iH_2O, overnight at 4 °C. Concentration of DNA was measured using Nanodrop and analysed on an agarose gel.

4.11.4 Restriction analysis

The isolated plasmids and PCR products were cleaved. The components in Table 6. were added into a new Eppendorf tube starting with the component with the biggest volume. Last were added restriction enzymes. The total volume of the reaction mixture was 40 µl. The mixture was incubated at 37°C for 3h. A sample was analysed on an agarose DNA gel and the enzymes in the mixture were usually inactivated by incubation at 65°C for 20 minutes. The temperature of inactivation depends on the enzyme. The samples were analysed on a 1 % agarose gel.

The mixture for digestion of the amplified PCR insert was prepared according to Table 6. The mixture was incubated for 1-2 hours at 37°C and then the enzymes were inactivated by incubation at 65°C for 20 min. The final volume was 20 µl.

After cloning was finished a restriction analysis was performed. The restriction analysis involved cleavage of the plasmids isolated using the QIAprep Spin Miniprep kit (Qiagen). The plasmids with the inserted ω subunit were cleaved with one enzyme (Table 7.) and two enzymes (Table 6.) both in final volume 20 µl. The samples were analysed on a 1.5 % agarose gel. The transformation was successful when the insert was cleaved out after cleavage with two enzymes.

Table 6 Plasmid cleavage (final volume 40 μl)

Component	Volume (μl)
Plasmid/insert (2000ng)	
RE(1)	0.8
RE(2)	0.8
Buffer (10x enzyme buffer)	4
iH₂O	

Table 7 Cleavage with 1 restriction enzyme (total volume 20 μl).

Component	Volume (μl)
Plasmid (300-500ng)	3
RE (1)	1
Buffer (10x enzyme buffer)	2
iH₂O	14

4.11.5 Horizontal agarose DNA electrophoresis

This method was used to separate and visualise DNA.

In an Erlenmeyer flask 0.5 g of agarose was melted in 50 ml of 1x TAE buffer using a microwave oven. This resulted in a 1% agarose. This mixture was then cooled, and an intercalation agent (Gel Red) was added in the ratio of 1:10 000 (5μl). After mixing the mixture was poured into a prepared electrophoretic system OWL^{TM}EasyCast B1A and a comb for well formation was added. The mixture was left to solidify for 30 minutes. The system was then filled with 1x TAE buffer to cover the gel and both electrodes. The comb was removed and 5 μl of DNA marker was loaded into the first well. The markers that were used in this thesis were: GeneRuler^{TM} Low Range DNA Ladder, GeneRuler 1kb DNA Ladder (250-10000bp) (Thermo Fisher).

The other wells were filled with samples mixed with a 10x Loading buffer (Takara) in a ratio of 1:10. This system was connected to a power source (PowerPac 3000) at the voltage of 5V/cm³ for ca an hour. The gel was analysed on a transilluminator (UVT-20M) at wavelength 320 nm and documented by Olympus Photocamera with UV filter.

4.11.6 Isolation of cleaved plasmid DNA from agarose gel

 Plasmid isolation was done using QIAquick gel extraction kit (from Qiagen).

A thermoblock was prewarmed to 50°C. The gel was inspected on a UV lamp. The required linear plasmid DNA was cut out form the agarose gel using a sterile scalpel and placed into an Eppendorf tube. The sample was then weighed. 3 volumes of QG buffer were added to

the cut-out gel with plasmid. This means that 900 µl of QG buffer was added when the sample weighed 300 mg. The gel was then melted in 50°C for 10 minutes (or until the whole sample was completely melted). The mixture was mixed using a vortex every 2 minutes. Once the sample melted completely, 1 volume of isopropanol was then added to the melted mixture (300 mg means 300 µl of isopropanol). This mixture was then applied to a QIAquick spin column containing a silica gel membrane placed in a 2 ml collection tube. Only 750 µl of mixture was applied at once and centrifuged at 17 900xg, for 1 min, at room temperature. The liquid that passed through the column was discarded and the collection tube was put back on the column. The remaining mixture was applied to the column and again centrifuged at 17 900xg, for 1 min, at room temperature. The flowthrough was discarded, and the column was again placed back in the collection tube. 500 µl of QG buffer was applied to the QIAquick spin column, the column was centrifuged at 17 900xg, room temperature for 1 minute. The flow-through was discarded. Then 750 µl of PE buffer was added. The column was centrifuged at 17 900xg, at room temperature for 1 minute. The flow-through was discarded, and the column centrifuged again to remove any remaining residues of the PE buffer containing ethanol. DNA was eluted. The column was placed into a new Eppendorf tube and 30 µl of iH$_2$O was applied to the centre of the column. The column was left standing for 1 minute and then centrifuged for 1 minute, at 17 900xg, room temperature. The eluate was analysed on an agarose gel.

4.11.7 Dephosphorylation of cleaved plasmids

Once the plasmid was cleaved and isolated from the gel dephosphorylation of 5' ends of DNA took place. This method is done to prevent self-ligation of the plasmid. The reaction mixture was prepared according to Table 8. Dephosphorylation took place at 37°C for 1 hour. The enzyme was then inactivated by incubation at 65°C for 15 min.

Table 8 Dephosphorylation reaction mixture (Final volume 10 µl)

Component	Volume (µl)
Plasmid	8
rSAP buffer (NEB)	1
rSAP (Shrimp Alkaline Phosphatase) (NEB)	1

4.11.8 Polymerase chain reaction

The polymerisation chain reaction (PCR) was used to amplify the required region for insertion into the cleaved plasmid (the insert). In this case the gene for the ω subunit. The primers that

were used are listed above in the primer section (Table 5). The Expand High Fidelity system from Roche was used.

The PCR reaction was mixed according to Table 9 into PCR Eppendorf tubes. These Eppendorf tubes with the mix were placed into a thermocycler. The DNA region was then amplified using the program in Table 10. The result was analysed on a 1.5 % horizontal agarose electrophoresis. (3 µl of the PCR sample was mixed with 1 µl of Loading Dye and analysed on the gel.)

Table 9 PCR reaction mix for 1 reaction (final volume 50µl)

Component	Volume (µl)
Expand High Fidelity Buffer with MgCl$_2$ (10x)	5
dNTP mix (10mM)	1
Forward primer (concentration 100 pmol/µl)	1
Reverse primer (concentration 100 pmol/µl)	1
DNA polymerase Expand High Fidelity PCR System (3.5 U/µl)	0.75
Chromosomal DNA template (100 ng)	2
iH$_2$O (injection water)	39.25

Table 10 PCR program

Number of cycles	Temperature (°C)	Time (s)
1	95	120
1	95 (denaturation)	15
	56 (annealing)	30
	72 (elongation)	45
5	95 (denaturation)	15
	52 (annealing)	30
	72 (elongation)	45
24	95 (denaturation)	15
	48 (annealing)	30
	72 (elongation)	45
∞	4	∞

4.11.9 Purification of PCR product using QIAquick gel extraction kit (Qiagen)

5 volumes of QG buffer were added to the DNA sample. This means that 235 µl of QG buffer was added when the amount of sample was 47 µl. The sample was then applied onto the QIAquick spin column and centrifuged at 17 900xg, at room temperature for 1 minute. The

flow-through was discarded and the QIAquick spin column was placed back into the collection tube. 750 µl of PE wash buffer was added to the spin column and was centrifuged at 17 900xg, at room temperature for 1 minute. The flow-through was discarded and the spin column was placed back into the collection tube. The spin column was again centrifuged at 17 900xg, at room temperature for 1 minute to remove any residue of the wash buffer. The QIAquick spin column was placed into a new 1.5 ml Eppendorf tube. The DNA was eluted using 30 µl of iH$_2$O. The iH$_2$O was applied to the centre of the QIAquick spin column, left standing for 1 minute and centrifuged at 17 900xg, at room temperature for 1 minute.

4.11.10 Ligation

The ligation reaction was set up according to Table 11. A negative control (the control of self-ligation of the plasmid) was made with all the components except for the insert. Ligation took place overnight (12-16 h) at 16°C.

Table 11 Reaction mix for ligation (final volume 10 µl)

Component	Volume added (µl)
Plasmid (40-100ng)	
T4 DNA ligase (25 U/µl) (NEB)	0,9
T4 DNA ligase Buffer (NEB)	1
Insert at a molar ratio to plasmid 5-10x:1	
iH$_2$O	

4.11.11 Transformation of *E. coli* DH5α and *E. coli* DE3 competent cells

Heat shock transformation was used in the case of *E. coli* (Hanahan, 1983). Competent cells were prepared in the lab.

Competent cells DH5α/DE3 were taken out of the -80 °C freezer and thawed on ice. New Eppendorf tubes with ligation mixtures or plasmid (1 ng - DH5α, 100 ng - DE3) for transformation were placed on ice to cool down and 100 µl of competent cells were added. A control sample was made containing only the competent cells. The mixture was gently mixed and incubated for 30 min on ice. Next the mixture was placed into 42°C for 90" and then incubated for 5 min on ice. 1 ml of LB media without antibiotics was added to each Eppendorf tube and this mixture was incubated at 37°C while shaking for 1 hour. After incubation the

Eppendorf tubes were centrifuged at 13 000xg, for 1 min at room temperature. The supernatant was quickly poured off and the pellet was resuspended in the supernatant that remained inside the Eppendorf tube. The cells were then plated on a dry Petri dish with LB agar containing the required antibiotic. The Petri dishes were then incubated at 37° overnight.

4.11.12 Miniprep isolation of plasmid DNA

Plasmid was isolated using the QIAprep Spin Miniprep kit (Qiagen).

The *E. coli* DH5α cells with the transformed plasmid were cultivated overnight in 10 ml of LB media with appropriate antibiotics (chapter 4.10.2). The next day the culture was cooled on ice and then centrifuged at 5000xg, 5 min, 4 °C. The supernatant was discarded, and the pellet was resuspended in 250 μl of P1 buffer and transferred into an Eppendorf tube. 250 μl of buffer P2 was added and the Eppendorf tube was turned over 4-6x. The mixture was left to stand for 5 min. Then 350 μ of neutralisation buffer N3 was added, and the Eppendorf tube was again mixed by turning over 4-6x. The mixture was centrifuged at 17 900xg, 10 min at room temperature. The supernatant was then transferred onto the QIA prep spin column and was centrifuged at 17 900xg, 1 min, at room temperature. The flowthrough was discarded and 750 μl of PE buffer was added. The column was then centrifuged at 17 900xg, 1 min, at room temperature. The flowthrough was discarded, and the column was again centrifuged at 17 900xg, 1 min, at room temperature in order to remove any remaining PE buffer. The spin column was transferred into a new Eppendorf tube and 30 μl of iH$_2$O was added. The column was left to stand for 1 min at room temperature and then the DNA was eluted by centrifugation at 17 900xg, 1 min, at room temperature.

4.12 Isolation and purification of proteins

In this chapter, isolation and purification of RNAP (ΔδΔω) and the ω subunit is described. The isolation using MBP-tag was inspired by the protocol for purification of plasmid pMAL-c5x using factor Xa from New England BioLabs (NEB). The isolation of RNAP and ω, containing a His-tag that has a high affinity towards nickel ions, was done using Ni-NTA agarose from Qiagen.

4.12.1 Test of the overexpression growth

The overexpression of ω was tested using the 1 ml samples taken before and after induction (from chapter 4.10.2). The pellets ware thawed on ice and resuspended with 500 μl of 1xP

buffer with 3mM β-mercaptoethanol. The samples were then sonicated until the samples cleared. The samples before induction were sonicated 5x10" with 1 minute intervals on ice and the samples after induction were sonicated 10x10" with 1 minute intervals on ice. The samples were then centrifuged at 16 000xg, 10 min, at 4°C. The supernatant was transferred into a new Eppendorf tube and the pellet was then resuspended using 500 µl of 1xP buffer with 3mM β-mercaptoethanol. The supernatant and pellet were then analysed on SDS-PAGE (chapter 4.12.4)

4.12.2 Isolation via MBP-tag

The pellet from 1 l-induced culture was resuspended in 25 ml of MBP buffer by vortexing. The resuspended culture was then sonicated 12x10" with 1 minute pause intervals on ice. This lysate was then centrifuged for 10 min, 27 000xg at 4°C. The supernatant was transferred into a new Falcon Tube.

4.12.2.1 Equilibration of Amylose resin beads

1.2 ml Amylose resin beads was used and washed with 12 ml of MBP buffer and centrifuged at 2000xg, for 3 min at 4°C. The supernatant was then removed using a pipet (a small amount of supernatant was always left in order not to lose any Amylose resin beads). The washing was 1x repeated. This was done to equilibrate the Amylose resin beads to the MBP buffer.

4.12.2.2 Binding and elution

The supernatant from the culture was mixed with the equilibrated Amylose resin beads and incubated for 1-2 h on ice (4°C) with constant shaking. After the incubation the mixture was centrifuged at 2000xg, for 3 minutes, at 4°C and the supernatant was removed. 10 µl of this supernatant was run on an SDS-PAGE. 12 ml of MBP buffer was added to the Amylose resin beads and centrifuged at 2000xg, 3 min, 4°C. This step was repeated 3 more times. Then 11 ml of Xa buffer was added to the beads and this was centrifuged at 2000xg, 4°C for 3 min. The supernatant was then removed. The Amylose resin beads were resuspended with the small amount of buffer left and transferred into a 5 ml Eppendorf tube.

Elution was done by adding 500 µl of Xa buffer with 10 mM maltose. The mixture was gently mixed and incubated overnight at 4°C with gentle rotating. After elution the mixture was centrifuged at 2000xg, 3, min, 4°C. The supernatant was transferred to a new Eppendorf tube (supernatant 1). The Amylose resin beads were washed with 200 µl of Xa buffer and again centrifuged at 2000xg, 3 min, 4°C. The supernatant (supernatant 2) was again transferred to a new Eppendorf tube. Another 200 µl was added to the Amylose resin beads, the mixture was

again centrifuged as before, and the supernatant was transferred to another new Eppendorf tube (supernatant 3).

Supernatants 1, 2 and 3 were centrifuged at 12 000xg, 5 min at 4°C to remove the residual beads and the supernatants without any residual resin were transferred into new Eppendorf tubes. Samples of supernatants were run on an SDS-PAGE and according to the results dialyzed into MBP storage buffer. 5 µl of the used Amylose resin beads were also ran on an SDS-PAGE gel.

4.12.2.3 Cleavage of protein from MBP tag

Factor Xa for cleavage of the MBP tag was added to the supernatants without any residual resin. 8 µl of factor Xa was added to supernatant 1 (500 µl) and 3 µl of factor Xa was added to supernatant 2 and 3 (200 µl each). Cleavage took place overnight at 4°C with gentle rotating. In the morning, 15 µl samples were taken from each supernatant and run on an SDS-PAGE to check cleavage efficiency. Once the cleavage was complete 1mM PMSF was added to each supernatant to inactivate factor Xa. Supernatant 1 was then centrifuged at 15 000xg, 4°C for 5 min and purified using gel filtration on FPLC.

4.12.3 Isolation via His tag

The pellet from 1 L of culture was resuspended in 20 ml of 1xP buffer with 3 mM β-mercatoethanol. The sample was then sonicated 20x 10" with 1 min intervals on ice. The lysate was centrifuged at 27 000xg, for 10 min, at 4 °C. The supernatant was placed into a clean Falcone tube.

4.12.3.1 Equilibration of Ni-NTA agarose

1 ml of Ni-NTA agarose beads was placed into a clean Falcon Tube and washed with 15 ml of 1xP buffer by centrifugation at 2000xg, 3 min, 4 °C. The supernatant was removed. This step was repeated once more.

4.12.3.2 Binding and elution

The supernatant from the culture was added to the equilibrated beads and incubated, 4°C for 1 h 30 min with gentle shaking on ice. A silicone hose was added to a Poly-Prep® Chromatography Column (Bio-Rad) and was placed into an Erlenmeyer flask. The column was preequilibrated with 10 ml of 1xP buffer. Supernatant with the Ni-NTA agarose beads was poured onto the column. The column was then washed with 30 ml of 1xP buffer and

subsequently with 30 ml of 1xP buffer with 30mM imidazole. The protein was then eluted using 1xP buffer with 400mM imidazole (7x0.5 ml fractions or 7x0.2 ml fractions in the case of ω). 7μl samples of each fraction were analysed on an SDS-PAGE gel. Fractions containing the purified protein were according to its purity dialysed into dialysis storage buffer or suitable buffer for gel filtration chromatography (FPLC) for further purification.

4.12.4 SDS-PAGE electrophoresis

SDS-PAGE, a sodium dodecyl sulphate polyacrylamide gel electrophoresis method, was used for separation of proteins according to their molecular weight.

Samples were mixed with 4x NuPAGE SDS sample buffer. The sample was then denatured for 5 minutes at 95°C. The XCell SureLock™ Mini-Cell (Invitrogen) was assembled with a NuPAGE Novex 4 – 12% Bis-Tris gradient gel. (**NuPAGE® Novex 4-12% Bis-Tris gels** (ThermoFisher Scientific) are gradient polyacrylamide gels for protein analysis with 10, 12 or 15 wells.) 1x NuPAGE MES SDS Running buffer was poured into the apparatus. The samples were loaded onto the gel. Also 5 μl of Novex™ Sharp Pre-stained Protein Standard was loaded. The electrophoresis was run at 200 V for 35 min. The proteins were visualised by staining with SimplyBlue™ SafeStain or Coomassie Blue. The disassembled gel was put into a plastic box with 100 ml of distilled water. The gel was microwaved for 1 minute and then put on a shaker with a rocking motion to cool down for 3 minutes. The water was then discarded. This step was repeated 2 more times. 20 ml of SimplyBlue™ SafeStain was added and the gel was microwaved for 45 s. The gel was then placed on the rocker for 5 minutes. SimplyBlue™ SafeStain was discarded, and 100 ml of distilled water were poured into the container and the gel was left to rock on the shaker for 15 minutes. The water was again discarded, and fresh 100 ml od water were added. This gel was then stored in the fridge until it was scanned. Staining with Coomassie Blue follows the same protocol.

4.12.5 Gel filtration chromatography

Gel filtration chromatography was used as an additional step in purification of proteins. The proteins were separated according to their size. The most concentrated fractions of isolated proteins that did not precipitate was selected. The sample was centrifuged at 17 000xg for 5 minutes and then the supernatant was transferred into a new tube. This (0.5 ml) was then loaded using ÄKTA pure 25L on the preequilibrated Superdex 75 column. 0.5 ml fractions of proteins were acquired. These fractions were then analysed on an SDS-PAGE gel and certain fractions

were then dialysed into the storage buffer. The buffer was used according to the protein. Buffers are described in the chapter 4.4.

4.12.6 Dialysis

This method was used to exchange one buffer with another buffer in a protein solution. Slide A Lyzer Dialysis Cassettes were used. These cassettes can have various pore sizes and volumes.

The selected dialysis cassette was placed into a plastic float and hydrated for 5 min in 500 ml of precooled dialysis buffer (4°C). The cassette was then taken out of the buffer and the protein solution was injected inside the cassette using a needle and syringe. After the whole volume of the sample was placed inside the cassette, the air was removed using the syringe. The cassette was then again placed into the plastic float and back into the buffer. A magnetic stirrer was placed in the buffer to enable stirring during dialysis. The sample was dialysed overnight (12-16 h) in the cold room at 4°C. The used dialysis buffer was discarded and replaced with 500 ml of fresh dialysis buffer. Dialysis took place for another 4 hours. The cassette was then taken out of the buffer and the protein solution was removed using another needle and syringe and stored in a new Eppendorf tube.

The buffer used for protein isolation of MBP-tag and ω with MBP tag was MBP buffer. This was then dialysed into MBP dialysis buffer.

When RNAP was isolated 1xP buffer was used and the protein was dialysed into a standard Storage buffer. When ω with His-tag was isolated 1xP buffer was used and was dialysed into Storage buffer for His-tag ω. The Storage buffer for His-tag ω and the standard Storage buffer differ only in the concentration of NaCl, the concentration is higher in the Storage buffer for His-tag ω (300mM). The compositions of the buffers are listed in chapter 4.4.

4.12.7 Measurement of protein concentration

Protein concentration was measured using the Bradford method and also using Qubit.

4.12.7.1 Qubit measurement

Qubit is a fluorometer that determines protein and nucleic acid concentrations using fluorescent dyes that bind specifically to the molecule being measured. The concentration was determined using the Qubit™ Protein Assay Kit. The components were left for 20 min to adapt to room temperature. First working solution was prepared by mixing 199 µl of Qubit working solution

buffer and 1 μl of the Qubit™ Protein Reagent for each sample and each protein standard. This was thoroughly mixed. This mixture was separated into Qubit assay tubes and protein sample/or standard was added, so that the final volume of the contents of each tube after the addition of the sample or Qubit™ protein standard was 200 μl. (1-10 μl of protein samples and 10 μl of protein standards). Each mixture was then mixed by vortexing for 2-3 min and incubated for 15 min and then measured. After incubation the Qubit™ protein standards were first read one by one using the Qubit^{TM} 4 Fluorometer to calibrate it. Then the protein samples were measured on the Qubit^{TM} Fluorometer.

4.12.7.2 The Bradford method

BSA (Bovine serum albumin) was used as a protein standard in this method. The calibration curve was mixed according to Table 12. The protein samples were then prepared and iH$_2$O was added to the final volume 100 μl. The reaction was started by the addition of 900 μl of Bradford reagent and subsequent vortexing. The absorbance was measured after 5 minutes at 595 nm by a spectrophotometer. A calibration curve was made, and the protein concentration was calculated (Bradford, 1976).

Table 12 Calibration curve for measuring protein concentration. BSA stock solution 400 ng/μl.

Sample	BSA (μg)	BSA (μl)	iH$_2$O (μl)
1	0	0	100
2	2	5	95
3	4	10	90
4	6	15	85
5	8	20	80
6	10	25	75

4.12.7.3 Measurement of concentration of the ω subunit

The protein concentration of the ω-His subunit could not be measured using the Bradford method. This was possibly caused by the fact that the ω subunit contains very little aromatic amino acids that are important for the measuring with this method. The aromatic amino acid tryptophane is not present in the ω subunit at all. Also, the low molecular weight of the protein could be a cause. For this reason, the ω subunit had to be measured using Qubit. This method is described in chapter 4.12.7.1.

4.13 *In vitro* transcription

In vitro transcription was used to study the activity of promoters regulated by vegetative σ factors (σ^A) and sporulation related σ factors (σ^E, σ^F) (Sudzinová et al., 2021). 30 ng/µl of DNA template was used except for the ribosomal promoter *rrnB* P1 where 100 ng/µl of DNA template was used. The DNA template was isolated using the Midiprep kit (4.11.1) with Phenol-chloroform extraction (4.11.2). The *in vitro* transcription was catalysed with a double knockout RNAP ΔδΔω (LK 1477) in the presence or absence of δ and ω subunits.

4.13.1 Reconstitution of RNAP with δ and or ω

RNAP was reconstituted first with δ/ω/dilution buffer or with both subunits at 37°C for 15 min. For titrations of ω and δ, the subunits were first serially diluted to required concentrations and then reconstituted with RNAP. The serial dilution of δ and ω and the combinations for reconstitution reactions can be seen in Tables 13 - 16. The serial dilutions were done from the highest concentration to the lowest concentration. Table 16 contains the combination for reconstitution with MBP-ω construct. All reconstitutions were done in dilution buffer.

Table 13 Serial dilation from higher concentration to lower concentration of δ.

	1:0.1563	1:0.3125	1:0.625	1:1,25	1:2,5	1:5	1:10	1:20
final concentration (µM)	**1500**	**3000**	**6000**	**12000**	**24000**	**48000**	**96000**	**192000**
δ of higher concentration (µl)	2	3	4	5	6	7	8	10
Dilution Buffer (µl)	2	3	4	5	6	7	8	0

Table 14 Serial dilution from higher concentration to lower concentration of ω-His

	1:0.125	1:0.25	1:0.5	1:1	1:2	1:3
final concentration (µM)	**1200**	**2400**	**4800**	**9600**	**19200**	**28800**
ω-His of higher concentration (µl)	2	3	4	5	6	10
Dilution buffer (µl)	2	3	4	5	3	0

Table 15 Reconstitution of RNAP with δ/ ω-His /dilution buffer

	RNAP (4.8 µM) (µl)	ω-His (28.8 µM) (µl)	δ (96 µM) (µl)	Dilution buffer (µl)
RNAP	2	-	-	2
RNAP +δ	2	-	1	1
RNAP+ω	2	1	-	1
RNAP+δ+ω	2	1	1	-

Table 16 Reconstitution of RNAP with δ/MBP-ω/MBP/dilution buffer

	RNAP (1.2 µM) (µl)	ω-MBP (24 µM) (µl)	MBP (24 µM) (µl)	δ (24 µM) (µl)	Dilution buffer (µl)
RNAP	2	-	-	-	2
RNAP +δ	2	-	-	1	1
RNAP+MBP-ω	2	1	-	-	1
RNAP+δ+MBP-ω	2	1	-	1	-
RNAP+MBP	2	-	1	-	1
RNAP+MBP+δ	2	-	1	1	-

The reconstitution of the serial dilution of δ/ω was done in the following way: 2 μl of RNAPΔδΔω was reconstituted with 1 μl of the serially diluted subunit δ/ω (Tables 13. and 14.) and with 1 μl of dilution buffer or the other subunit δ/ω. The combinations with the serially diluted subunits were then reconstituted with σ^A as is described below (4.13.2).

4.13.2 Reconstitution with σ factors

This reconstituted RNAP with or without the subunits was then reconstituted with 4 μl of 24 μM σ^A, σ^E or σ^F for another 15 min in 37°C (in the case of MBP experiment σ^A was 3 μM). The final concentration of RNAP was 120 nM and the concentrations of other components of RNAP are listed in Table 17. The final concentration of RNAP used in experiments with MBP-ω was 30 nM and the concentrations of other components of RNAP used are listed in Table 18.

Table 17 Concentrations and components of RNAP (ω-His experiment).

Component	Stock concentration	Final concentration	Ratio of RNAP: subunit
σ factors	24 μM	1200 nM	1:10
δ subunit	96 μM	1200 nM	1:10
ω-His subunit	28.8 μM	360 nM	1:3

Table 18 Concentrations and components of RNAP (ω-MBP experiment)

Component	Stock concentration	Final concentration	Ratio of RNAP:subunit
σ factors	3 μM	150 nM	1:5
δ subunit	24 μM	300 nM	1:10
MBP-ω subunit	24 μM	300 nM	1:10
MBP	24 μM	300 nM	1:10

4.13.3 Master mix preparation

The Master mix was prepared according to Table 19 and contained: 1x transcription buffer (40mM Tris-HCl, pH 8, 10 mM $MgCl_2$, 1mM dithiothreitol (DTT)), 0.1 mg/ml BSA, 150 mM KCl, 200 μM CTP, ATP, GTP and non-radioactive 10 μM UTP and 2 μM radiolabelled [α^{32}P] UTP and 30 ng/μl or 100 ng/μl of diluted DNA template.

Table 19 Master mix calculated for one reaction (final volume for one reaction 9µl)

Component	Volume (µl)
20x transcription buffer	0.45
20 mM CTP (200 µM)	0.1
20 mM GTP (200 µM)	0.1
20 mM ATP (200 µM)	0,1
1 mM UTP (10 µM)	0.1
$\alpha^{32}P$ (2 µM)	0.1
Plasmid 30 ng/µl (P*veg*, P*spoIIQ*, P*katX*, P*yknT*)/ 100 ng/µl (*rrnB* P1)	1
100x BSA	0.1
KCl (150 mM)	1.5
iH₂O	5.45

4.13.4 *In vitro* transcription

The Master mix was pipetted into new Eppendorf tubes (9 µl per Eppendorf tube) and incubated in 37 °C for 5 min. The *in vitro* transcription reaction was initiated using 1 µl of reconstituted RNAP. The reaction took place in for 15 min at 37°C in final volume 10 µl and was stopped by 10 µl of STOP solution. The samples were vortexed and placed on ice. The reactions were analysed using polyacrylamide gel electrophoresis as described in 4.13.5.

4.13.5 Polyacrylamide gel electrophoresis

Vertical Polyacrylamide gel electrophoresis was used to separate RNA transcripts.

First the apparatus was assembled using two electrophoresis glasses. Two spacers were placed on the sides. The glasses with spacers were clamped together and the bottom was tapped with PVC tape.

Second, the polyacrylamide gel solution was prepared according to Table 20. inside a fume hood and mixed gently. The solution was then poured between the glasses and a comb was placed 1 cm deep into the gel. The gel was left to solidify for at least 1 hour.

After gel polymerization the clamps and tape were removed, and the glasses with the gels were placed into the electrophoretic apparatus. 1x TBE buffer was poured between the glasses and on the outside to cover the cathode and anode. The comb was removed, and the wells were rinsed with the 1x TBE buffer using a syringe. Then 10 µl of each sample was loaded into the wells. The apparatus was closed with a lid and connected to a power source at 180 V for approximately 2 hours. The electrophoresis was then disassembled, and the gel was transferred onto a Whatman filter paper and covered with plastic foil. The gel was then dried at 80°C for 1 hour and then left to cool down for approximately 45 minutes. The gel was then

placed into a cassette with a ^{32}P-sensitive screen and left to be exposed overnight. The next day the screen was scanned using Amersham^{TM} Typhoon (GE Healthcare) and results were analysed using programme ImageQuantTL.

Table 20 Components of polyacrylamide gel

Components	Volume
7 % Polyacrylamide	35 ml
10 % Ammonium persulfate	350 μl
Tetrametyletylendiamin (TEMED)	35 μl

5.Results

5.1 Cloning

Constructs for overexpression of the ω subunit were prepared according to chapter 4.11 using plasmids pGEX-1 and pMAL-c5x. The design of the constructs is shown in Fig. 19. Primers 3398 (forward) and 3399 (reverse) (Table 5) were used for PCR amplification of the *rpoZ* insert for the construct with the GST-tag. Primers 3400 (forward) and 3399 (reverse) were used for amplification of the *rpoZ* insert for the construct with the MBP-tag. The amplified inserts are shown in Fig. 20A. The inserts were purified as described in (chapter 4.11.9). The pGEX-1 and pMAL-c5x plasmids were isolated and cleaved (chapter 4.11.1 and 4.11.4). The isolated plasmids pGEX-1 and pMAL-c5x are depicted in Fig. 20B along with the cut out cleaved linear plasmids (chapter 4.11.4) that were then isolated from the gel (chapter 4.11.6). The pGEX-1 plasmid and *rpoZ* insert were cleaved using restriction endonucleases *BamHI* and *EcoRI* (chapter 4.11.4). The pMAL-c5x plasmid and *rpoZ* insert were cleaved using restriction endonucleases *NdeI* and *EcoRI* (chapters 4.11.4). The plasmids were dephosphorylated (chapter 4.11.7) and inserts were ligated into the linear dephosphorylated plasmids (chapter 4.11.10). The ligation mixtures were transformed into *E. coli* DH5α competent cells (chapter 4.11.11). Three colonies from each plate were used for miniprep purification (chapter 4.11.12) and analysed by restriction analysis. Restriction analysis of plasmids obtained from colonies after transformation was carried out in order to check if the selected clones contained the *rpoZ* insert (4.11.4). The result is shown below in Fig. 20C.

The restriction analysis appeared to show that the ligation was successful in all cases. The plasmids were sequenced using primer 301 (reverse) for pGEX-1 clones and using primer 1318 (forward) (primer sequences chapter 4.9) for pMAL-c5x clones. The sequences were then analysed. Validated clones 1 (pGEX-1/*rpoZ*, clone 1) and 5 (pMAL-c5x/*rpoZ*, clone 5) were selected and transformed into *E. coli* DE3 (BL21) for overexpression. Glycerol stocks of constructs in *E. coli* DE3 (BL21) with numbers LK 2685 (pGEX-1/*rpoZ*, clone 1), and LK 2687 (pMAL-c5x/*rpoZ*, clone 5) were made. Glycerol stocks of constructs in *E. coli* DH5α cells were also made according to chapter 4.10.5 under numbers LK 2688 (pGEX-1/*rpoZ*, clone 1), LK 2690 (pMAL-c5x/*rpoZ*, clone 5). List of bacterial strains is in Table 4. The constructs LK 2685 (pGEX1/*rpoZ*) and LK 2687 (pMAL-c5x/*rpoZ*) were used in further experiments.

Figure 19. Visualisation of the constructs with GST-tag and MBP-tag.
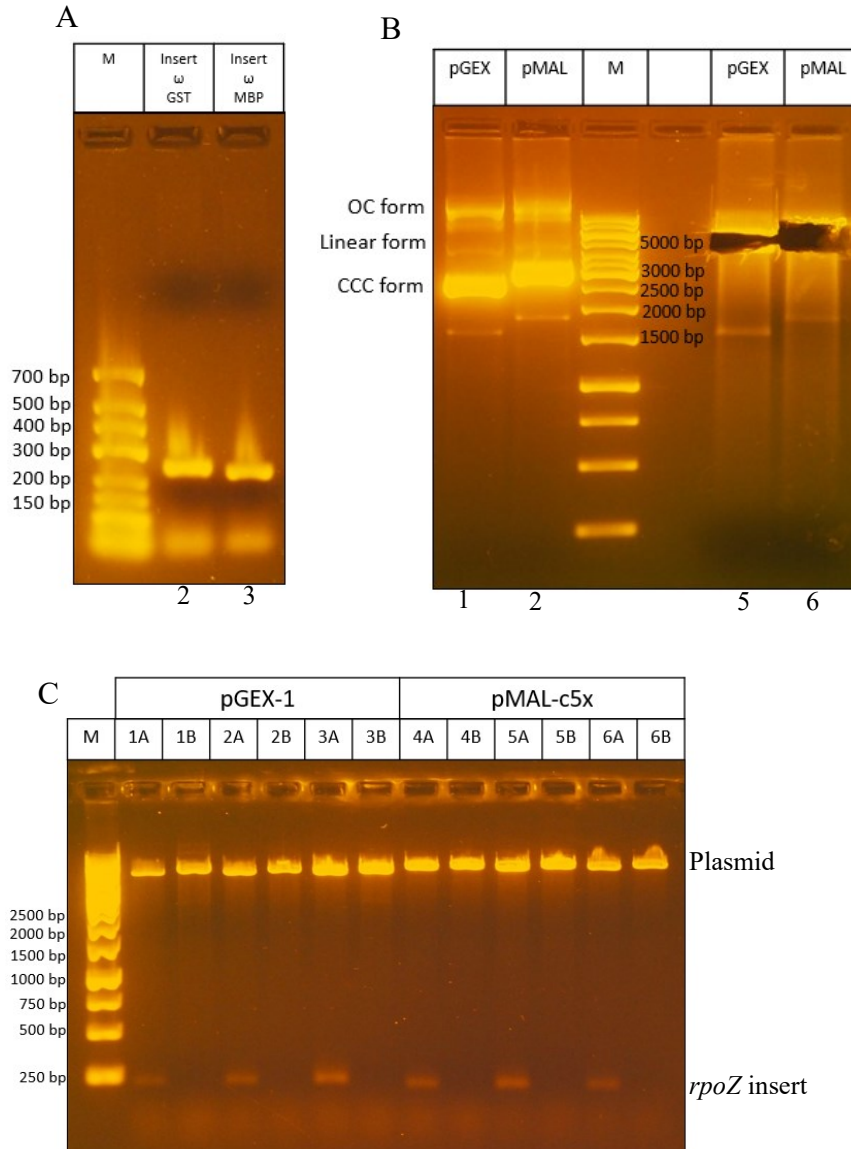
Figure 20. PCR amplification, isolation and restriction analysis of constructs bearing the gene *rpoZ* for the ω subunit. A: PCR amplified inserts. Lane M, 5 μl of the GeneRuler Low range DNA Ladder; Lane 2, the amplified *rpoZ* (204 bp) insert prepared for insertion into pGEX-1; Lane 3, the amplified *rpoZ* (204 bp) insert prepared for insertion into pMAL-c5x. Both samples contain 3 μl of the insert, 7 μl of iH$_2$O and 1.1 μl of 10x DNA loading dye. 1.5 % agarose gel. **B:** Plasmid midipreps. Lane 1, isolated pGEX-1; Lane 2., pMAL-c5x (both samples 0.5 μl of plasmid DNA, 0.8 μl of 10x DNA loading dye and 6.7 μl of iH$_2$O); Lane M, 5 μl of GeneRuler 1kb DNA Ladder. OC-open circular DNA, and CCC is covalently closed circular DNA. The linear form can be seen between these two forms. Lanes 5 and 6 display cut out linear forms of the plasmids pGEX-1 and pMAL-c5x respectively. 1 % agarose gel. **C:** Minipreps of plasmids with *rpoZ* insert (Miniprep chapter 4.10.12) from transformed DH5α cell clones 1,2,3,4,5,6 (from left to right). Samples labelled 1-3 contain pGEX-1 and samples labelled 4-6 contain pMAL-c5x. The first samples (samples A) of the individual clones were always cleaved with two enzymes and the second samples (samples B) were always cleaved with one enzyme. The samples (20 μl) were mixed with 2 μl of 10x DNA loading dye. The smallest band (the band that migrated the longest distance) is the *rpoZ* insert (ca 200 bp). GeneRuler 1kb DNA Ladder (5 μl) is in lane M. 1% agarose gel.

5.2. Overexpression of the ω subunit

5.2.1 Test of overexpression of ω from prepared constructs

Overexpression of the ω subunit was tested using three different constructs: two previously mentioned constructs LK 2685 (pGEX1/*rpoZ*) and LK 2687 (pMAL-c5x/*rpoZ*), and the LK 700 (pET22b/*rpoZ*) construct. The LK 700 construct had been previously constructed in the Krásný laboratory and contains ω with a His-tag. Purification from the overexpression of LK 700 was not successful in the past. Therefore, one of the new constructs was to be tested in isolation of the protein first. The MBP-tag and GST-tag were selected in order to increase the solubility of the protein and increase expression. The constructs MBP-ω (LK 2687) and GST-ω (LK 2685) were grown in 200 ml according to chapter 4.10.2. The overexpression of these constructs was then tested using 1 ml samples according to chapter 4.12.1. When overexpressed at room temperature the culture was induced with 0.3 mM IPTG for 3 h. When the overexpression took place at 16°C the culture was induced with 0.05 mM overnight. Overexpression of ω was seen with all constructs (Fig. 21 and 22).

Furthermore, the construct LK 2687 with the MBP-tag was used further, because the expressed protein was found predominantly in the soluble (supernatant) fraction and less in the insoluble (pellet/inclusion bodies) fraction (Fig. 21 right part). In the case of the construct LK 2685 with the GST-tag, the overexpression was higher in the pellet (in the red rectangle) and lower in the supernatant (Fig. 21 left part). Due to the slightly higher amount of protein with MBP-tag produced at 16°C in comparison with room temperature the protocol for induction at 16 °C was used further on (Fig. 21).

The overexpression of ω with His-tag can be seen in Fig. 22. In this case the strain LK 700 with His-tag, was grown in 1L of LB media according to chapter 4.10.2. The overexpression took place at 16°C, the concentration of IPTG varied. The amount of ω-His was found to be about the same in the supernatant (black frames) and in the pellet (Fig. 22). The overexpression into the supernatant was higher when the culture was induced by 0.05 mM IPTG than when it was induced by 0.005 mM IPTG.
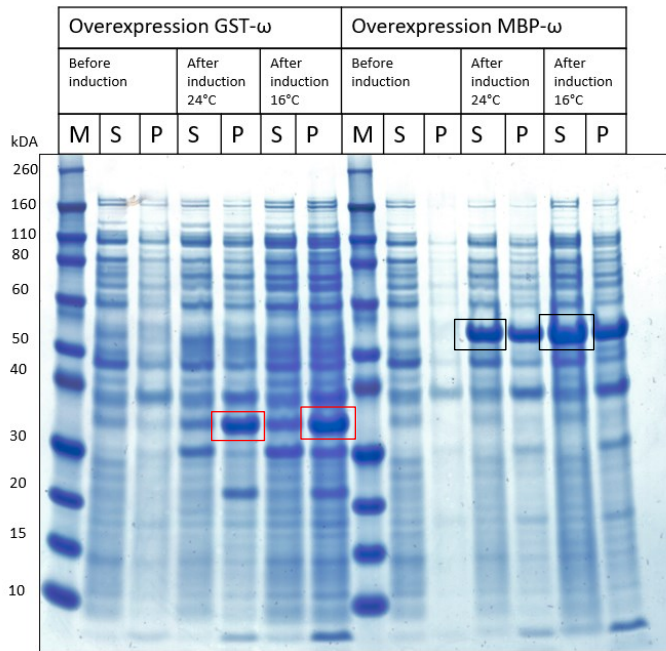
Figure 21. Overexpression of the ω subunit with MBP-tag (LK 2687) and GST-tag (LK 2685). M-Marker Novex^R Sharp Pre-Stained Protein Standard 6 μl. The first 2 samples (from left to right) are always from culture before induction, the next 2 samples are always from cultures after induction at 24°C 0.3 mM IPTG, and the last 2 samples are always from cultures after induction at 16°C 0.05 mM IPTG. The first 6 samples are of overexpression with GST-tag. The other 6 samples are of overexpression with MBP-tag. S stands for supernatant samples (10 μl of sample+ 3 μl of 4xSDS loading dye) and P for pellet samples (3 μl of sample+7 μl of 1xP buffer+3 μl of 4xSDS loading dye). The red rectangles show the ω subunit with GST-tag in the pellet. The black rectangles show the ω subunit with MBP-tag in the supernatant.
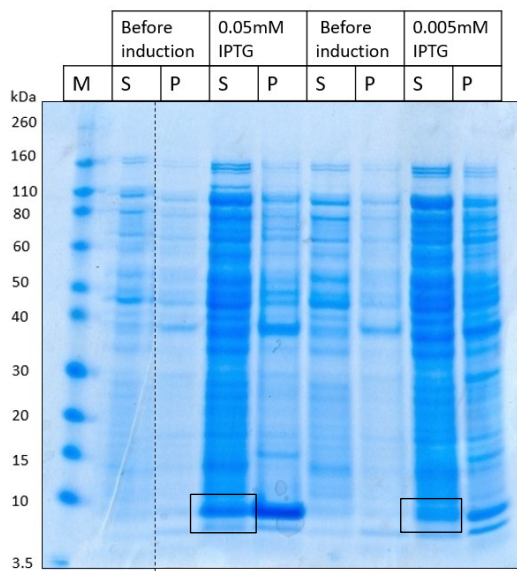
Figure 22. Overexpression of the ω subunit with His-tag using construct LK 700. Lane M contains 5 μl of Novex^R Sharp Pre-Stained Protein Standard. From left to right the first two samples are samples before induction and the next two samples are after induction with 0.05 mM IPTG. The next two samples are before induction and the last two are after induction with 0.005 mM IPTG. or 0.005 mM IPTG. S- supernatant, P-pellet. All lanes contain 20 μl of sample with 5 μl of 4x SDS loading dye. The black rectangles show the ω subunit with His-tag in the supernatant.

5.3. Isolation of the ω subunit, MBP and RNAP

RNAP was isolated using affinity chromatography with Ni-NTA agarose as it contains a His-tag. The ω subunit was isolated in two forms with His-tag and with MBP-tag. The ω-His form was isolated also using affinity chromatography with Ni-NTA agarose. The MBP-ω was isolated using Amylose resin beads. To acquire only MBP, the plasmid pMAL-c5x (LK 1340) was transformed into *E. coli* DE3 (BL21) cells for overexpression of MBP (chapter 4.11.11). Glycerol stock with the number LK 3033 was made. MBP was isolated also using Amylose resin beads (chapter 4.12.2).

5.3.1 Isolation of ω with MBP-tag

After the overexpression was tested the ω subunit with the MBP-tag was selected for its solubility for further purification. LK 2687 was grown in 2L of LB media according to chapter 4.10.3 and then MBP-ω was isolated using Amylose resin beads. The protocol for this isolation is described in chapter 4.12.2. The eluates after isolation of MBP-ω and the result of cleavage by factor Xa (described in chapter 4.12.2.3) can be seen in Fig. 23A. The amount of MBP-ω left in the supernatant after binding to Amylose Resin beads (labelled SPNT in Fig. 23A) was low. The concentration of each eluate (E1, E2, E3) was quite high. However, the amount of MBP-ω that had remained bound on the Amylose Resin beads (labelled AR in Fig. 23A) was also quite high (approximately the same amount as in eluate 2) even after a thorough elution. The cleaved ω subunit is shown in (Fig. 23A). The ω subunit was centrifuged before gel filtration as was described in chapter 4.12.5 and a large pellet was visible. A sample of this pellet and a sample of the remaining supernatant were run on an SDS-PAGE gel (chapter 4.12.4) to verify if the ω subunit was still in the supernatant or aggregated in the pellet. As is shown in Fig. 23B, the ω subunit indeed aggregated in the pellet because only MBP was present in the supernatant. Various modifications of the MBP buffer were done (i.e. increase in salt concentration), but it always led to the aggregation of ω after cleavage.

The isolation of the ω subunit with MBP-tag was successful. However, once the MBP-tag was cleaved off, the ω subunit began to aggregate and could not be used for further experiments. Therefore, MBP-ω was grown and isolated again and isolated MBP-ω (eluate 1, eluate 2 and eluate 3 shown in Fig. 23A) was dialysed without cleavage (chapter 4.12.6) into MBP storage buffer (composition in chapter 4.4) for further *in vitro* experiments. MBP was isolated separately. The MBP-ω protein after dialysis is shown in Fig. 23C. The concentration of MBP-ω was then measured using the Bradford method (4.12.7.2).
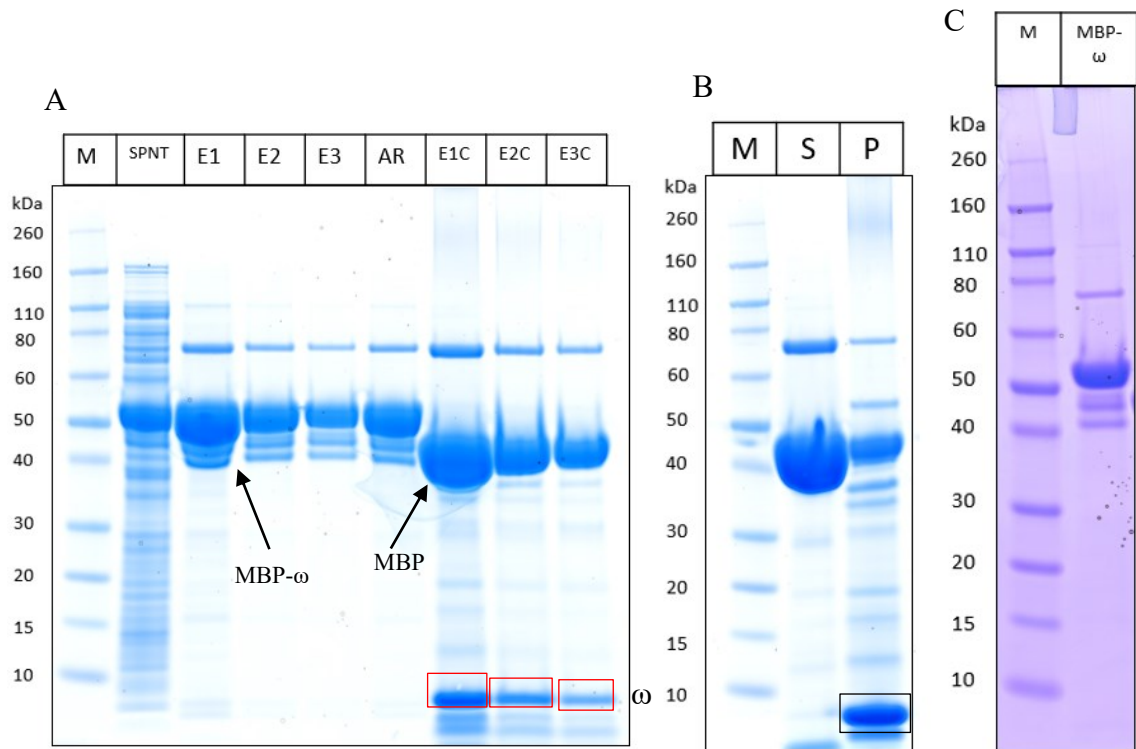
Figure 23. SDS-PAGE of isolation of MBP-ω, cleavage of ω by factor Xa and precipitation of ω in the pellet. MBP-ω after dialysis into storage buffer. A: Gel after elution of MBP-ω and after cleavage of ω. (From left to right) M-Marker Novex^R Sharp Pre-Stained Protein Standard., SPNT-supernatant after binding of MBP-ω to Amylose resin beads, E1-first eluate of MBP-ω, E2-second eluate of MBP-ω, E3-third eluate of MBP-ω, AR-amylose resin beads after elution. The last three lanes E1C, E2C, E3C-each eluate of MBP-ω after cleavage with factor Xa. MBP-ω and only MBP are indicated by arrows. The ω subunit is shown in the red frames. **B:** SDS-PAGE of supernatant and pellet after cleavage with factor Xa. M-Marker Novex^R Sharp Pre-Stained Protein Standard. S-supernatant, P-pellet. ω is shown in the black frame, where it aggregated and formed a pellet. **C:** SDS-PAGE gel of MBP-ω after dialysis. M-Marker Novex^R Sharp Pre-Stained Protein Standard. MBP-ω contains protein eluates E1, E2 and E3 with MBP-ω after dialysis. The concentration was 11.27 μg/μl (200 μM).

5.3.2 Isolation of MBP

The procedure for overexpression and isolation of MBP was identical with the procedure for MBP-ω. LK 3033 was grown in 1 L of LB medium (chapter 4.10.2) and the culture was induced with 0.05 mM IPTG for 3 h at room temperature. Overexpression and isolation were done according to chapters 4.10.2 and 4.12.2. The SDS-PAGE gel (chapter 4.12.4) of the isolation of MBP is shown below in Fig. 24A. After the isolation, eluates E1, E2 and E3 with MBP were dialysed together. The result of dialysis is shown in Fig. 24B. The dialysed MBP was then measured by Bradford method (4.12.7.2).
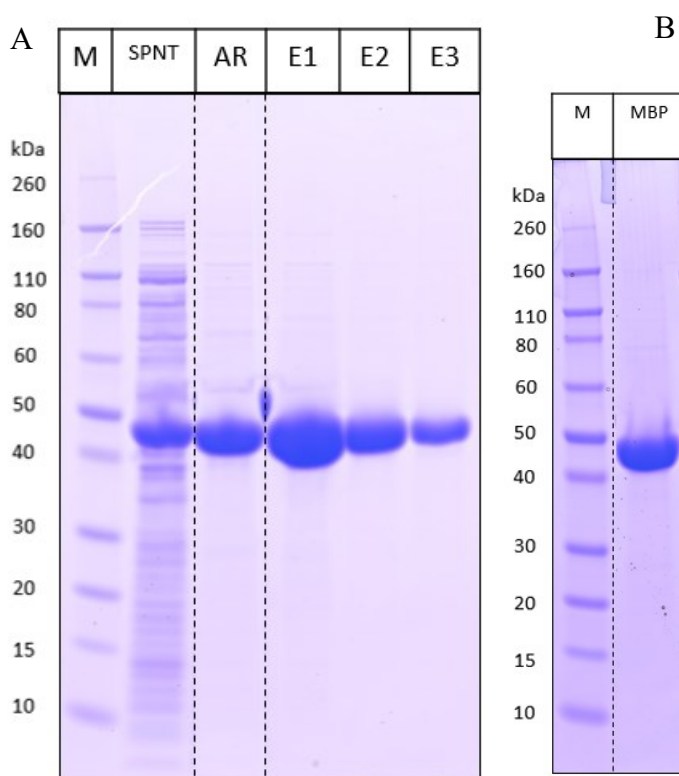
Figure 24. **Isolation of MBP and MBP after dialysis in MBP storage buffer. A:** SDS-PAGE after of the isolation of MBP. M-marker Novex[R] Sharp Pre-Stained Protein Standard, SPNT-supernatant after binding of MBP to the Amylose Resin beads, AR-Amylose Resin beads after elution of MBP, E1, E2, E3-eluates containing MBP. **B:** SDS-PAGE of dialysed MBP. M- marker Novex[R] Sharp Pre-Stained Protein Standard, MBP-The eluates of MBP E1, E2, E3 after dialysis. The concentration was 17.49 μg/μl (400 μM).

5.3.3 Isolation of ω with His-tag

As mentioned above, the ω-subunit aggregated after cleavage with factor Xa. The use of the fused ω protein with the MBP-tag was not ideal, because the MBP-tag is quite large. Therefore, isolation of the ω subunit with His-tag was also performed. LK 700 was grown in 1L of LB media and overexpressed according to chapter 4.10.2. In this case, the culture was induced with 0.05 mM IPTG in 16°C overnight. The isolation was done according to chapter 4.12.3 and in Fig. 25 we can see the 7 eluted fractions (200 μl each) containing the ω-His protein (indicated in the black frame). As is visible in Fig. 25, the isolated fractions contained various contaminations. In order to remove these contaminations, gel filtration chromatography (FPLC) was performed.
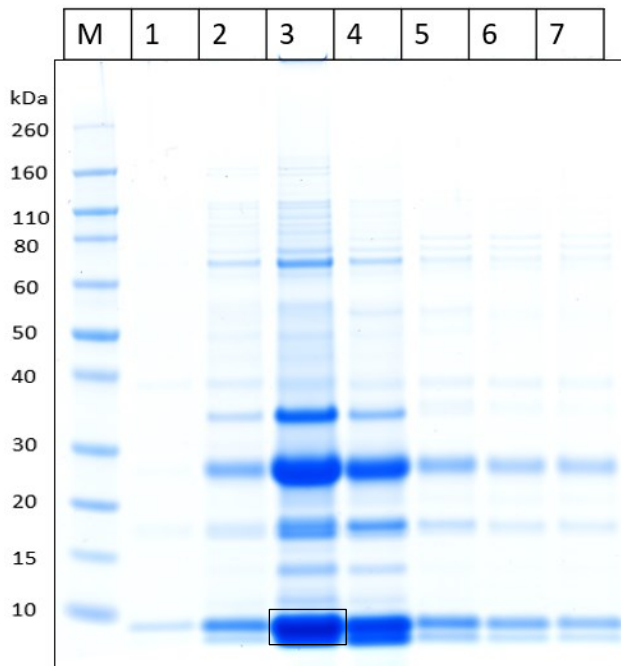
Figure 25. SDS-PAGE showing results of isolation of ω subunit with His-tag. M- marker 5 μl of Novex[R] Sharp Pre-Stained Protein Standard. Lanes 1 to 7 contain samples of each isolated fraction 1-7. All lanes contain 7 μl of each sample and 3 μl of 4x SDS loading dye. The black frame shows the ω-His.

5.3.4 Purification of the ω subunit by gel chromatography

First, the fractions with the highest ω level were combined in a final volume of 500 μl (fractions 3,4 and part of fraction 2). These 500 μl were centrifuged to remove any precipitations and gel filtration chromatography was performed (chapter 4.12.5) Fig. 26 shows the gel filtration

chromatogram. Certain fractions from the gel filtration were analysed on an SDS-PAGE gel (chapter 4.12.4). This can be seen in Fig. 27. Fractions D5 and D6 (Fig. 27) contained the most pure and concentrated ω-His. Therefore, these fractions (D5 and D6) were processed further. The red asterisk in Fig. 26 marks the fractions D5 and D6 in the chromatogram from gel filtration.

To achieve the highest possible concentration of ω-His, a second gel filtration was performed using fractions 2, 5 and 6 (Fig. 25.). A second chromatogram is shown in Fig. 28 and fraction D6 is indicated with the red asterisk. Again, selected fractions (the fractions around the peaks) were analysed on an SDS-PAGE gel (Fig. 29A) to check the presence and the purity of ω-His. Fraction D6 was the most pure and most concentrated and was therefore selected for further use. Fractions D5 and D6 from the first gel filtration were combined with fraction D6 from the second gel filtration and dialysed into Storage buffer for ω-His (composition in chapter 4.4). The final ω-His prep after dialysis is shown in Fig. 29B. The concentration of ω-His after dialysis was measured using Qubit (chapters 4.12.7.1 and 4.12.7.3).
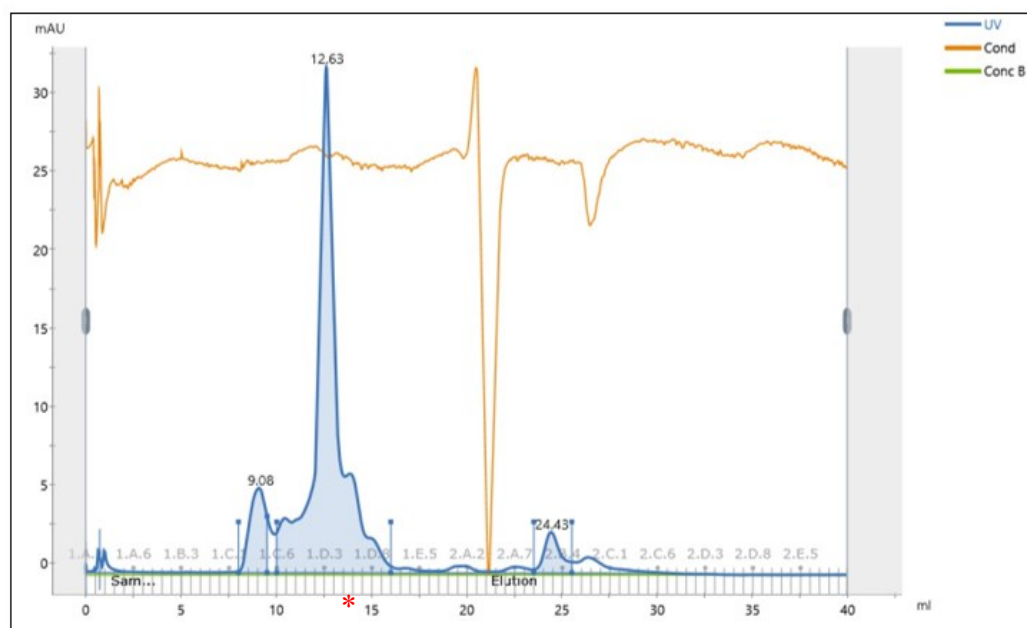
Figure 26. Chromatogram from the first gel filtration of the strongest fractions containing isolated ω subunit with His-tag (Fig. 25). On x axes is the amount of ml collected into fractions. Y axes shows the amount of protein in mAU (absorption units UV λ 280 nm). Cond. stands for conductivity The red asterisk * marks the location of the fractions D5 and D6 that contained the ω-His protein.
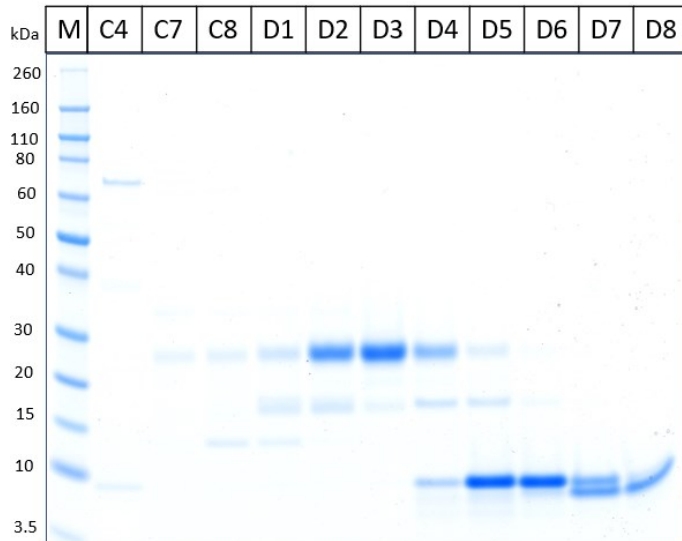
Figure 27. SDS-PAGE protein gel analysis of the first gel filtration according to the chromatogram in Fig. 26. Lane M contains Novex[R] Sharp Pre-Stained Protein Standard. Further lanes C4-D8 contain samples from fraction collected during gel chromatography (18 μl of samples and 4 μl of 4x SDS loading dye).
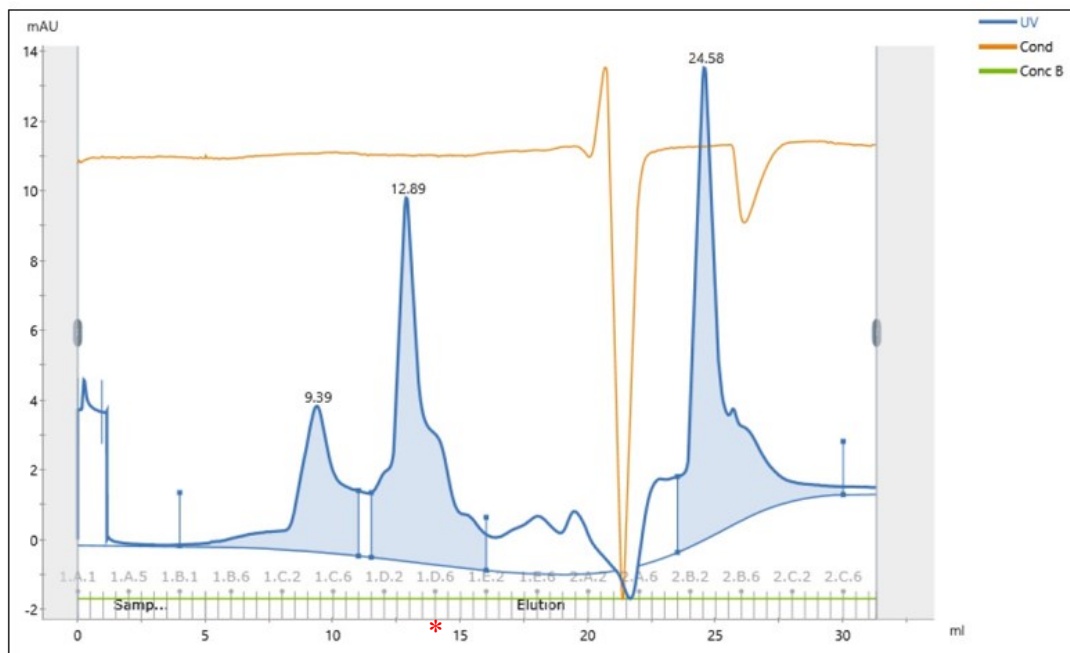
Figure 28. **Gel chromatogram of the second gel filtration of weaker fractions containing ω subunit with His-tag** (Fig.25). On x axes is the amount of ml collected into fractions. Y axes shows the amount of protein in mAU (absorption units UV λ 280 nm). The red asterisk * marks the fraction D6 containing the purified ω-His protein. Cond.- stands for conductivity.
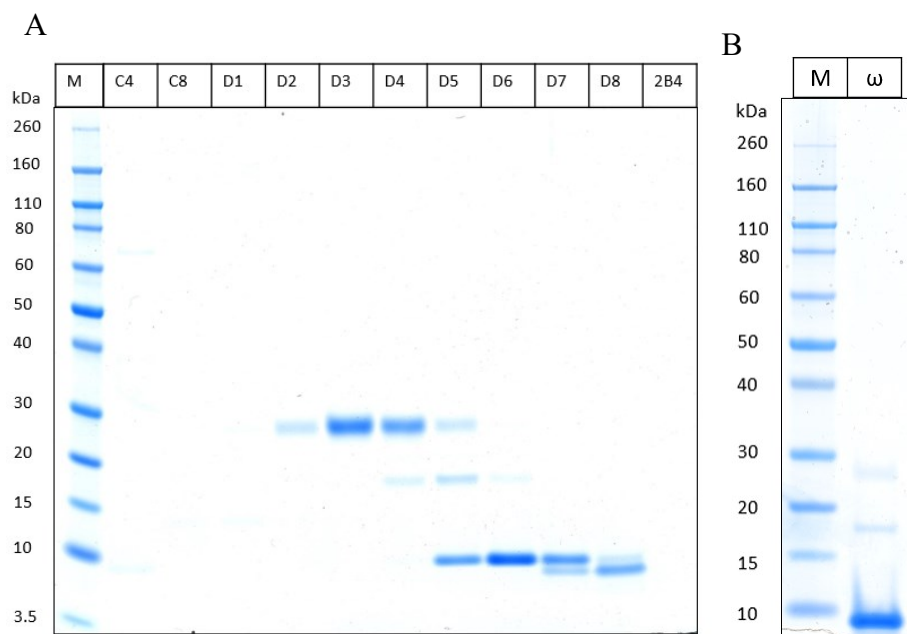
Figure 29. SDS-PAGE of fractions of the second gel filtration and ω after dialysis. A: SDS-PAGE protein analysis of the second gel filtration according to the gel chromatogram in Fig. 28. Lane M contains Novex[R] Sharp Pre-Stained Protein Standard. Further lanes C4-2B4 contain samples from fractions collected during gel chromatography (18 μl of samples and 4 μl of 4x SDS loading dye). **B:** SDS-PAGE ω-His after dialysis. The concentration was 0.310 μg/μl (40.7 μM).

5.3.5 Isolation of RNA polymerase

The strain with mutant RNAPΔδΔω without ω and δ subunits (LK 1477) was constructed in the Krásný lab. RNAPΔδΔω was isolated according to chapter 4.12.3. The isolation was done from 1 L as well as from 2 L of the cultivated cells. The isolation from 2 litres was tested because there was a need for a more concentrated RNAP for the *in vitro* transcription experiments. The fractions (500 μl), obtained after elution from Ni-NTA agarose, from both isolations are shown in Fig. 30A. Both isolations were successful. The isolated RNAPΔδΔω from 2 L was visibly more concentrated than the RNAPΔδΔω isolated from 2 L. The most concentrated fractions (fractions 1 and 2) were in both cases combined and dialysed into Standard storage buffer. The RNAPΔδΔω after dialysis from 1 L and 2 L is shown in Fig. 30B. The concentrations of the dialysed RNAPs ΔδΔω were measured using the Bradford method (chapter 4.12.7.2). The concentration from 2L-culture was more than 2x higher than from 1 L-culture A more concentrated RNAPΔδΔω was successfully isolated.
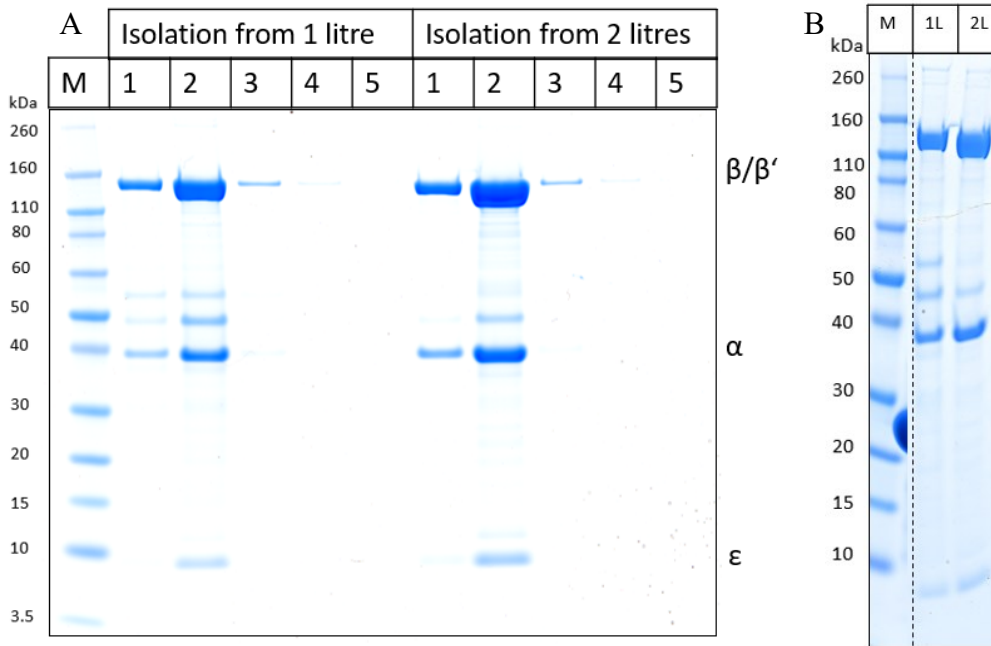
Figure 30. Isolation of RNAP. **A:** First lane M contains 5 µl of Novex[R] Sharp Pre-Stained Protein Standard. The first lanes labelled 1-5 contain samples from isolation from 1 litre of culture, while the second lanes labelled 1-5 contain samples from isolation from 2 l of culture. All samples consist of 7 µl of isolated fraction sample and 3 µl of 4x SDS loading dye. **B:** SDS-PAGE of isolated RNAP after dialysis. M-Marker Novex[R] Sharp Pre-Stained Protein Standard, 1 L-RNAP isolated from 1 L of culture after dialysis, 2 L- RNAP isolated from 2 L of culture after dialysis. The concentration of RNAP isolated from 1 L was 1.73 µg/µl (5.2 µM) and the concentration of RNAP isolated from 2 L was 4.42 µg/µl (13.2 µM).

5.4 *In vitro* transcription

The above mentioned isolated and purified proteins (MBP, MBP-ω, ω-His and RNAPΔδΔω) were tested in *in vitro* transcription experiments. *In vitro* transcription was performed according to chapter 4.13. The RNA transcripts were then visualised on a polyacrylamide gel according to chapter 4.13.5 and quantified using program ImageQuantTL. All the experiments were done with RNAPΔδΔω (LK 1477). This RNAP was selected because it had been previously shown that the deletion of both δ and ω subunit had a major negative effect on sporulation (unpublished data, Kálalová) and I wanted to determine how these subunits influence transcription of the primary as well as sporulation-specific σ factors.

The δ subunit and σ factors were isolated in the lab. In *B. subtilis*, σ[E] (LK 2580) and σ[F] (LK 1425) were grown and isolated according to (Sudzinová et al., 2021). σ[E] is first synthesized as an inactive pro-σ[E] and then is activated by being cleaved by SpoIIGA. Therefore, the pro-σ[E] was shortened according to (Imamura et al., 2011) and only the active σ[E] was cloned (LK 2580).

This σ^E was used in my Thesis. σ^A (LK 1365) was isolated according to (Chang and Doi, 1990). The δ subunit (RLG 7023) was isolated according to (De Saro et al., 1995).

5.4.1 *In vitro* transcription using ω with MBP-tag and His-tag

The first pilot *in vitro* transcription experiment was done to verify the functionality of the isolated proteins and was performed on a σ^A-dependent promoter P*veg*. RNAP was reconstituted with either dilution buffer (composition in chapter 4.2) /δ/MBP-ω or MBP. The MBP was used as a negative control to test whether the MBP-tag itself had any effect on transcription. These combinations were prepared according to Table 16. Furthermore, RNAP was also reconstituted with δ and ω-His (Table 15). The *in vitro* transcriptions were done as described in chapter 4.13 and the results are shown in Fig. 31. The final concentration of RNAP was 30 nM.
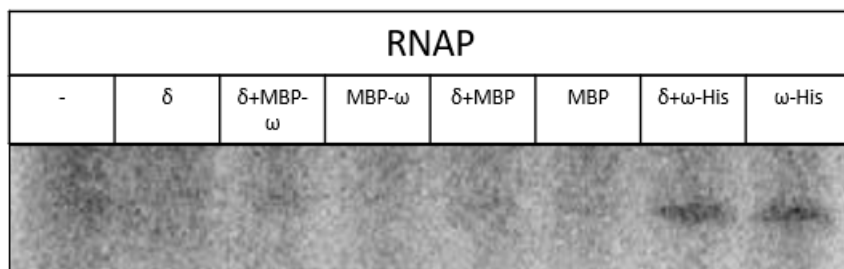
Figure 31. Transcription from the σ^A-dependent P*veg* promoter with the addition of MBP, MBP-ω or ω-His. A pilot experiment done with (from left to right): RNAPΔδΔω, RNAPΔδΔω+δ, RNAPΔδΔω+δ+MBP-ω, RNAPΔδΔω+MBP-ω, RNAPΔδΔω+MBP, RNAPΔδΔω+δ+His-ω and RNAPΔδΔω+ω-His. RNAP:σ^A 1:5, RNAP:MBP-ω 1:10, RNAP:MBP 1:10, RNAP:δ 1:10, RNAP:His-ω. P*veg*:30ng/μl.

As can be seen in Fig. 31., *in vitro* transcription was not visible when using only RNAP or RNAP with δ, RNAP with MBP-ω or with MBP-ω and δ. The negative control consisting of RNAP with only MBP also showed no transcription. When RNAP was combined with ω-His and ω-His+δ, transcription signal was detected.

Since there was no visible transcript when MBP-ω was used, the ω-His variant was used in further experiments. As there was no visible transcript when only RNAP was used, the *in vitro* transcription had to be optimised: the concentration of RNAP was increased 4-fold (120 nM).

5.4.1 RNAP affinity for the δ subunit

The first experiments carried out after the optimalisation were titration experiments, i.e. increase in concentration of a certain component in *in vitro* experiments. These experiments

were done to determine the concentration when RNAP becomes saturated and also to determine the relative affinity of RNAP for ω and δ subunits.

Since the RNAP was ΔδΔω the titration of the δ subunit was carried out. The δ subunit was diluted using the dilution buffer according to chapter 4.13.1. The exact concentrations of δ are listed in Table 13. The *in vitro* transcription was performed on the σ^A-dependent promoter P*veg* (30 ng/μl). P*veg* is a vegetative promoter.

Two separate experiments were done. The first one was only with the increasing amount of δ subunit. The second experiment was the same, but in the presence of ω (constant concentration). Results are shown in Fig. 32. Fig. 32A displays the experiment only with δ and Fig. 32B shows the experiment with titration of δ in the presence of ω (RNAP:ω 1:3). The RNAPΔδΔω was saturated once the transcription reached a maximum. The concentration of the subunits used in further experiments was higher than the saturation point, so that the subunits were in excess compared to the RNAPΔδΔω. The saturation of RNAPΔδΔω by δ was at about the same concentration in both cases (1:1.25). The relative transcription was higher when ω was present.
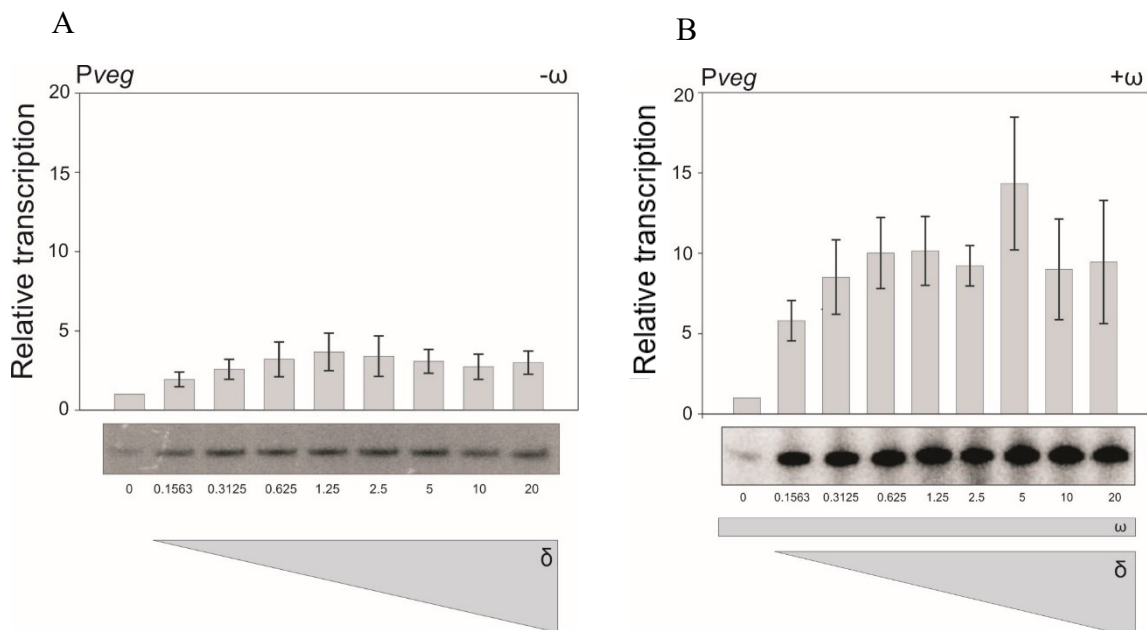
Figure 32. Titration of the δ subunit in the absence and presence of the ω subunit using the P*veg* promoter. **A:** Titration of δ. The concentration of δ rises from left to right. **B:** Titration of δ in the presence of ω (The concentration of ω is constant and in ratio 1:3). The ratios of δ:RNAP are indicated below the transcripts. 120 nM RNAPΔδΔω was used. The primary data is shown below the graphs and the graphs are normalized to transcription in the absence of δ. The transcripts are quantified in the graph above them. The experiments were performed 3x. The bars represent the average relative transcription.

5.4.2 RNAP affinity for the ω subunit

Next, *in vitro* transcription experiment was performed with increasing ω. ω was diluted with dilution buffer according to chapter 4.13.1. The exact concentrations of ω are listed in Table 14. The experiment was carried out with and without the presence of δ. When δ was present its concentration was constant (RNAP:δ 1:10). The *in vitro* transcription was performed with 30 ng/µl of the vegetative promoter P*veg* dependent on σ^A. Results are shown in Fig. 33. Fig. 33A shows the titration of ω without δ and Fig. 33B shows the titration of ω in the presence of δ. In the absence of δ the saturation of RNAP by ω was 1:0.5 (RNAP:ω). In the presence of δ the saturation of RNAP by ω was 1:2 (RNAP:ω). The experiment revealed that a higher concentration of ω is required to saturate RNAP in the presence of δ. Furthermore, the relative transcription was higher when δ was present.
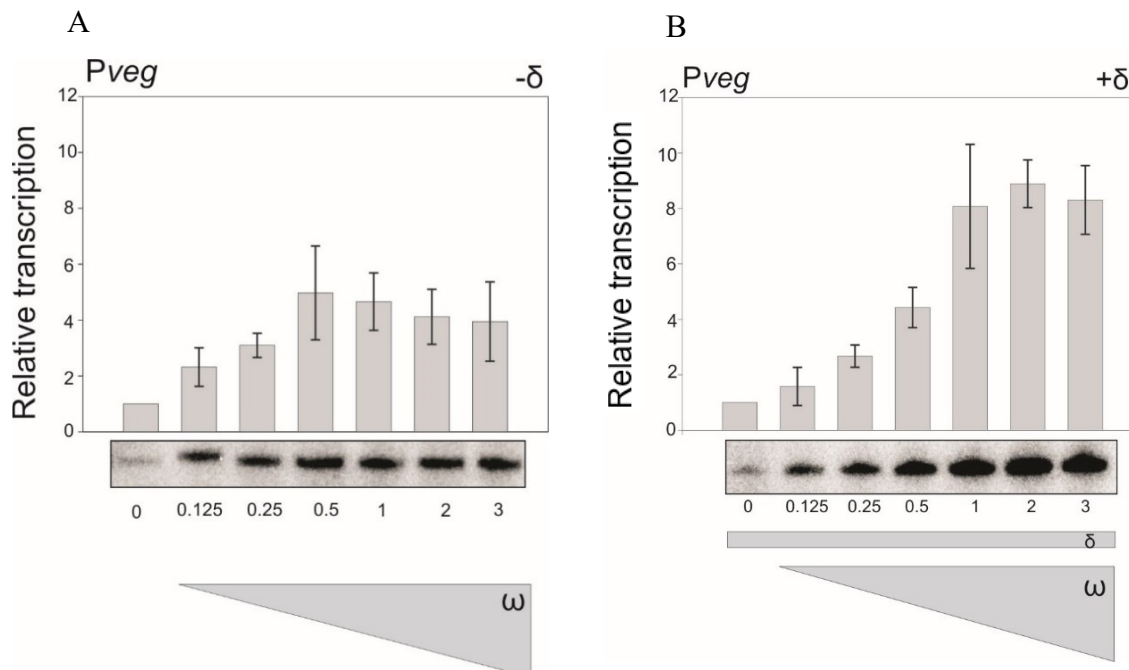
Figure 33. Titration of the ω subunit in the absence and presence of the δ subunit using P*veg* promoter. A: Titration of ω. The concentration of δ rises from left to right. **B:** Titration of ω in the presence of δ (The concentration of δ is constant and in ratio 1:10). The ratios of ω:RNAP are indicated below the transcripts. 120 nM RNAPΔδΔω was used. The primary data is shown below the graphs and the graphs are normalized to transcription in the absence of ω. The transcripts are quantified in the graph above them. The experiments were performed 3x. The bars represent the average relative transcription.

5.4.3 Influence of the ω subunit on vegetative promoters

Next to be tested was the effect of ω on the transcription from vegetative promoters. Two σ^A-dependent promoters P*veg* and *rrnB* P1 were used. P*veg* is a non-ribosomal promoter and *rrnB* P1 is a ribosomal promoter. The ribosomal promoter *rrnB* P1 was selected to test whether the effect of ω was the same on non-ribosomal promoters and ribosomal promoters. The effect might have been different because it had been previously shown that ribosomal promoters behave differently than non-ribosomal promoters. This is the case, because ribosomal promoters are regulated by the concentrations of iGTP. The open complexes of ribosomal promoters are unstable and therefore sensitive to iGTP (Krásný and Gourse, 2004; Natori et al., 2009; Rabatinová et al., 2013; Sudzinová et al., 2021).

Transcriptions were performed with RNAP without, with δ or ω, and with δ and ω. The combinations were prepared according to Table 15 and *in vitro* transcriptions were carried out according to chapter 4.13.4. The results of experiments with P*veg* promoter are shown in Fig. 34A and with *rrnB* P1 in Fig. 34B. The trend is the same for both promoters. The transcription without any of the two small subunits was quite low. However, transcription increased when δ was added. From P*veg*, transcription increased ~4x and from *rrnB* P1 ~5x. Transcription increased even more when only ω was added, from ~6x P*veg* and ~8x from *rrnB* P1. When both δ and ω were added, there was an even larger increase in transcription, for ~32x P*veg* and ~31x for *rrnB* P1.

The experiments with P*veg* were done with a lower concentration of DNA template (30 ng/μl) and experiments with *rrnB* P1 were done with a higher concentration of DNA template (100 ng/μl). The concentration of DNA template (promoter *rrnB* P1) was increased because transcription from promoter *rrnB* P1 using 30 ng/μl of template the was too low to be quantified. For further interpretation see Discussion.
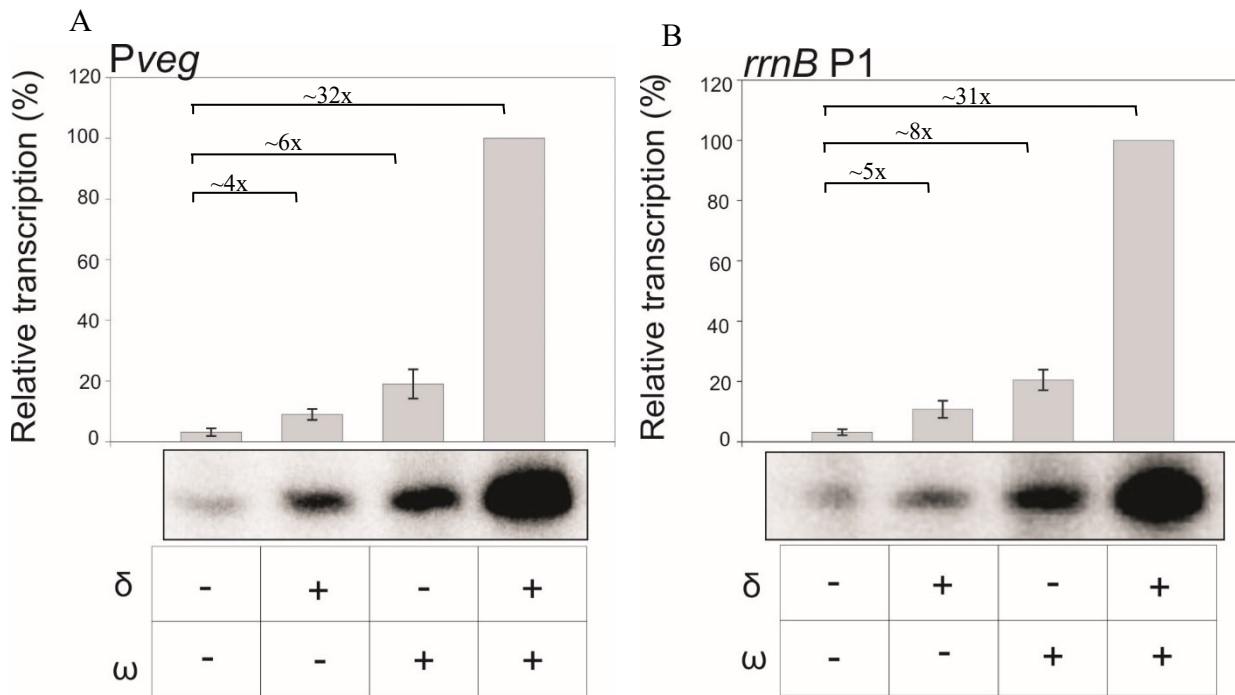
Figure 34. *In vitro* **transcription of the σ^A-dependent promoters P***veg* **and** *rrnB* **P1. A:** Transcription from P*veg* (30 ng/μl). **B:** Transcription from *rrnB* P1 (100 ng/μl). The first bar represents transcription with only RNAPΔδΔω, the second bar is after addition of δ, the third bar is after addition of ω, and the fourth bar is after addition of both subunits. RNAP:δ 1:10, RNAP:ω 1:3, RNAP:σ 1:10. The primary data is shown below the graph and the graph is normalized to maximum transcription. The experiments were performed 3x. The bars represent the average relative transcription. 120 nM RNAPΔδΔω

5.4.4 Influence of the ω subunit on sporulation related promoters

As described earlier in the introduction (chapter 3.5.3) some results indicated that the δ and ω subunit affect sporulation (unpublished data, Kálalová). Therefore, *in vitro* experiments addressing the role of the ω subunit in transcriptions from sporulation-related promoters were performed. For this purpose, promoters that are dependent on σ^F and σ^E were used because these σ factors regulate the early stage of sporulation. The used sporulation related promoters were P*spoIIQ*, P*katX* and P*yknT*. P*spoIIQ* and P*katX* are σ^F-dependent and P*yknT* is σ^E-dependent. The same *in vitro* transcription experiments as for the σ^A-dependent vegetative promoters were performed.

The *in vitro* transcriptions were performed as described in chapter 4.13 and the experiment was prepared according to Table 15. The RNA transcripts obtained from P*spoIIQ* and P*katX* promoters along with quantification are shown in Fig. 35. Fig. 35A shows RNA transcripts of P*spoIIQ* and Fig. 35B shows RNA transcripts of P*katX*. The transcription when only the RNAP was present was very low. The addition of only δ increased the transcription from both σ^F dependent promoters. When only ω was added transcription increased but less than when only δ was added. In the case of P*spoIIQ* when δ was added the transcription increased ~20x and

when ω was added it increased only ~7x. From the P*katX* promoter, the transcription after addition of δ increased ~21x, but when ω was added, transcription increased only ~3x.

However, when both δ and ω were added the transcription from both promoters increased massively. Transcription from P*spoIIQ* increased ~114x and transcription from P*katX* increased ~195x. For interpretation see Discussion.
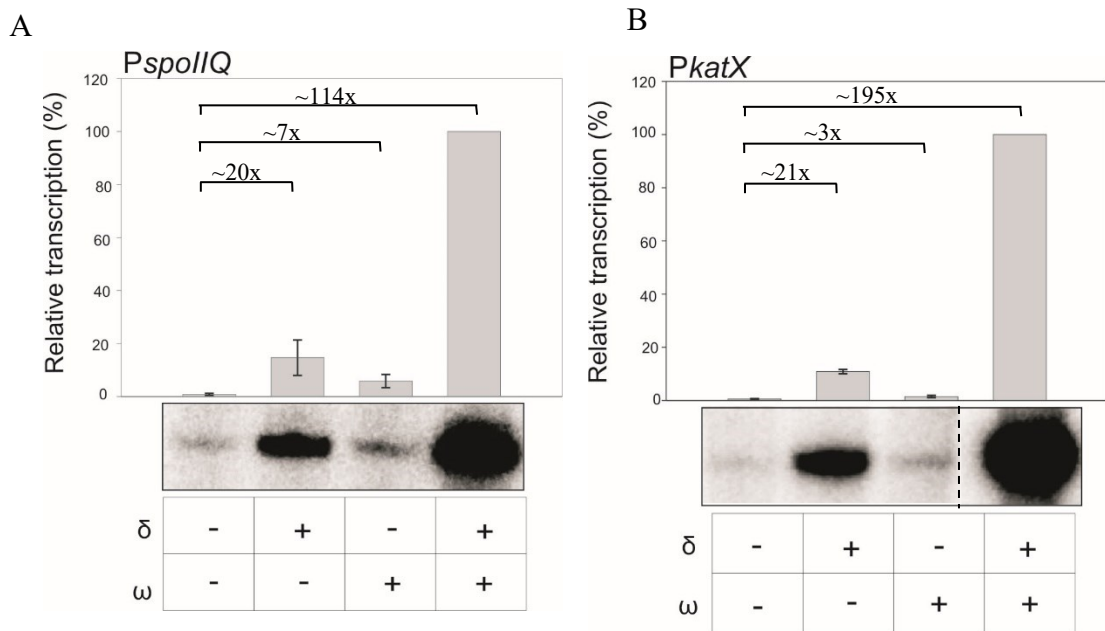
Figure 35. *In vitro* **transcription of σ^F-dependent promoters P*spoIIQ* and P*katX*. A:** Transcription from P*spoIIQ* (30 ng/μl). **B:** Transcription from *PkatX* (30 ng/μl). The first bar represents transcription with only RNAPΔδΔω, the second bar is after addition of δ, the third bar is after addition of ω, and the fourth bar is after addition of both subunits. RNAP:δ 1:10, RNAP:ω 1:3, RNAP:σ 1:10. The primary data is shown below the graph and the graph is normalized to maximum transcription. The experiments were performed 3x. The bars represent the average relative transcription. 120 nM RNAPΔδΔω

Fig. 36. Shows the effect of the ω subunit on transcription from the σ^E-dependent promoter P*yknT*. In this case, again transcription with only RNAP present was very weak and when δ was added transcription increased (~4x). Transcription increased ~3x when ω was added, when compared to RNAPΔδΔω. When both subunits were added, transcription increased ~13x.
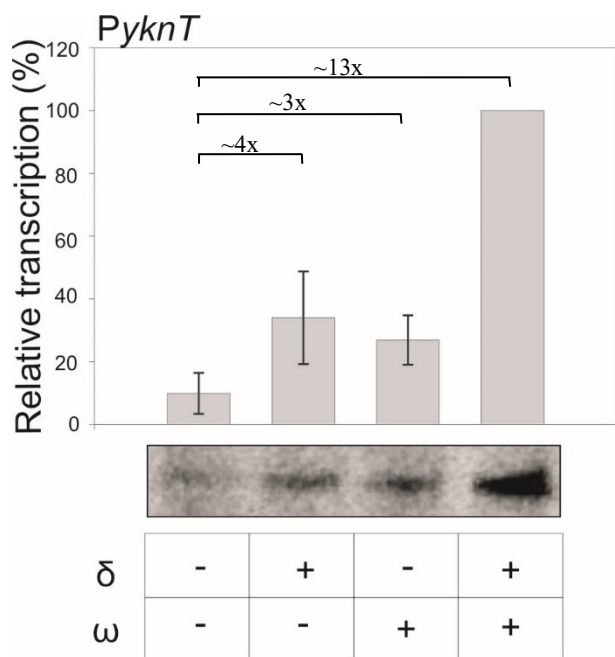
Figure 36. *In vitro* transcription of the σ^E dependent *PyknT* promoter. Transcription from *PyknT* (30 ng/µl). The first bar represents transcription with only RNAP$\Delta\delta\Delta\omega$, the second bar is after addition of δ, the third bar is after addition of ω, and the fourth bar is after addition of both subunits. RNAP:δ 1:10, RNAP:ω 1:3, RNAP:σ 1:10. The primary data is shown below the graph and the graph is normalized to maximum transcription. The experiments were performed 3x. The bars represent the average relative transcription. 120 nM RNAP$\Delta\delta\Delta\omega$

6.Discussion

In this Thesis I have contributed to characterization of the ω subunit from *B. subtilis*. First, constructs with the gene for the ω subunit were designed and prepared. Then, the ω subunit was successfully overexpressed, and, after optimisation, isolated. The isolated ω-His subunit was then tested in *in vitro* transcription experiments with vegetative (P*veg* and *rrnB* P1) and sporulation-related promoters (P*spoIIQ*, P*katX*, P*yknT*). A synergistic effect of δ and ω was found, revealing a novel aspect of the *B. subtilis* transcription machinery.

6.1 Cloning and overexpression of ω

The gene for the ω subunit was cloned with GST-tag and MBP-tag to increase solubility and yield. As shown in Fig. 21, the increase in solubility was successful in the case of the MBP-tag, where more ω was found in the supernatant than in the inclusion bodies. The solubility was not increased as much in the case of the GST-tag as it shown in Fig. 21 because more ω was found in the pellet (inclusion bodies) than in the supernatant. This indicates that MBP-tag version of ω is more soluble.

Overexpression was then optimized, and regardless of the tag, it was higher when induced at 16 °C rather than at room temperature. Two relatively low concentrations of the inducer, IPTG, were tested in the case of ω-His (0.05 mM and 0.005 mM), and both functioned equally well, yielding sufficient amounts of the proteins in the soluble fraction. An important observation in the case of ω-His was that the OD of the culture was critical. The ideal yield was reached when the OD after induction was around 4.

6.2 Isolation of ω and further functionality

The ω subunit was successfully isolated using MBP-tag and His-tag. The yield was higher when ω was isolated using the MBP-tag. However, the MBP-tag is quite large, and the cleavage of the MBP-tag was not possible because ω aggregated. The cleaved ω subunit could be found in the supernatant only for a short period of time (it started precipitating) and so it could not be processed by gel filtration chromatography. This aggregation could have been caused by the high concentration of the protein or perhaps also because of the concentration of the salt in the buffer being too low. The cleavage of the MBP-tag could have also caused a change in solubility of ω in the used buffer (MBP buffer). Furthermore, it could also have been caused by the change in flexibility of ω. This aggregation supports the idea that the flexibility of ω is important and

that the exact folding of ω occurs only once it is located on RNAP and in this way can regulate transcription. This was found in *E. coli* by (Bhowmik et al., 2017; Patel et al., 2019). Nevertheless, other studies also reported in *E. coli* that they were not able to isolate the ω subunit (Geertz et al., 2011). This indicates that the struggle with isolating this protein is not uncommon.

Most of the MBP-ω in the supernatant bound to the Amylose resin beads (Fig. 23A). This means that the concentration of Amylose resin beads was sufficient for efficient binding of MBP and MBP-ω. However, the isolation of the MBP-ω construct or MBP could have been further optimised at the elution stage to gain even higher concentrations of MBP-ω. This could be achieved by repeating the elution several more times or increasing the volume of buffer used for elution.

To avoid the aggregation, I focused on purification of ω-His with the hope that it will behave differently. The isolated ω-His was highly contaminated and was therefore further purified using gel filtration chromatography. It still aggregated but to a lesser degree than the previous construct. To prevent aggregation, a higher concentration of salt (300 mM) was used for the storage of the purified ω-His and this greatly improved its solubility.

When the functionality of the fusion proteins, ω-His and MBP-ω, was tested by *in vitro* transcription experiments (Fig. 31.) it was discovered that the MBP-ω fusion protein was not functional. This was most probably caused by size of the MBP-tag or perhaps by a possible interaction of MBP with either the ω subunit or RNAP. Fortunately, the ω-His variant was functional in *in vitro* transcription experiments (Fig. 31).

Even though the isolation of the ω subunit had been unsuccessful in the past, the induction (using small concentrations of IPTG) overnight at 16°C, the purification using FPLC and the increase in the salt concentration proved to be crucial for the successful isolation. To summarize this part, the ω subunit was successfully purified, an essential prerequisite for subsequent transcription experiments.

6.3 Influence of ω on transcription from vegetative promoters

First, several *in vitro* transcription experiments were performed to determine saturation levels of ω and δ for RNAP. Then, the influence of ω on transcription from two different vegetative promoters was studied. Transcription with RNAPΔδΔω associated only with σ^A was used as a

reference control. When transcription was carried out using P*veg* and *rrnB* P1 promoters, the addition of ω had a major stimulatory effect on transcription from both promoters. Additionally, the influence of δ, another small subunit of Firmicutes RNAP was also tested. The δ subunit was added alone or together with ω. The addition of δ alone had a stimulatory effect on transcription, but this effect was smaller than the effect of ω. Importantly, after the addition of both subunits, the stimulatory effect was synergistic. The effect of δ correlates with the finding of Wiedermannová *et al.*,2014, where δ is implicated in the recycling of RNAP, that in turn increases transcription (Wiedermannová et al., 2014).

Interestingly, it was previously reported that δ stimulated transcription from P*veg* (the same result as in this Thesis) but inhibited transcription from *rrnB* P1 (an opposite result) (Kubáň et al., 2019). The reason for this difference is not apparent. A possibility is that Kuban et al. used slightly different reaction conditions and a different type of RNAP - lacking only δ. These differences will have to be addressed by future experiments.

Finally, *rpoZ* is co-transcribed together with the *gmk* gene involved in GTP biosynthesis (Abecasis et al., 2013; Nicolas et al., 2012). Similarly, as the ω subunit in *E. coli* is co-transcribed with the gene *spoT* (Gentry and Burgess, 1989). Both these genes are through the regulation of GTP in the cell connected with the stringent response. As many promoters in *B. subtilis* are regulated by the concentration of GTP (Krásný et al., 2008), it is tempting to speculate that ω may affect the affinity of RNAP for this molecule or possibly even the stringent response. Future experiments are required to test this hypothesis.

6.4 Influence of ω on transcription from sporulation-specific promoters

The influence of ω on transcription from sporulation-specific promoters was tested by the addition of ω in *in vitro* transcription experiments using sporulation-related σ factors (σ[F] and σ[E]). The transcription of only RNAPΔδΔω associated with σ[F] or σ[E] was used as a control. The promoters used were σ[F]-dependent P*spoIIQ*, P*katX* and σ[E]-dependent P*yknT*. All these promoters are expressed in the early stages of sporulation (McKenney and Eichenberger, 2012; Steil et al., 2005; Wang et al., 2006). Additionally, the δ subunit was added either alone or together with ω. In the case of the σ[F]-dependent promoters, the addition of δ had a stimulating effect on transcription. The addition of ω had a small stimulating effect, but the effect was smaller than the addition of δ had. However, when both the subunits were added there was a very high increase in transcription. This stimulating effect was even bigger than in the case of

the vegetative promoters. When we compare the two σ^F-dependent promoters we can see that the synergic effect of δ and ω was higher when P*katX* was used.

When the σ^E-dependent P*yknT* promoter was tested, the addition of δ increased transcription. The presence of ω increased transcription as well. The increase in transcription was in this case similar. The effect of δ was only slightly more pronounced. The addition of both subunits increased transcription even more, but the increase was smaller than in the case of σ^F-dependent promoters.

This synergistic effect of ω and δ, and its magnitude (especially for transcription with σ^F relative to transcription with the other σ factors), then imply that these RNAP subunits either have an effect on the recruitment of sporulation-specific σ factors to RNAP, similarly as reported in (Geertz et al., 2011; Gunnelius et al., 2014a), or they affect some kinetic step during transcription initiation. This correlates well with the unpublished findings of Kálalová where a massive effect of the absence of these subunits on sporulation was observed (see Chapter 3.5.3.).

The importance of ω for sporulation is also supported by the fact that it is part of the SigF regulon (Abecasis et al., 2013; Nicolas et al., 2012; Raeymaekers et al., 2002). The most interesting form of transcript of the *rpoZ* operon (in the SigF regulon) is in this case yloB-yloC-remA-gmk-yloH *(rpoZ)*. The *rpoZ* gene is co-transcribed with *yloB*, which encodes an ATP-driven Ca^{2+} pump that transports calcium ions from the mother cell to the forespore (Abecasis et al., 2013; Raeymaekers et al., 2002), *yloC* that encodes an endoribonuclease, *remA* (*ylzA*) encoding a transcriptional regulator of the extracellular matrix genes (found in the forespore) and *gmk* a guanylate kinase (Nicolas et al., 2012) This operon is intriguing because multiple genes are in some way connected with the process of sporulation or could possibly lead to further regulation connected with the synthesis of the ω subunit.

Furthermore, when we put this into context with the fact that only half of RNAPs in *B. subtilis* contain the ω subunit (Doherty et al., 2010) it leads me to the idea of additional synthesis of ω could possibly have regulatory function in sporulation. The location of the gene for ω (*rpoZ*) in the *B. subtilis* 168 chromosome is shown in Fig. 37. Future experiments will

address the mechanistic relationship between ω, δ, and sporulation σ factors.
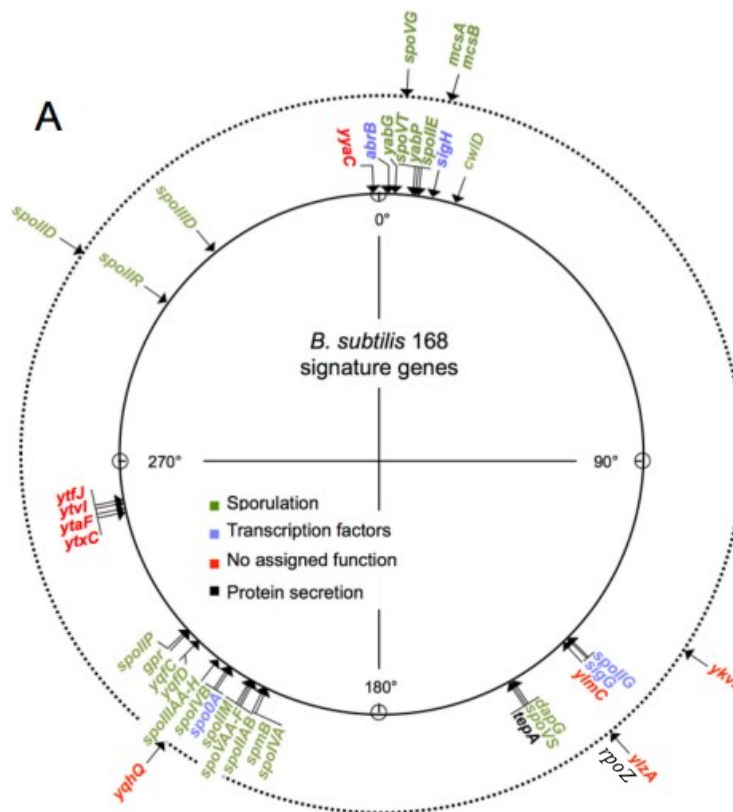
Figure 37. The Genomic signature of sporulation. The signature is defined as genes present in 90 % of sporulating bacteria, in no more than 5 % (the inner circle) or 10 % (the outer circle) of the rest of bacterial species. The diagram shows genes with an established role in endosporulation, genes encoding for the sporulation related σ factors, genes coding for global transcriptional regulators and gen *tepA*, that has a predicted function in secretion of proteins, but has not yet been connected with sporulation. Genes with unknown function are also shown. The position of the genes is shown in degrees in the chromosome of *B. subtilis* 168. Adapted from (Abecasis et al., 2013).

6.5 Further study of the influence of ω

In order to prove any of the mechanisms mentioned above more experiments will have to be done. It would be interesting to also test the influence on various σ^H-dependent and more σ^E dependent promoters. More *in vitro* transcription experiments will have to be done to determine the affinity of RNAPΔδΔω towards various σ factors in order to uncover any changes related with the deletion of the ω subunit. Furthermore, the effect of the ω subunit on the stability of the open complex should be tested especially in the case of the ribosomal promoter *rrnB* P1. This would have to be tested by a single-round *in vitro* transcription using a competitor to inhibit repeated binding of RNAP to DNA before initiating transcription with NTPs. Also *in vivo* experiments, with perhaps GFP, should be done to establish how it works in the cell itself as it is possible that other proteins that are not present in the *in vitro* experiments could play an important role.

7. Conclusions

The ω subunit was isolated successfully in two forms: MBP-ω and ω-His. This was a significant achievement as previous attempts to purify ω in the Krásný lab had been unsuccessful. Of the two forms, ω-His was more active and was selected for subsequent transcription experiments.

Transcription experiments were then performed with vegetative (P*veg* and *rrnB* P1) and sporulation-related promoters [P*spoIIQ*, P*katX* (σ^F-dependent) and P*yknT* (σ^E-dependent)]. The experiments revealed a stimulatory effect of ω on transcription with *B. subtilis* RNAP. This effect was larger in the case of transcription from vegetative promoters compared to sporulation-specific promoters. The experiments also demonstrated a synergistic effect of δ and ω subunits on transcription. In this case, the effect was markedly more prominent for transcription from σ^F-dependent promoters.

In summary, this Thesis has led to a successful isolation of the ω subunit. It has also contributed to the further uncovering of the potential role of the ω subunit in transcription of *B. subtilis*, especially together with the δ subunit in the early stages of sporulation.

8.References

Abecasis, A.B., Serrano, M., Alves, R., Quintais, L., Pereira-Leal, J.B., and Henriques, A.O. (2013). A genomic signature and the identification of new sporulation genes. J. Bacteriol. *195*, 2101–2115.

Alon, U. (2019). An Introduction to Systems Biology: Design Principles of Biological Circuits,2nd Edition (Chapman and Hall: Boca Raton).

Amaya, E., Khvorova, A., and Piggot, P.J. (2001). Analysis of Promoter Recognition *In Vivo* Directed by σF of *Bacillus subtilis* by Using Random-Sequence Oligonucleotides. J. Bacteriol. *183*, 3623–3630.

Arnaouteli, S., Bamford, N.C., Stanley-Wall, N.R., and Kovács, Á.T. (2021). *Bacillus subtilis* biofilm formation and social interactions. Nat. Rev. Microbiol. *19*, 600–614.

Asayama, M., and Imamura, S. (2008). Stringent promoter recognition and autoregulation by the group 3 σ-factor SigF in the cyanobacterium Synechocystis sp. strain PCC 6803. Nucleic Acids Res. *36*, 5297–5305.

Bagyan, I., Casillas-Martinez, L., and Setlow, P. (1998). The *katX* Gene, Which Codes for the Catalase in Spores of *Bacillus subtilis*, Is a Forespore-Specific Gene Controlled by σF , and KatX Is Essential for Hydrogen Peroxide Resistance of the Germinating Spore. J. Bacteriol. *180*, 2057–2062.

Barbe, V., Cruveiller, S., Kunst, F., Lenoble, P., Meurice, G., Sekowska, A., Vallenet, D., Wang, T., Moszer, I., Médigue, C., et al. (2009). From a consortium sequence to a unified sequence: the *Bacillus subtilis* 168 reference genome a decade later. Microbiology *155*, 1758–1775.

Barne, K.A., Bown, J.A., Busby, S.J.W., and Minchin, S.D. (1997). Region 2.5 of the *Escherichia coli* RNA polymerase σ 70 subunit is responsible for the recognition of the "extended-10" motif at promoters. EMBO J. *16*, 4034–4040.

Benoit, I., Esker, M.H. van den, Patyshakuliyeva, A., Mattern, D.J., Blei, F., Zhou, M., Dijksterhuis, J., Brakhage, A.A., Kuipers, O.P., Vries, R.P. de, et al. (2015). *Bacillus subtilis* attachment to *Aspergillus niger* hyphae results in mutually altered metabolism. Environ. Microbiol. *17*, 2099–2113.

Bhardwaj, N., Syal, K., and Chatterji, D. (2018). The role of ω-subunit of *Escherichia coli* RNA polymerase in stress response. Genes to Cells *23*, 357–369.

Bhaya, D., Watanabe, N., Ogawa, T., and Grossman, A.R. (1999). The role of an alternative sigma factor in motility and pilus formation in the cyanobacterium *Synechocystis* sp. strain PCC6803. Proc. Natl. Acad. Sci. U. S. A. *96*, 3188–3193.

Bhowmik, D., Bhardwaj, N., and Chatterji, D. (2017). Influence of Flexible "ω" on the Activity of *E. coli* RNA Polymerase: A Thermodynamic Analysis. Biophys. J. *112*, 901–910.

Borukhov, S., Sagitov, V., and Goldfarb, A. (1993). Transcript cleavage factors from *E. coli*. Cell *72*, 459–466.

Bradford, M.M. (1976). A rapid and sensitive method for the quantitation of microgram quantities of protein utilizing the principle of protein-dye binding. Anal. Biochem. *72*, 248–254.

Browning, D.F., and Busby, S.J.W. (2004). The regulation of bacterial transcription initiation. Nat. Rev. Microbiol. *2*, 57–65.

Burbulys, D., Trach, K.A., and Hoch, J.A. (1991). Initiation of sporulation in *B. subtilis* is controlled by a multicomponent phosphorelay. Cell *64*, 545–552.

Campbell, E.A., Masuda, S., Sun, J.L., Muzzin, O., Olson, C.A., Wang, S., and Darst, S.A. (2002). Crystal structure of the *Bacillus stearothermophilus* anti-sigma factor SpoIIAB with the sporulation sigma factor σF. Cell *108*, 795–807.

Cano, R.J., and Borucki, M.K. (1995). Revival and identification of bacterial spores in 25- to 40-million-year-old Dominican amber. Science. *268*, 1060–1064.

Caulier, S., Nannan, C., Gillis, A., Licciardi, F., Bragard, C., and Mahillon, J. (2019). Overview of the

antimicrobial compounds produced by members of the *Bacillus subtilis* group. Front. Microbiol. *10*, 1–19.

Chang, B.Y., and Doi, R.H. (1990). Overproduction, purification, and characterization of Bacillus subtilis RNA polymerase σA factor. J. Bacteriol. *172*, 3257–3263.

Chang, B.Y., Chen, K.Y., Wen, Y.D., and Liao, C.T. (1994). The response of a *Bacillus subtilis* temperature-sensitive *sigA* mutant to heat stress. J. Bacteriol. *176*, 3102–3110.

Chen, Y.F., and Helmann, J.D. (1995). The *Bacillus subtilis* Flagellar Regulatory Protein σD: Overproduction, Domain Analysis and DNA-binding Properties. J. Mol. Biol. *249*, 743–753.

Chen, I., Christie, P.J., and Dubnau, D. (2005). The Ins and Outs of DNA Transfer in Bacteria. Science. *310*, 1456–1460.

Chhakchhuak, P.I.R., Khatri, A., and Sen, R. (2019). Mechanism of action of bacterial transcription terminator rho. Proc. Indian Natl. Sci. Acad. *85*, 157–168.

Cook, H., and Ussery, D.W. (2013). Sigma factors in a thousand *E. coli* genomes. Environ. Microbiol. *15*, 3121–3129.

Crick, F. (1970). Central dogma of molecular biology. Nature *227*, 561–563.

Davis, M.C., Kesthely, C.A., Franklin, E.A., and MacLellan, S.R. (2017). The essential activities of the bacterial sigma factor. Can. J. Microbiol. *63*, 89–99.

Decker, K.B., and Hinton, D.M. (2013). Transcription Regulation at the Core: Similarities Among Bacterial, Archaeal, and Eukaryotic RNA Polymerases. Annu. Rev. Microbiol. *67*, 113–139.

Doherty, G.P., Fogg, M.J., Wilkinson, A.J., and Lewis, P.J. (2010). Small subunits of RNA polymerase: Localization, levels and implications for core enzyme composition. Microbiology *156*, 3532–3543.

Dove, S.L., and Hochschild, A. (1998). Conversion of the ω subunit of *Escherichia coli* RNA polymerase into a transcriptional activator or an activation target. Genes Dev. *12*, 745–754.

Eichenberger, P., Fujita, M., Jensen, S.T., Conlon, E.M., Rudner, D.Z., Wang, S.T., Ferguson, C., Haga, K., Sato, T., Liu, J.S., et al. (2004). The program of gene transcription for a single differentiating cell type during sporulation in *Bacillus subtilis*. PLoS Biol. *2*, 1664–1683.

Fujita, M. (2000). Temporal and selective association of multiple sigma factors with RNA polymerase during sporulation in *Bacillus subtilis*. Genes to Cells *5*, 79–88.

Fujita, M., and Sadaie, Y. (1998a). Promoter selectivity of the *Bacillus subtilis* RNA polymerase σA and σH holoenzymes. J. Biochem. *124*, 89–97.

Fujita, M., and Sadaie, Y. (1998b). Rapid isolation of RNA polymerase from sporulating cells of *Bacillus subtilis*. Gene *221*, 185–190.

Fujita, M., González-Pastor, J.E., and Losick, R. (2005). High- and low-threshold genes in the Spo0A regulon of *Bacillus subtilis*. J. Bacteriol. *187*, 1357–1368.

Fukushima, T., Ishikawa, S., Yamamoto, H., Ogasawara, N., and Sekiguchi, J. (2003). Transcriptional, Functional and Cytochemical Analyses of the *veg* Gene in *Bacillus subtilis*. J. Biochem. *133*, 475–483.

Geertz, M., Travers, A., Mehandziska, S., Sobetzko, P., Janga, S.C., Shimamoto, N., and Muskhelishvilia, G. (2011). Structural coupling between RNA polymerase composition and DNA supercoiling in coordinating transcription: A global role for the omega subunit? MBio *2*, 1–11.

Gentry, D.R., and Burgess, R.R. (1989). *rpoZ*, encoding the omega subunit of *Escherichia coli* RNA polymerase, is in the same operon as *spoT*. J. Bacteriol. *171*, 1271–1277.

Gentry, D.R., and Burgess, R.R. (1990). Overproduction and purification of the ω subunit of *Escherichia coli* RNA polymerase. Protein Expr. Purif. *1*, 81–86.

Gentry, D., Xiao, H., Burgess, R., and Cashel, M. (1991). The omega subunit of *Escherichia coli* K-12 RNA polymerase is not required for stringent RNA control *in vivo*. J. Bacteriol. *173*, 3901–3903.

Gholamhoseinian, A., and Piggot, P.J. (1989). Timing of *spoII* Gene Expression Relative to Septum Formation during Sporulation of *Bacillus subtilis*. J. Bacteriol. *171*, 5747–5749.

Ghosh, P., Ishihama, A., and Chatterji, D. (2001). *Escherichia coli* RNA polymerase subunit ω and its N-terminal domain bind full-length β′ to facilitate incorporation into the α2β subassembly. Eur. J. Biochem. *268*, 4621–4627.

González-Pastor, J.E. (2011). Cannibalism: a social behavior in sporulating *Bacillus subtilis*. FEMS Microbiol. Rev. *35*, 415–424.

Gopalkrishnan, S., Nicoloff, H., and Ades, S.E. (2014). Co-ordinated regulation of the extracytoplasmic stress factor, sigmaE, with other *Escherichia coli* sigma factors by (p)ppGpp and DksA may be achieved by specific regulation of individual holoenzymes. Mol. Microbiol. *93*, 479–493.

Gopalkrishnan, S., Ross, W., Chen, A.Y., and Gourse, R.L. (2017). TraR directly regulates transcription initiation by mimicking the combined effects of the global regulators DksA and ppGpp. PNAS *114*, 5539–5548.

Gruber, T.M., and Gross, C.A. (2003). Multiple Sigma Subunits and the Partitioning of Bacterial Transcription Space. Annu. Rev. Genet. *57*, 441–466.

Gunnelius, L., Hakkila, K., Kurkela, J., Wada, H., Tyystjärvi, E., and Tyystjärvi, T. (2014a). The omega subunit of the RNA polymerase core directs transcription efficiency in cyanobacteria. Nucleic Acids Res. *42*, 4606–4614.

Gunnelius, L., Kurkela, J., Hakkila, K., Koskinen, S., Parikainen, M., and Tyystjärvi, T. (2014b). The ω Subunit of RNA Polymerase Is Essential for Thermal Acclimation of the Cyanobacterium *Synechocystis* Sp. PCC 6803. PLoS One *9*, 1–9.

Haldenwang, W.G. (1995). The sigma factors of *Bacillus subtilis*. Microbiol. Rev. *59*, 1–30.

Hanahan, D. (1983). Studies on Transformation of *Escherichia coli* with Plasmids. J. Mol. Biol *166*, 557–580.

Heil, A., and Zillig, W. (1970). Reconstitution of bacterial DNA-dependent RNA-polymerase from isolated subunits as a tool for the elucidation of the role of the subunits in transcription. FEBS Lett. *11*, 165–168.

Hein, P.P., and Landick, R. (2010). The bridge helix coordinates movements of modules in RNA polymerase. BMC Biol. *8*, 1–4.

Helmann, J.D. (1995). Compilation and analysis of *Bacillus subtilis* σA-dependent promoter sequences: evidence for extended contact between RNA polymerase and upstream promoter DNA. Nucleic Acids Res. *23*, 2351–2360.

Helmann, J.D., and DeHaseth, P.L. (1999). Protein-nucleic acid interactions during open complex formation investigated by systematic alteration of the protein and DNA binding partners. Biochemistry *38*, 5959–5967.

Henriques, A.O., Bryan, E.M., Beall, B.W., and Moran, C.P. (1997). cse15, cse60, and csk22 Are New Members of Mother-Cell-Specific Sporulation Regulons in *Bacillus subtilis*. J. Bacteriol. *179*, 389–398.

Höfler, C., Heckmann, J., Fritsch, A., Popp, P., Gebhard, S., Fritz, G., and Mascher, T. (2016). Cannibalism stress response in *Bacillus subtilis*. Microbiol. (United Kingdom) *162*, 164–176.

Hood, R.D., Higgins, S.A., Flamholz, A., Nichols, R.J., and Savage, D.F. (2016). The stringent response regulates adaptation to darkness in the cyanobacterium Synechococcus elongatus. PNAS *113*, 4867–4876.

De Hoon, M.J.L., Eichenberger, P., and Vitkup, D. (2010). Hierarchical evolution of the bacterial sporulation network. Curr. Biol. *20*, 735–745.

Huang, L., McCluskey, M.P., Ni, H., and LaRossa, R.A. (2002). Global Gene Expression Profiles of the Cyanobacterium *Synechocystis* sp. Strain PCC 6803 in Response to Irradiation with UV-B and White Light. J. Bacteriol. *184*, 6845–6858.

Igoshin, O.A., Price, C.W., and Savageau, M.A. (2006). Signalling network with a bistable hysteretic switch controls developmental activation of the σF transcription factor in *Bacillus subtilis*. Mol. Microbiol. *61*, 165–184.

Imamura, D., Zhou, R., Feig, M., and Kroos, L. (2008). Evidence that the *Bacillus subtilis* SpoIIGA protein is a novel type of signal-transducing aspartic protease. J. Biol. Chem. *283*, 15287–15299.

Imamura, D., Kuwana, R., Kroos, L., Feig, M., Takamatsu, H., and Watabe, K. (2011). Substrate specificity of SpoIIGA, a signal-transducing aspartic protease in *Bacilli*. J. Biochem. *149*, 665–671.

De Jong, L., De Koning, E.A., Roseboom, W., Buncherd, H., Wanner, M.J., Dapic, I., Jansen, P.J., Van Maarseveen, J.H., Corthals, G.L., Lewis, P.J., et al. (2017). In-Culture Cross-Linking of Bacterial Cells Reveals Large-Scale Dynamic Protein-Protein Interactions at the Peptide Level. J. Proteome Res. *16*, 2457–2471.

Ju, J., Mitchell, T., Peters III, H., and Haldenwang, W.G. (1999). Sigma Factor Displacement from RNA Polymerase during *Bacillus subtilis* Sporulation. J. Bacteriol. *181*, 4969–4977.

Karow, M.L., Glaser, P., and Piggot, P.J. (1995). Identification of a gene, *spoIIR*, that links the activation of σE to the transcriptional activity of σF during sporulation in *Bacillus subtilis*. PNAS *92*, 2012–2016.

Kashtan, N., Itzkovitz, S., Milo, R., and Alon, U. (2004). Topological generalizations of network motifs. Phys. Rev. E. Stat. Nonlin. Soft Matter Phys. *70*, 1–12.

Kearns, D.B., and Losick, R. (2003). Swarming motility in undomesticated *Bacillus subtilis*. Mol. Microbiol. *49*, 581–590.

Kojima, I., Kasuga, K., Kobayashi, M., Fukasawa, A., Mizuno, S., Arisawa, A., and Akagawa, H. (2002). The *rpoZ* Gene, Encoding the RNA Polymerase Omega Subunit, Is Required for Antibiotic Production and Morphological Differentiation in *Streptomyces kasugaensis*. J. Bacteriol. *184*, 6417–6423.

Koskinen, S., Hakkila, K., Kurkela, J., Tyystjärvi, E., and Tyystjärvi, T. (2018). Inactivation of group 2 σ factors upregulates production of transcription and translation machineries in the cyanobacterium *Synechocystis* sp. PCC 6803. Sci. Rep. *8*, 1–12.

Kouba, T., Koval', T., Sudzinová, P., Pospíšil, J., Brezovská, B., Hnilicová, J., Šanderová, H., Janoušková, M., Šiková, M., Halada, P., et al. (2020). Mycobacterial HelD is a nucleic acids-clearing factor for RNA polymerase. Nat. Commun. *11*, 1–13.

Kovács, Á.T. (2019). *Bacillus subtilis*. Trends Microbiol. *27*, 724–725.

Koval', T., Sudzinová, P., Perháčová, T., Trundová, M., Skálová, T., Fejfarová, K., Šanderová, H., Krásný, L., Dušková, J., and Dohnálek, J. (2019). Domain structure of HelD, an interaction partner of *Bacillus subtilis* RNA polymerase. FEBS Lett. *593*, 996–1005.

Krásný, L., and Gourse, R.L. (2004). An alternative strategy for bacterial ribosome synthesis: *Bacillus subtilis* rRNA transcription regulation. EMBO J. *23*, 4473–4483.

Krásný, L., Tišerová, H., Jonák, J., Rejman, D., and Šanderová, H. (2008). The identity of the transcription +1 position is crucial for changes in gene expression in response to amino acid starvation in *Bacillus subtilis*. Mol. Microbiol. *69*, 42–54.

Kriel, A., Bittner, A.N., Kim, S.H., Liu, K., Tehranchi, A.K., Zou, W.Y., Rendon, S., Chen, R., Tu, B.P., and Wang, J.D. (2012). Direct Regulation of GTP Homeostasis by (p)ppGpp: A Critical Component of Viability and Stress Resistance. Mol. Cell *48*, 231–241.

Kroos, L., Kunkel, B., and Losick, R. (1989). Switch protein alters specificity of RNA polymerase containing a compartment-specific sigma factor. Science *243*, 526–529.

Kubáň, V., Srb, P., Štégnerová, H., Padrta, P., Zachrdla, M., Jaseňáková, Z., Šanderová, H., Vítovská, D., Krásný, L., Koval, T., et al. (2019). Quantitative Conformational Analysis of Functionally Important Electrostatic Interactions in the Intrinsically Disordered Region of Delta Subunit of Bacterial RNA Polymerase. J. Am. Chem. Soc. *141*, 16817–16828.

Kunst, F., Ogasawara, N., Moszer, I., Albertini, A.M., Alloni, G., Azevedo, V., MG., B., Bessières, P., Bolotin, A., Borchert, S., et al. (1997). The complete genome sequence of the gram-positive bacterium Bacillus subtilis. Nature *390*, 249–256.

Kurkela, J., Hakkila, K., Antal, T., and Tyystjärvi, T. (2017). Acclimation to High CO2 Requires the ω Subunit of the RNA Polymerase in Synechocystis. Plant Physiol. *174*, 172–184.

Kurkela, J., Fredman, J., Salminen, T.A., and Tyystjärvi, T. (2021). Revealing secrets of the enigmatic omega subunit of bacterial RNA polymerase. Mol. Microbiol. *115*, 1–11.

Kuwana, R., Okumura, T., Takamatsu, H., and Watabe, K. (2005). The *ylbO* gene product of *Bacillus subtilis* is involved in the coat development and lysozyme resistance of spore. FEMS Microbiol. Lett. *242*, 51–57.

LaBell, T.L., Trempy, J.E., and Haldenwang, W.G. (1987). Sporulation-specific σ factor σ29 of *Bacillus subtilis* is synthesized from a precursor protein, P31. PNAS *84*, 1784–1788.

Lampe, M., Binnie, C., Schmidt, R., and Losick, R. (1988). Cloned gene encoding the delta subunit of *Bacillus subtilis* RNA polymerase. Gene *67*, 13–19.

Landick, R. (2005). NTP-entry routes in multi-subunit RNA polymerases. TRENDS Biochem. Sci. *30*, 651–654.

Liu, K., Myers, A.R., Pisithkul, T., Claas, K.R., Satyshur, K.A., Amador-Noguez, D., Keck, J.L., and Wang, J.D. (2015). Molecular mechanism and evolution of guanylate kinase regulation by (p)ppGpp. Mol. Cell *57*, 735–749.

López, D., Vlamakis, H., Losick, R., and Kolter, R. (2009). Cannibalism Enhances Biofilm Development in *Bacillus subtilis*. Mol. Microbiol. *74*, 609–618.

Lord, M., Barillà, D., and Yudkin, M.D. (1999). Replacement of vegetative σA by sporulation-specific σF as a component of the RNA polymerase holoenzyme in sporulating *Bacillus subtilis*. J. Bacteriol. *181*, 2346–2350.

Losick, R., and Stragier, P. (1992). Crisscross regulation of cell-type-specific gene expression during development in *B. subtilis*. Nature *355*, 601–604.

Lozinski, T., Adrych-Rozek, K., Markiewicz, W.T., and Wierzchowski, K. (1991). Effect of DNA bending in various regions of a consensus-like *Escherichia coli* promoter on its strength *in vivo* and structure of the open complex *in vitro*. Nucleic Acids Res. *19*, 2947–2953.

Mao, C., Zhu, Y., Lu, P., Feng, L., Chen, S., and Hu, Y. (2018). Association of ω with the C-Terminal Region of the β′ Subunit Is Essential for Assembly of RNA Polymerase in *Mycobacterium tuberculosis*. J. Bacteriol. *200*, 1–9.

Marzorati, M., Van den Abbeele, P., Bubeck, S.S., Bayne, T., Krishnan, K., Young, A., Mehta, D., and Desouza, A. (2020). *Bacillus subtilis* HU58 and *Bacillus coagulans* SC208 Probiotics Reduced the Effects of Antibiotic-Induced Gut Microbiome Dysbiosis in an M-SHIME® Model. Microorganisms *8*, 1–15.

Mathew, R., Ramakanth, M., and Chatterji, D. (2005). Deletion of the gene *rpoZ*, encoding the ω subunit of RNA polymerase, in *Mycobacterium smegmatis* results in fragmentation of the β′ subunit in the enzyme assembly. J. Bacteriol. *187*, 6565–6570.

Mathew, R., Mukherjee, R., Balachandar, R., and Chatterji, D. (2006). Deletion of the *rpoZ* gene, encoding the ω subunit of RNA polymerase, results in pleiotropic surface-related phenotypes in *Mycobacterium smegmatis*. Microbiology *152*, 1741–1750.

McKenney, P.T., and Eichenberger, P. (2012). Dynamics of Spore Coat Morphogenesis in *Bacillus subtilis*. Mol. Microbiol. *83*, 245–260.

Mechold, U., Potrykus, K., Murphy, H., Murakami, K.S., and Cashel, M. (2013). Differential regulation by ppGpp versus pppGpp in *Escherichia coli*. Nucleic Acids Res. *41*, 6175–6189.

Minakhin, L., Bhagat, S., Brunning, A., Campbell, E.A., Darst, S.A., Ebright, R.H., and Severinov, K. (2001). Bacterial RNA polymerase subunit ω and eukaryotic RNA polymerase subunit RPB6 are sequence, structural, and functional homologs and promote RNA polymerase assembly. PNAS *98*, 892–897.

Mitra, P., Ghosh, G., Hafeezunnisa, M., and Sen, R. (2017). Rho Protein: Roles and Mechanisms. Annu. Rev. Microbiol. *71*, 687–709.

Molle, V., Fujita, M., Jensen, S.T., Eichenberger, P., González-Pastor, J.E., Liu, J.S., and Losick, R. (2003). The Spo0A regulon of *Bacillus subtilis*. Mol. Microbiol. *50*, 1683–1701.

Molodtsov, V., Sineva, E., Zhang, L., Huang, X., Cashel, M., Ades, S.E., and Murakami, K.S. (2018). Allosteric effector ppGpp potentiates the inhibition of transcript initiation by DksA. Mol. Cell *69*, 828–839.

Mukherjee, K., and Chatterji, D. (1999). Alteration in template recognition by *Escherichia coli* RNA polymerase lacking the ω subunit: A mechanistic analysis through gel retardation and foot-printing studies. J. Biosci. *24*, 453–459.

Mukherjee, K., Nagai, H., Shimamoto, N., and Chatterji, D. (1999). GroEL is involved in activation of *Escherichia coli* RNA polymerase devoid of the ω subunit *in vivo*. Eur. J. Biochem. *266*, 228–235.

Murakami, K.S., Masuda, S., Campbell, E.A., Muzzin, O., and Darst, S.A. (2002). Structural basis of transcription initiation: An RNA polymerase holoenzyme-DNA complex. Science. *296*, 1285–1290.

Mustaev, A., Roberts, J., and Gottesman, M. (2017). Transcription elongation. Transcription *8*, 150–161.

Natori, Y., Tagami, K., Murakami, K., Yoshida, S., Tanigawa, O., Moh, Y., Masuda, K., Wada, T., Suzuki, S., Nanamiya, H., et al. (2009). Transcription Activity of Individual *rrn* Operons in *Bacillus subtilis* Mutants Deficient in (p)ppGpp Synthetase Genes, *relA*, *yjbM*, and *ywaC*. J. Bacteriol. *191*, 4555–4561.

Newing, T.P., Oakley, A.J., Miller, M., Dawson, C.J., Brown, S.H.J., Bouwer, J.C., Tolun, G., and Lewis, P.J. (2020). Molecular basis for RNA polymerase-dependent transcription complex recycling by the helicase-like motor protein HelD. Nat. Commun. *11*, 1–11.

Nicolas, P., Mäder, U., Dervyn, E., Rochat, T., Leduc, A., Pigeonneau, N., Bidnenko, E., Marchadier, E., Hoebeke, M., Aymerich, S., et al. (2012). Condition-dependent transcriptome reveals high-level regulatory architecture in *Bacillus subtilis*. Science. *335*, 1103–1106.

Nudler, E. (2009). RNA Polymerase Active Center: The Molecular Engine of Transcription. Annu. Rev. Biochem. *78*, 335–361.

Patel, U.R., Gautam, S., and Chatterji, D. (2019). Unraveling the Role of Silent Mutation in the ω-Subunit of *Escherichia coli* RNA Polymerase: Structure Transition Inhibits Transcription. ACS Omega *4*, 17714–17725.

Paul, B.J., Barker, M.M., Ross, W., Schneider, D.A., Webb, C., Foster, J.W., and Gourse, R.L. (2004a). DksA: A critical component of the transcription initiation machinery that potentiates the regulation of rRNA promoters by ppGpp and the initiating NTP. Cell *118*, 311–322.

Paul, B.J., Ross, W., Gaal, T., and Gourse, R.L. (2004b). rRNA transcription in *Escherichia coli*. Annu. Rev. Genet. *38*, 749–770.

Paul, B.J., Berkmen, M.B., and Gourse, R.L. (2005). DksA potentiates direct activation of amino acid promoters by ppGpp. PNAS *102*, 7823–7828.

Pei, H.H., Hilal, T., Chen, Z.A., Huang, Y.H., Gao, Y., Said, N., Loll, B., Rappsilber, J., Belogurov, G.A., Artsimovitch, I., et al. (2020). The δ subunit and NTPase HelD institute a two-pronged mechanism for RNA polymerase recycling. Nat. Commun. *11*, 1–14.

Perederina, A., Svetlov, V., Vassylyeva, M.N., Tahirov, T.H., Yokoyama, S., Artsimovitch, I., and Vassylyev, D.G. (2004). Regulation through the secondary channel - Structural framework for ppGpp-DksA synergism during transcription. Cell *118*, 297–309.

Pero, J., Nelson, J., and Fox, T.D. (1975). Highly asymmetric transcription by RNA polymerase containing phage-SP01-induced polypeptides and a new host protein. PNAS *72*, 1589–1593.

Prajapati, R.K., Sengupta, S., Rudra, P., and Mukhopadhyay, J. (2016). *Bacillus subtilis* δ Factor Functions as a Transcriptional Regulator by Facilitating the Open Complex Formation. J. Biol. Chem. *291*, 1064–1075.

Price, C.W., and Doi, R.H. (1985). Genetic mapping of *rpoD* implicates the major sigma factor of *Bacillus subtilis* RNA polymerase in sporulation initiation. Mol. Gen. Genet. *201*, 88–95.

Rabatinová, A., Šanderová, H., Matějčková, J.J., Korelusová, J., Sojka, L., Barvík, I., Veronika, P., Sklenář, V., Žídek, L., and Krásný, L. (2013). The δ Subunit of RNA Polymerase Is Required for Rapid Changes in Gene Expression and Competitive Fitness of the Cell. J. Bacteriol. *195*, 2603–2611.

Raeymaekers, L., Wuytack, E.Y., Willems, I., Michiels, C.W., and Wuytack, F. (2002). Expression of a P-type Ca(2+)-transport ATPase in *Bacillus subtilis* during sporulation. Cell Calcium *32*, 93–103.

Ray-Soni, A., Bellecourt, M.J., and Landick, R. (2016). Mechanisms of Bacterial Transcription Termination: All Good Things Must End. Annu. Rev. Biochem. *85*, 319–347.

Richard, C.L., Tandon, A., Sloan, N.R., and Kranz, R.G. (2003). RNA Polymerase Subunit Requirements for Activation by the Enhancer-binding Protein *Rhodobacter capsulatus* NtrC. J. Biol. Chem. *278*, 31701–31708.

Roberts, J.W. (2019). Mechanisms of Bacterial Transcription Termination. J. Mol. Biol. *431*, 4030–4039.

Roberts, J., and Park, J.S. (2004). Mfd, the bacterial transcription repair coupling factor: Translocation, repair and termination. Curr. Opin. Microbiol. *7*, 120–125.

Ross, W., Thompson1, J.F., Newlands, J.T., and Gourse, R.L. (1990). *E.coli* Fis protein activates ribosomal RNA transcription *in vitro* and *in vivo*. EMBO J. *9*, 3733–3742.

Ross, W., Vrentas, C.E., Sanchez-Vazquez, P., Gaal, T., and Gourse, R.L. (2013). The Magic Spot: A ppGpp Binding Site on E. coli RNA Polymerase Responsible for Regulation of Transcription Initiation. Mol. Cell *50*, 420.

Ross, W., Sanchez-Vazquez, P., Chen, A.Y., Lee, J.H., Burgos, H.L., and Gourse, R.L. (2016). ppGpp binding to a site at the RNAP-DksA interface accounts for its dramatic effects on transcription initiation during the stringent response. Mol. Cell *62*, 811.

Ruff, E.F., Thomas Record, M., and Artsimovitch, I. (2015). Initial Events in Bacterial Transcription Initiation. Biomolecules *5*, 1035–1062.

Santos-Beneit, F., Barriuso-Iglesias, M., Fernández-Martínez, L.T., Martínez-Castro, M., Sola-Landa, A., Rodríguez-García, A., and Martín, J.F. (2011). The RNA Polymerase Omega Factor RpoZ Is Regulated by PhoP and Has an Important Role in Antibiotic Biosynthesis and Morphological Differentiation in *Streptomyces coelicolor*. Appl. Environ. Microbiol. *77*, 7586–7594.

Sarkar, P., Sardesai, A.A., Murakami, K.S., and Chatterji, D. (2013). Inactivation of the Bacterial RNA Polymerase Due to Acquisition of Secondary Structure by the ω Subunit. J. Biol. Chem. *288*, 25076–25087.

De Saro, F.J.L., Woody, A.Y.M., and Helmann, J.D. (1995). Structural analysis of the *Bacillus subtilis* delta factor: a protein polyanion which displaces RNA from RNA polymerase. J. Mol. Biol. *252*, 189–202.

Shin, Y., Qayyum, M.Z., Pupov, D., Esyunina, D., Kulbachinskiy, A., and Murakami, K.S. (2021). Structural basis of ribosomal RNA transcription regulation. Nat. Commun. *12*, 1–12.

Šiková, M., Wiedermannová, J., Převorovský, M., Barvík, I., Sudzinová, P., Kofroňová, O., Benada, O., Šanderová, H., Condon, C., and Krásný, L. (2020). The torpedo effect in *Bacillus subtilis* : RNase J1 resolves stalled transcription complexes. EMBO J. *39*, 1–17.

Smith, A.J., Pernstich, C., and Savery, N.J. (2012). Multipartite control of the DNA translocase, Mfd. Nucleic Acids Res. *40*, 10408–10416.

Sojka, L., Kouba, T., Barvík, I., Šanderová, H., Maderová, Z., Jonák, J., and Krásný, L. (2011). Rapid changes in gene expression: DNA determinants of promoter regulation by the concentration of the transcription initiating NTP in *Bacillus subtilis*. Nucleic Acids Res. *39*, 4598–4611.

Steil, L., Serrano, M., Henriques, A.O., and Völker, U. (2005). Genome-wide analysis of temporally regulated and compartment-specific gene expression in sporulating cells of *Bacillus subtilis*. Microbiology *151*, 399–420.

Stragier, P., Bonamy, C., and Karmazyn-Campelli, C. (1988). Processing of a sporulation sigma factor in *Bacillus subtilis*: How morphological structure could control gene expression. Cell *52*, 697–704.

Sudzinová, P., Kambová, M., Ramaniuk, O., Benda, M., Šanderová, H., and Krásný, L. (2021). Effects of DNA Topology on Transcription from rRNA Promoters in *Bacillus subtilis*. Microorganisms *9*, 1–17.

Sutherland, C., and Murakami, K.S. (2018). An Introduction to the Structure and Function of the catalytic core enzyme of *Escherichia coli* RNA polymerase. EcoSal Plus *8*, 1–14.

Svetlov, V., and Nudler, E. (2020). Towards the unified principles of transcription termination. EMBO J. *39*, 1–3.

van Tilburg, A.Y., Cao, H., van der Meulen, S.B., Solopova, A., and Kuipers, O.P. (2019). Metabolic engineering and synthetic biology employing *Lactococcus lactis* and *Bacillus subtilis* cell factories. Curr. Opin. Biotechnol. *59*, 1–7.

Toulokhonov, I., and Landick, R. (2003). The Flap Domain Is Required for Pause RNA Hairpin Inhibition of Catalysis by RNA Polymerase and Can Modulate Intrinsic Termination. Mol. Cell *12*, 1125–1136.

Tuominen, I., Pollari, M., Tyystjärvi, E., and Tyystjärvi, T. (2006). The SigB σ factor mediates high-temperature responses in the cyanobacterium *Synechocystis* sp. PCC6803. FEBS Lett. *580*, 319–323.

Uptain, S.M., Kane, C.M., and Chamberlin, M.J. (1997). Basic mechanisms of transcript elongation and its regulation. Annu. Rev. Biochem. *66*, 117–172.

Valabhoju, V., Agrawal, S., and Sen, R. (2016). Molecular Basis of NusG-mediated Regulation of Rho-dependent Transcription Termination in Bacteria. J. Biol. Chem. *291*, 22386–22403.

Vlamakis, H., Chai, Y., Beauregard, P., Losick, R., and Kolter, R. (2013). Sticking together: building a biofilm the *Bacillus subtilis* way. Nat. Rev. Microbiol. *11*, 157–168.

Vrentas, C.E., Gaal, T., Ross, W., Ebright, R.H., and Gourse, R.L. (2005). Response of RNA polymerase to ppGpp: requirement for the ω subunit and relief of this requirement by DksA. Genes Dev. *19*, 2379–2387.

Vrentas, C.E., Gaal, T., Burgess, R.R., and Gourse, R.L. (2010). An improved procedure for the purification of the *Escherichia coli* RNA polymerase ω subunit. Protein Expr. Purif. *71*, 190–194.

Wang, S.T., Setlow, B., Conlon, E.M., Lyon, J.L., Imamura, D., Sato, T., Setlow, P., Losick, R., and Eichenberger, P. (2006). The forespore line of gene expression in *Bacillus subtilis*. J. Mol. Biol. *358*, 16–37.

Watson, J.D., and Crick, F.H.C. (1953). Genetical implications of the structure of deoxyribonucleic acid. Nature *171*, 964–967.

Weiss, A., and Shaw, L.N. (2015). Small things considered: the small accessory subunits of RNA polymerase in Gram-positive bacteria. FEMS Microbiol. Rev. *39*, 541–554.

Weiss, A., Moore, B.D., Tremblay, M.H.J., Chaput, D., Kremer, A., and Shaw, L.N. (2017). The ω subunit governs RNA polymerase stability and transcriptional specificity in *Staphylococcus aureus*. J. Bacteriol. *199*, 1–16.

Westbye, A.B., O'Neill, Z., Schellenberg-Beaver, T., and Thomas Beatty, J. (2017). The *Rhodobacter capsulatus* gene transfer agent is induced by nutrient depletion and the RNAP omega subunit. Microbiology *163*, 1355–1363.

Whipple, F.W., and Sonenshein, A.L. (1992). Mechanism of initiation of transcription by *Bacillus subtilis* RNA polymerase at several promoters. J. Mol. Biol. *223*, 399–414.

Wiedermannová, J., and Krásný, L. (2021). β-CASP proteins removing RNA polymerase from DNA: when a torpedo is needed to shoot a sitting duck. Nucleic Acids Res. *49*, 10221–10234.

Wiedermannová, J., Sudzinová, P., Kovaľ, T., Rabatinová, A., Šanderová, H., Ramaniuk, O., Rittich, Š., Dohnálek, J., Fu, Z., Halada, P., et al. (2014). Characterization of HelD, an interacting partner of RNA polymerase from *Bacillus subtilis*. Nucleic Acids Res. *42*, 5151–5163.

York, K., Kenney, T.J., Satola, S., Moran, C.P., Poth, H., and Youngman, P. (1992). Spo0A controls the σA-dependent activation of *Bacillus subtilis* sporulation-specific transcription unit *spoIIE*. J. Bacteriol. *174*, 2648–2658.

Zhang, G., Campbell, E.A., Minakhin, L., Richter, C., Severinov, K., and Darst, S.A. (1999). Crystal Structure of *Thermus aquaticus* Core RNA Polymerase at 3.3 A ̊ Resolution. Cell *98*, 811–824.

Zhang, S.R., Lin, G.M., Chen, W.L., Wang, L., and Zhang, C.C. (2013). ppGpp Metabolism Is Involved in Heterocyst Development in the Cyanobacterium *Anabaena* sp. Strain PCC 7120. J. Bacteriol. *195*, 4536–4544.

Zuo, Y., Wang, Y., and Steitz, T.A. (2013). The Mechanism of *E. coli* RNA Polymerase Regulation by ppGpp Is Suggested by the Structure of Their Complex. Mol. Cell *50*, 430–436.